

For Reference

NOT TO BE TAKEN FROM THIS ROOM

For Reference

NOT TO BE TAKEN FROM THIS ROOM

EX LIBRIS
UNIVERSITATIS
ALBERTAENSIS



THESIS
1965 (F)
10 D

THE UNIVERSITY OF ALBERTA

ULTIMATE STRENGTH AND

BEHAVIOR OF PLATES

by

AUNG GYI, B.S (M.I.T.), M.S.(M.I.T.)

A THESIS

SUBMITTED TO THE FACULTY OF GRADUATE STUDIES

IN PARTIAL FULFILMENT OF THE REQUIREMENTS FOR THE DEGREE OF

DOCTOR OF PHILOSOPHY

DEPARTMENT OF CIVIL ENGINEERING

EDMONTON, ALBERTA

NOVEMBER 1965

UNIVERSITY OF ALBERTA

FACULTY OF GRADUATE STUDIES

The undersigned certify that they have read, and recommend to the Faculty of Graduate Studies for acceptance, a thesis entitled "ULTIMATE STRENGTH AND BEHAVIOR OF PLATES" submitted by AUNG GYI in partial fulfilment of the requirements for the degree of Doctor of Philosophy.

ABSTRACT

The object of the investigation was to obtain a better understanding of the ultimate strength and behavior of building slabs. With this in mind, a method of analysis was developed which gives the progression of yielding, the loads and deflections throughout the elastic and plastic ranges until the formation of collapse mechanisms in the plates.

The method is based on a modification of Newmark's plate analog and the superposition of elastic solutions. The required finite difference operators were derived using this physical model at each stage of yielding in the plate, and the solutions were superposed to establish the progressive yielding of the plate until the formation of a collapse mechanism. The deflections and bending moments at each grid point for every stage of yielding were determined. The twisting moment and elastic bending which are neglected in the yield line theory were taken into consideration. The "square yield criterion" was used as the yield criterion for the plates.

The investigation was restricted to single panel rectangular plates and four parameters, namely, aspect ratio, support conditions, loading pattern and Poisson's ratio were considered. Aspect ratio ($\frac{b}{a}$) was varied from 0.5 to 1.0, support conditions were for simply supported and fixed edge cases, and the types of loading considered were uniform load, symmetrical line load and concentrated load at the center. The variation of Poisson's ratio was from 0 to 0.3.

An electronic digital computer IBM 7040 was used to perform the required numerical calculations. The load-deflection characteristics were

plotted and the progression of yielding traced for all the plates considered.

A procedure for the application of results in the design of reinforced concrete slabs was suggested, and the investigation of the concrete and steel strains for these slabs was carried out to determine whether the strain hardening in the steel or whether crushing of concrete took place prior to the formation of collapse mechanism.

The advantage of this method of analysis over the other ultimate strength procedures, is that it computes the ultimate load and gives the correct final yield pattern without the necessity of assuming many possible collapse mechanisms of the plate or without requiring to assume the possible distributions of moments at ultimate load. In addition, it gives the loads and deflections at every discrete point of the plate for each stage of yielding until the formation of a collapse mechanism.

ACKNOWLEDGMENTS

The author wishes to express his sincere gratitude and appreciation to his thesis supervisor, Dr. S.H. Simmonds, Associate Professor in the Department of Civil Engineering, under whose valuable direction this investigation was carried out.

He is also grateful to the Canadian Colombo Plan Scholarship Committee for providing him the financial assistance and to the Government of Burma for granting him a leave of absence from Rangoon Institute of Technology, without which this study would not be feasible.

The numerical results in this investigation were obtained by making use of IBM 7040, at the Computing Science Department, University of Alberta. The author is thankful to the Computing Science Department as a whole, but especially to D.D. Simpson and C.L. Meek for providing him help during the computer programming for this investigation.

Appreciation is also acknowledged here to the following:

Miss H. Wozniuk for typing the manuscript and the personnel of the technical illustrating services of the Faculty of Engineering for tracing the drawings.

TABLE OF CONTENTS

	PAGE
Title Page	i
Approval Sheet	ii
Abstract	iii
Acknowledgements	v
Table of Contents	vi
List of Tables	viii
List of Figures	x
Notation	xv
 CHAPTER I INTRODUCTION	
1.1 General Remarks	1
1.2 Object	1
1.3 Scope	2
1.4 Historical Review	2
 CHAPTER II METHOD OF ANALYSIS	
2.1 Introduction	5
2.2 Basic Assumptions	8
2.3 Extension of Newmark's Plate Analog into Plastic Range	9
2.4 Derivation of Difference Operators	11
2.5 Determination of Dimensionless Parameters for Loads and Deflections	19
 CHAPTER III LIMITATIONS OF METHOD OF ANALYSIS	
3.1 General Limitations	24
3.2 Tolerances used in establishing the yielding of Grid Points	24
3.3 Grid Spacing	25

TABLE OF CONTENTS (Continued)

	PAGE
CHAPTER IV	OUTLINE OF INVESTIGATION
4.1	General Remarks 26
4.2	Aspect Ratio 26
4.3	Support Conditions 27
4.4	Loading Pattern 27
4.5	Poisson's Ratio 27
CHAPTER V	PRESENTATION AND DISCUSSION OF RESULTS
5.1	Introduction 29
5.2	Uniform Load 30
5.3	Line Load 50
5.4	Concentrated Load 57
CHAPTER VI	APPLICATION TO REINFORCED CONCRETE SLABS
6.1	General Remarks 114
6.2	Stiffness of a Reinforced Concrete Slab 114
6.3	Comparison of the Theoretical Deflection with Measured Value 115
6.4	Suggested Procedure for Design of a Rein- forced Concrete Slab 118
CHAPTER VII	CONCRETE AND STEEL STRAINS
7.1	General Remarks 123
7.2	Assumptions 123
7.3	Investigation based on Average Stiffness 124
CHAPTER VIII	SUMMARY AND GENERAL CONCLUSIONS
8.1	Summary 130
8.2	Conclusions 131
LIST OF REFERENCES	
APPENDIX A	YIELD CRITERIA
A.1	Square Yield Criterion A1
A.2	Tresca's Yield Criterion A3
A.3	Von Mises' Yield Criterion A5
APPENDIX B	SCHEMATIC FLOW DIAGRAM FOR COMPUTER PROGRAM B1

LIST OF TABLES

TABLE		PAGE
4.1	Plates Considered in this Investigation	28
5.1	Comparison of Moments from Analyses and Moments from Westergaard or Timoshenko in Elastic Range. Simply Supported Plates, Uniform Loading	36
5.2	Comparison of Ultimate Loads from Analyses and Ultimate Loads from Yield Line Theory. Simply Supported Plates, Uniform Loading	38
5.3	Comparison of Moments from Analyses and Moments from Westergaard or Timoshenko in Elastic Range. Fixed Edge Plates, Uniform Loading	41
5.4	Comparison of Ultimate Loads from Analyses and Ultimate Loads from Yield Line Theory Fixed Edge Plates, Uniform Loading	42
5.5	Comparison of Deflections from Analyses and Deflections from Timoshenko. Simply Supported Plates, Uniform Loading	44
5.6	Comparison of Deflections at First Yield and Deflections at Ultimate. Simply Supported Plates, Uniform Loading	44
5.7	Comparison of Deflections from Analyses and Deflections from Timoshenko. Fixed Edge Plates, Uniform Loading	47
5.8	Comparison of Deflections at First Yield and Deflections at Ultimate. Fixed Edge Plates, Uniform Loading	47
5.9	Comparison of First Yield Loads and Ultimate Loads from Analyses. Simply Supported Plates, Line Load	54
5.10	Comparison of First Yield Loads and Ultimate Loads from Analyses. Fixed Edge Plates, Line Load	54

LIST OF TABLES (Continued)

TABLE		PAGE
5.11	Comparison of Deflections at First Yield and Deflections at Ultimate. Simply Supported Plates, Line Load	56
5.12	Comparison of Deflections at First Yield and Deflections at Ultimate. Fixed Edge Plates, Line Load	56
5.13	Comparison of Deflections at First Yield and Deflections at Ultimate. Simply Supported Plates, Concentrated Load at the Center	62
5.14	Comparison of Deflections at First Yield and Deflections at Ultimate. Fixed Edge Plates, Concentrated Load at the Center	62
7.1	Coefficients of Curvature at Ultimate Load, Uniform Load, Poisson's Ratio = 0	129

LIST OF FIGURES

FIGURE		PAGE
2.1	Newmark's Plate Analog	6
2.2	Forces Affecting Equilibrium of Hinge "o" of Newmark's Plate Analog	7
5.1	Load-Maximum Deflection Characteristics of Simply Supported Plate, $b/a = 0.5$, $\mu = 0$, Uniform Load	63
5.2	Load-Maximum Deflection Characteristics of Simply Supported Plate, $b/a = 0.5$, $\mu = 0.1$, Uniform Load	64
5.3	Load-Maximum Deflection Characteristics of Simply Supported Plate, $b/a = 0.5$, $\mu = 0.2$, Uniform Load	65
5.4	Load-Maximum Deflection Characteristics of Simply Supported Plate, $b/a = 0.5$, $\mu = 0.3$, Uniform Load	66
5.5	Load-Maximum Deflection Characteristics of Fixed Edge Plate, $b/a = 0.5$, $\mu = 0$, Uniform Load	67
5.6	Load-Maximum Deflection Characteristics of Simply Supported Plate, $b/a = 0.6$, $\mu = 0$, Uniform Load	68
5.7	Load-Maximum Deflection Characteristics of Simply Supported Plate, $b/a = 0.6$, $\mu = 0.1$, Uniform Load	69
5.8	Load-Maximum Deflection Characteristics of Simply Supported Plate, $b/a = 0.6$, $\mu = 0.2$, Uniform Load	70
5.9	Load-Maximum Deflection Characteristics of Simply Supported Plate, $b/a = 0.6$, $\mu = 0.3$, Uniform Load	71
5.10	Load-Maximum Deflection Characteristics of Fixed Edge Plate, $b/a = 0.6$, $\mu = 0$, Uniform Load	72

LIST OF FIGURES (Continued)

FIGURE		PAGE
5.11	Load-Maximum Deflection Characteristics of Fixed Edge Plate, $b/a = 0.6$, $\mu = 0$, Uniform Load	73
5.12	Load-Maximum Deflection Characteristics of Simply Supported Plate, $b/a = 0.75$, $\mu = 0$, Uniform Load	74
5.13	Load-Maximum Deflection Characteristics of Simply Supported Plate, $b/a = 0.75$, $\mu = 0.3$, Uniform Load	75
5.14	Load-Maximum Deflection Characteristics of Fixed Edge Plate, $b/a = 0.75$, $\mu = 0$, Uniform Load	76
5.15	Load-Maximum Deflection Characteristics of Simply Supported Plate, $b/a = 1.0$, $\mu = 0$, Uniform Load	77
5.16	Load-Maximum Deflection Characteristics of Simply Supported Plate, $b/a = 1.0$, $\mu = 0.1$, Uniform Load	78
5.17	Load-Maximum Deflection Characteristics of Simply Supported Plate, $b/a = 1.0$, $\mu = 0.2$, Uniform Load	79
5.18	Load-Maximum Deflection Characteristics of Simply Supported Plate, $b/a = 1.0$, $\mu = 0.3$, Uniform Load	80
5.19	Load-Maximum Deflection Characteristics of Fixed Edge Plate, $b/a = 1.0$, $\mu = 0$, Uniform Load	81
5.20	Load-Maximum Deflection Characteristics of Fixed Edge Plate, $b/a = 1.0$, $\mu = 0.3$, Uniform Load	82
5.21	Yield Patterns (Uniform Load)	83
5.22	Load-Deflection Plot for 4" Thick Elasto-Plastic Plate, Simply Supported, 6' x 10', Uniform Load	84

LIST OF FIGURES (Continued)

FIGURE		PAGE
5.23	Load-Deflection Plot for 4" Thick Elasto-Plastic Plate, Fixed Edge, 6' x 10', Uniform Load	85
5.24	Load-Deflection Plot for 4" Thick Elasto-Plastic Plate, Simply Supported, 6' x 6', Uniform Load	86
5.25	Load-Deflection Plot for 4" Thick Elasto-Plastic Plate, Fixed Edge, 6' x 6', Uniform Load	87
5.26	Deflections and Bending Moments Along Axes of Symmetry, Simply Supported Plate, $b/a = 0.6$, $\mu = 0$, Uniform Load	88
5.27	Deflections and Bending Moments Along Axes of Symmetry, Fixed Edge Plate, $b/a = 0.6$, $\mu = 0$, Uniform Load	89
5.28	Deflections and Bending Moments Along Axes of Symmetry, Simply Supported Plate, $b/a = 1.0$, $\mu = 0$, Uniform Load	90
5.29	Deflections and Bending Moments Along Axes of Symmetry, Fixed Edge Plate, $b/a = 1.0$, $\mu = 0$, Uniform Load	91
5.30	Load-Maximum Deflection Characteristics of Simply Supported Plate, $b/a = 0.6$, $\mu = 0$, Line Load (X - X)	92
5.31	Load-Maximum Deflection Characteristics of Fixed Edge Plate, $b/a = 0.6$, $\mu = 0$, Line Load (X - X)	93
5.32	Load-Maximum Deflection Characteristics of Simply Supported Plate, $b/a = 0.6$, $\mu = 0$, Line Load (Y-Y)	94
5.33	Load-Maximum Deflection Characteristics of Fixed Edge Plate, $b/a = 0.6$, $\mu = 0$, Line Load (Y-Y)	95
5.34	Load-Maximum Deflection Characteristics of Simply Supported Plate, $b/a = 1.0$, $\mu = 0$, Line Load (X-X)	96

LIST OF FIGURES (Continued)

FIGURE		PAGE
5.35	Load-Maximum Deflection Characteristics of Fixed Edge Plate, $b/a = 1.0$, $\mu = 0$, Line Load (X-X)	97
5.36	Yield Patterns (Line Load)	98
5.37	Deflections and Bending Moments Along Axes of Symmetry, Simply Supported Plate, $b/a = 0.6$, $\mu = 0$, Line Load (X-X)	99
5.38	Deflections and Bending Moments Along Axes of Symmetry, Fixed Edge Plate, $b/a = 0.6$, $\mu = 0$, Line Load (X-X)	100
5.39	Deflections and Bending Moments Along Axes of Symmetry, Simply Supported Plate, $b/a = 0.6$, $\mu = 0$, Line Load (Y-Y)	101
5.40	Deflections and Bending Moments Along Axes of Symmetry, Fixed Edge Plate, $b/a = 0.6$, $\mu = 0$, Line Load (Y-Y)	102
5.41	Deflections and Bending Moments Along Axes of Symmetry, Simply Supported Plate, $b/a = 1.0$, $\mu = 0$, Line Load (X-X)	103
5.42	Deflections and Bending Moments Along Axes of Symmetry, Fixed Edge Plate, $b/a = 1.0$, $\mu = 0$, Line Load (X-X)	104
5.43	Load-Maximum Deflection Characteristics of Simply Supported Plate, $b/a = 0.5$, $\mu = 0$, Concentrated Load at Center	105
5.44	Load-Maximum Deflection Characteristics of Fixed Edge Plate, $b/a = 0.5$, $\mu = 0$, Concentrated Load at Center	106
5.45	Load-Maximum Deflection Characteristics of Simply Supported Plate, $b/a = 1.0$, $\mu = 0$, Concentrated Load at Center	107
5.46	Load-Maximum Deflection Characteristics of Fixed Edge Plate, $b/a = 1.0$, $\mu = 0$, Concentrated Load at Center	108

LIST OF FIGURES (Continued)

FIGURE		PAGE
5.47	Yield Patterns (Concentrated Load)	109
5.48	Deflections and Bending Moments Along Axes of Symmetry, Simply Supported Plate, $b/a = 0.5$, $\mu = 0$, Concentrated Load	110
5.49	Deflections and Bending Moments Along Axes of Symmetry, Fixed Edge Plate, $b/a = 0.5$, $\mu = 0$, Concentrated Load	111
5.50	Deflections and Bending Moments Along Axes of Symmetry, Simply Supported Plate, $b/a = 1.0$, $\mu = 0$, Concentrated Load	112
5.51	Deflections and Bending Moments Along Axes of Symmetry, Fixed Edge Plate, $b/a = 1.0$, $\mu = 0$, Concentrated Load	113
6.1	Ultimate Moment per Unit Width-Effective Depth Relationship for a Reinforced Concrete Slab	121
6.2	Comparison of Load-Deflection Plots from Analyses and From Reference (15)	122
7.1	Stress and Strain Diagrams Across a Reinforced Concrete Section	125
A.1	Square Yield Criterion	A1
A.2	Tresca's Yield Criterion	A4
A.3	Von Mises' Yield Criterion	A6
B.1	Schematic Flow Diagram for Computer Program	B1

NOTATION

The following notation has been adopted for use in this thesis.

A_s	= area of reinforcement in a reinforced concrete section
a	= longer span length of a rectangular plate
b	= shorter span length of a rectangular plate or span length of a square plate
b'	= width of a reinforced concrete section
B_D	= dimensionless coefficient for deflection of a plate subjected to concentrated load at the center
B_L	= dimensionless coefficient for concentrated load at the center of a plate
c_1	= depth of neutral axis from compressive outer fibre of a reinforced concrete section
C_D	= dimensionless coefficient for deflection of a plate subjected to symmetrical line load
C_L	= dimensionless coefficient for the symmetrical line load placed on a plate
C	= compressive force on a reinforced concrete section
d	= effective depth of a reinforced concrete section
E	= Young's Modulus of elasticity
E_c	= modulus of elasticity of concrete
E_s	= modulus of elasticity of steel
f'_c	= standard cylinder strength of concrete
f_y	= yield stress of steel
h	= square grid length of Newmark's plate analog
h_x	= grid length of Newmark's plate analog in the x direction

NOTATION (Continued)

h_y	= grid length of Newmark's plate analog in the y direction
k	= coefficient of depth to neutral axis of a reinforced concrete section
K_D	= dimensionless coefficient for deflection of a plate subjected to uniform load
K_L	= dimensionless coefficient for uniform load placed on a plate
M	= bending moment or twisting moment per unit width of a plate
\bar{M}	= bending moment or twisting moment acting on a width of h , h_x or h_y
M_p	= plastic moment per unit width of a plate or ultimate moment per unit width of a reinforced concrete slab
N	= plate stiffness = $\frac{Et^3}{12(1 - \mu^2)}$
n	= modular ratio = $\frac{E_s}{E_c}$
P	= concentrated load
P_y	= concentrated load at first yield
p	= $\frac{A_s}{b'd}$
Q	= total load acting at a node point or joint of the plate analog
q	= uniform load
q_y	= uniform load at first yield
q'	= line load
q'_y	= line load at first yield
t	= thickness of a plate
T	= tensile force of a reinforced concrete section
w	= vertical deflection of a plate

NOTATION (Continued)

x, y, z = rectangular reference coordinates

μ = Poisson's ratio

ϵ_c = concrete strain

ϵ_s = steel strain

β = moment coefficient

$\sigma_1, \sigma_2, \sigma_3$, principal stresses

τ = shear stress

CHAPTER I

INTRODUCTION

1.1 General Remarks

In recent years there has been a distinct attempt by engineers to base designs on ultimate strength rather than arbitrary stresses, in order to obtain more economical structures. This has necessitated a better understanding of the fundamental behavior of structures in order to ensure satisfactory performance under service conditions in addition to obtaining the required strength. While considerable progress in this direction has been made for beams and columns, little work has been done for plate elements. In an attempt to further contribute to the behavior of plate in the post elastic range this study was undertaken.

In this study the words slab and plate are used interchangeably.

1.2 Object

The primary aim of this investigation is to obtain a better understanding of the ultimate strength and behavior of building slabs. With this in mind, a method of analysis is developed assuming elasto-plastic behavior which would enable one to investigate the bending moments, deflections, and progressive yielding of rectangular plates due to successive increments of loading until the formation of collapse mechanisms. It is desired to use these results to suggest a procedure for the design of reinforced concrete slabs which would consider the ultimate strength and

serviceability. Thus, in addition to knowing deflections at ultimate load, it is required to determine whether strain-hardening has taken place in the reinforcement or whether crushing has occurred in the concrete prior to the formation of a collapse mechanism.

1.3 Scope

In this study, analyses are restricted to single panel rectangular plates. In an attempt to investigate some of the effects certain parameters have on the strength and behavior of these plates, four parameters, namely, aspect ratio, support conditions, loading pattern and Poisson's ratio were considered. Aspect ratio ($\frac{b}{a}$) was varied from 0.5 (rectangular plate) to 1.0 (square plate). To approximate the conditions most frequently encountered in building slabs, both simply supported and fixed edge cases, as well as uniform load, symmetrical line load, and concentrated load at the center were considered. The variation of Poisson's ratio was from 0 to 0.3.

1.4 Historical Review

Various attempts have been made to determine the load-carrying capacities of homogeneous, isotropic plates. These solutions assumed perfect elasto-plastic action and were required to satisfy either von Mises' or Tresca's yield criterion. (See APPENDIX A). They are confined almost exclusively to the case of rotational symmetry, as, for example in the works of Hopkins and Prager (1) and Hopkins and Wang (2).

Hopkins (3) has attempted to discuss the non-rotationally symmetric plates made of a rigid, perfectly plastic material with Tresca's yield condition. Although this paper presents the general plastic theory of plates, it does not provide solutions of practical plate problems.

Mansfield (4) made collapse analyses of rigid-plastic plates using the "square yield criterion", although this criterion is not strictly applicable to steel or metal plates. However, Wood (5) has pointed out that it is roughly suitable for design purposes in view of the beneficial effects of membrane action.

Brotchie (6) has discussed the flexural behavior of thin plates in the post elastic range and has shown applications to an infinite plate, circular plates, and a continuous plate on cylindrical supports. The Tresca yield criterion was used.

The ultimate strength of a reinforced concrete slab can be determined by the yield line theory which was developed by Johansen as early as 1931 (7, 8). This theory is considered to give an upper bound on the ultimate load in terms of limit analysis and thus it is important that correct yield patterns be assumed to obtain correct ultimate loads. To determine the correct yield patterns for most practical slabs, investigators like Metz (9) have carried out small scale tests on plaster models.

The ultimate load of a slab can also be found by using a "lower bound" solution. The basis for the lower bound solutions for the square and rectangular reinforced concrete slabs is given in Reference (10) as follows:

"If a distribution of moments can be found which satisfies the plate equilibrium and boundary conditions for a given external load, and if the plate is at every point able to carry these moments, then the given external load will represent a lower limit of the carrying capacity of the plate".

As for the design of reinforced concrete slabs based on the

yield line theory, European Committee for Concrete has produced important works such as the Bulletins No. 27, No. 29 and No. 35. Crawford (10) has discussed the combination of the yield line theory (upper bound) and the strip method (lower bound) proposed by Hillerborg for actual designs of reinforced concrete slabs.

In the works mentioned above the behavior of the plate or slab is not given. In other words, the progression of yielding and the corresponding deflections of the plate until the formation of a collapse mechanism is not known. The behavior of the plate or slab is important from the design point of view as the ultimate load divided by an arbitrary factor of safety may give a load in the post elastic range which might result in unsatisfactory cracks and deflection of the slab. Therefore, it seems desirable to find a method which will give both the strength and behavior of a slab without the necessity of assuming the yield patterns or assuming the distribution of moments.

CHAPTER II

METHOD OF ANALYSIS

2.1 Introduction

The governing differential equation, based on the ordinary theory of flexure of plates, which expresses the deflections in terms of the loading and plate stiffness in the elastic range is as follows:

$$\frac{\partial^4 w}{\partial x^4} + 2 \frac{\partial^4 w}{\partial x^2 \partial y^2} + \frac{\partial^4 w}{\partial y^4} = \frac{q}{N} \quad (2.1)$$

In general, there are two techniques available to solve this plate equation by the method of finite differences. One is a mathematical technique where straight substitutions of finite differences are made for the derivatives in the plate equation. The other is the use of a discrete physical model approximating the behavior of a plate as a means of analysis. One such physical model that approximates the behavior of a plate is Newmark's plate analog. The use of this analog is preferable when boundary conditions or discontinuity conditions cannot be formulated accurately and/or easily.

Ang (12), Prescott, Ang and Siess (13), and Simmonds and Siess (14) have successfully used the Newmark's plate analog to solve the plate problems with realistic boundary conditions in the elastic range. Diagrammatic representation of this model is shown in FIGURES 2.1 and 2.2, and detailed descriptions of it are given in the References mentioned above. In using

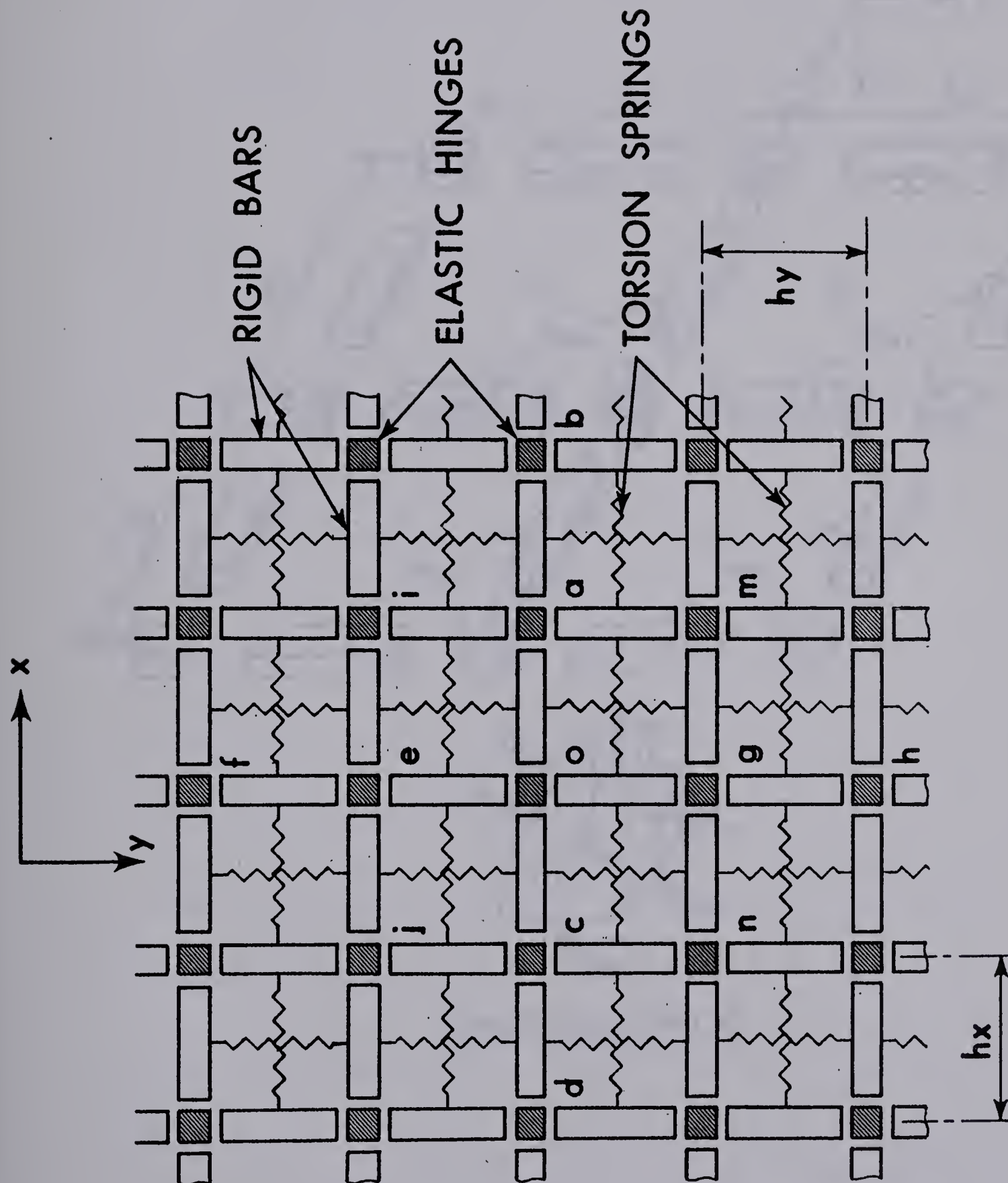


FIGURE 2.1 NEWMARK'S PLATE ANALOG

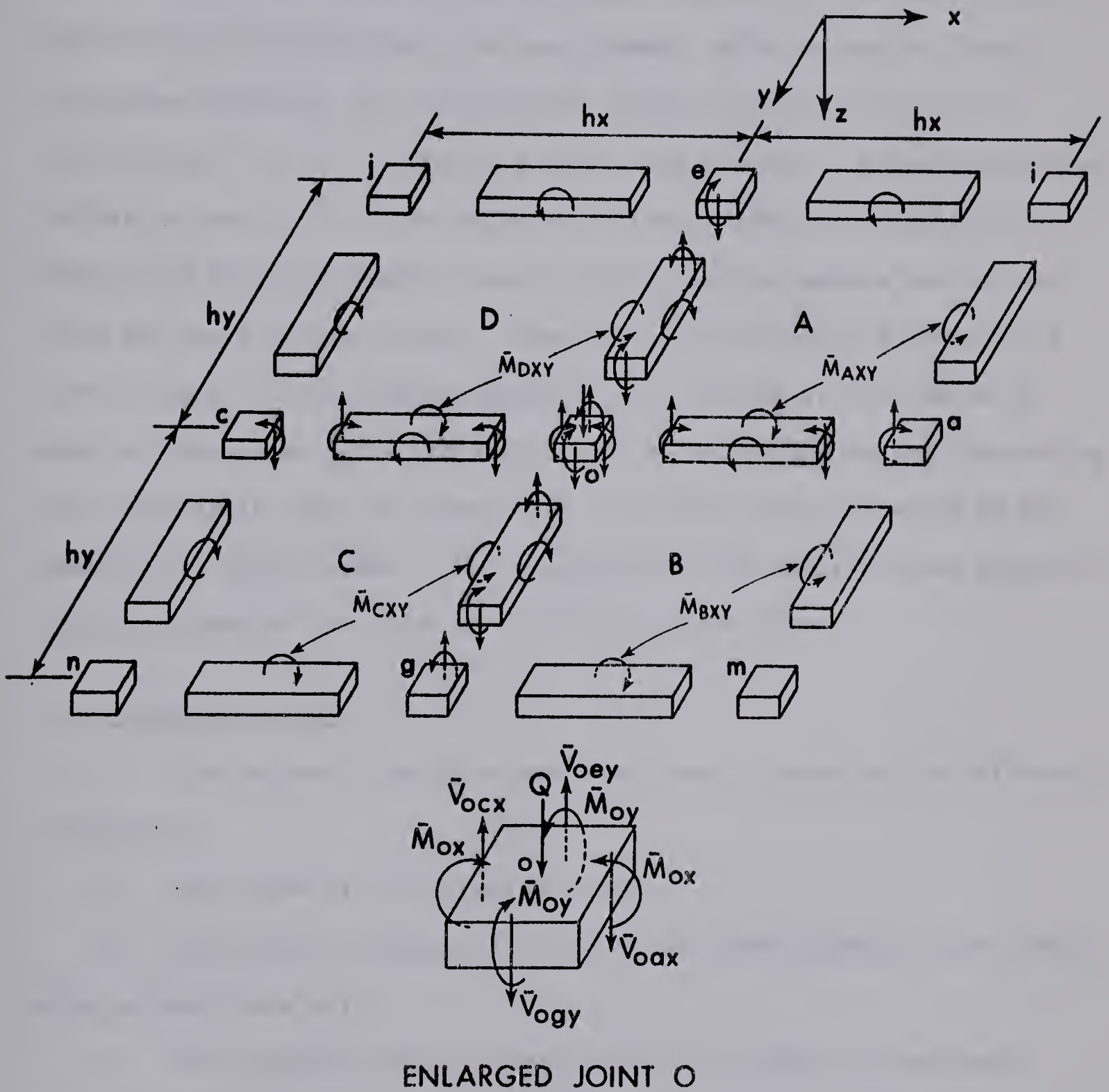


FIGURE 2.2 FORCES AFFECTING EQUILIBRIUM OF HINGE O

this procedure, equations of equilibrium involving the stress resultants are written for every discrete point of the analog. By expressing the stress resultants in terms of the vertical deflections, the difference operators for every discrete point are formed. With the use of these difference operators, the simultaneous linear equations for unknown deflections (w) of the discrete points are obtained. After determining the deflections (w) by the solution of the simultaneous equations, the bending and twisting moments, and principal bending moments can be computed for every discrete point. When the principal bending moment at a point is equal to the plastic moment (M_p), yielding is considered to occur at that point. The problem is then to extend the use of this analog into the plastic range to account for the discontinuities caused by the formation of yield hinges. The considerations and modifications required for this extension are given in the following sections.

2.2 Basic Assumptions

The method of analysis presented here is based on the following assumptions:

- (1) The plate is of uniform thickness.
- (2) The plate is subjected to short-time loads normal to the middle plane of the plate only.
- (3) The stresses acting on any cross section have no resultant force in the direction of the plane of the plate i.e. there are no membrane stresses.
- (4) The deflections of the plate are the deflections of its middle plane.

- (5) There is linear distribution of strains from top to bottom of the plate at all times.
- (6) Hooke's Law is valid in the elastic range.
- (7) The plate yields due to flexure only according to the "square yield criterion".
- (8) An idealized moment-curvature diagram assuming perfect elasto-plastic action is applicable.
- (9) Deflections of the plate are small and there is little change in the geometry of the plate.
- (10) Instability does not occur in any form.
- (11) The unloaded plate is initially flat.

2.3 Extension of Newmark's Plate Analog into Plastic Range

In extending the use of Newmark's plate analog into the plastic range, it is necessary to consider the possible yield conditions that can occur in the plate. The criterion used for yielding of a discrete point is as follows:

$$|M_I|, |M_{II}| = |M_p|, \text{ where}$$

M_I, M_{II} = the principal bending moments and M_p = plastic moment of the plate.

$$M_I, M_{II} = \frac{1}{2} (M_x + M_y) \pm \sqrt{\frac{1}{4} (M_x - M_y)^2 + (M_{xy})^2}$$

According to the "square yield criterion" (APPENDIX A), there can be three types of yielding in the plate.

TYPE I: The first type of yielding will occur at a point where the following conditions exist:

$$M_{xy} = 0 , \quad |M_x| = |M_p| \quad \text{and} \quad |M_y| < |M_p|$$

In this case M_x is the maximum principal moment, and yielding is parallel to the y direction. M_y can still increase in magnitude until its value reaches the value of the plastic moment (M_p).

TYPE II: The second type of yielding will occur at a point where

$$M_{xy} = 0 , \quad |M_y| = |M_p| \quad \text{and} \quad |M_x| < |M_p|$$

In this case M_y is the maximum principal moment, and yielding is parallel to the x direction. M_x can still increase in magnitude until its value reaches the value of the plastic moment (M_p).

TYPE III: The third type of yielding will occur at a point where

$$M_{xy} \neq 0 , \quad \text{and either} \quad |M_I| = |M_p| \quad \text{or} \quad |M_{II}| = |M_p|$$

In this case M_x , M_y , M_{xy} cannot increase in magnitude and yielding is not parallel to either x or y direction.

Using the above yield criterion, the analysis begins by considering the purely elastic plate. To obtain the first yield hinge, the applied load is adjusted until the maximum principal bending moment at a point is equal to the plastic moment of the plate. At this point, the deflections (w), the moments M_x , M_y , M_{xy} and the principal bending moments for every discrete point are similarly adjusted and set aside. This is the first stage of the analysis. In the subsequent stage, a new

set of simultaneous equations for deflections are written through the use of difference operators, which are derived by using the modified plate analog approximating the plate with a yield hinge or discontinuity in it. Solving this new set of equations, a new set of deflections (w), M_x , M_y , M_{xy} are obtained at every discrete point under the new applied load. This new applied load is proportioned in such a way that the resulting new set of M_x , M_y , and M_{xy} when added to the previously set aside values, will cause the next yield hinge. In short, the second solution is superposed on the first solution to establish the next yield hinge. This process is continued until enough yield hinges are established in the system to produce a collapse mechanism. The ultimate load will be the summation of all the loads; and the deflection at a point will be the summation of all the deflections for that point.

The problem is then to derive the required difference operators corresponding to the different types of yielding.

2.4 Derivation of Difference Operators

The derivation of expressions for the bending and twisting moments for a general point by using the plate analog can be found in Reference (12). Referring to FIGURE 2.2 in this study, the typical expressions for the bending and twisting moments per unit width are:

$$\begin{aligned}
 M_{ox} &= -N \left[\frac{w_a - 2w_o + w_c}{h_x^2} + \mu \frac{(w_e - 2w_o + w_g)}{h_y^2} \right] \\
 M_{oy} &= -N \left[\frac{(w_e - 2w_o + w_g)}{h_y^2} + \mu \frac{(w_a - 2w_o + w_c)}{h_x^2} \right]
 \end{aligned} \tag{2.2}$$

$$M_{Axy} = -N (1 - \mu) \left[\frac{(w_a - w_o) - (w_i - w_e)}{h_x h_y} \right] \quad (2.2)$$

The above relationships are the same as the finite difference forms of the bending and twisting moment equations. It should be pointed out that in FIGURE 2.2, \bar{M}_{ox} , which is the total bending moment across the grid width = $(M_{ox}) \cdot h_y$. Similarly, $\bar{M}_{oy} = (M_{oy}) \cdot h_x$, and $\bar{M}_{Axy} = (M_{Axy}) \cdot h_x$ or $\bar{M}_{Axy} = (M_{Axy}) \cdot h_y$.

EQUATIONS (2.2) are used to express the stress resultants in terms of the deflections for the equations of equilibrium of discrete points, and for convenience of application are repeated below in operator forms. Since the analyses are restricted to an analog with square grids, i.e. $h_x = h_y = h$ in FIGURE 2.2, this simplification is used.

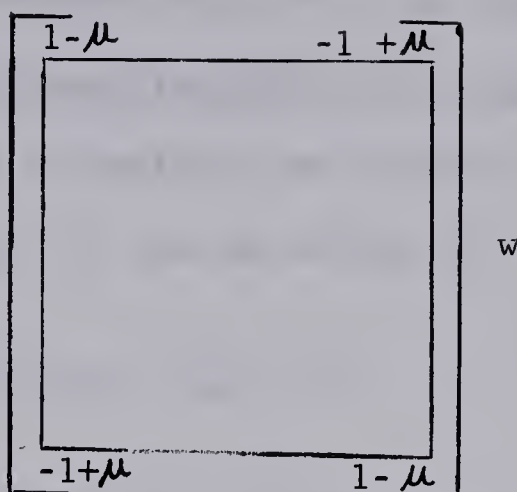
For a typical point "o"

$$M_{ox} = - \frac{N}{h^2} \left[\begin{array}{cc} \mu & \\ 1 & -2-2\mu+1 \\ & \mu \end{array} \right] w \quad (2.3)$$

$$M_{oy} = - \frac{N}{h^2} \left[\begin{array}{cc} & 1 \\ \mu & -2-2\mu \\ & \mu \end{array} \right] w$$

For a typical grid panel "A"

$$M_{AXY} = - \frac{N}{h^2}$$

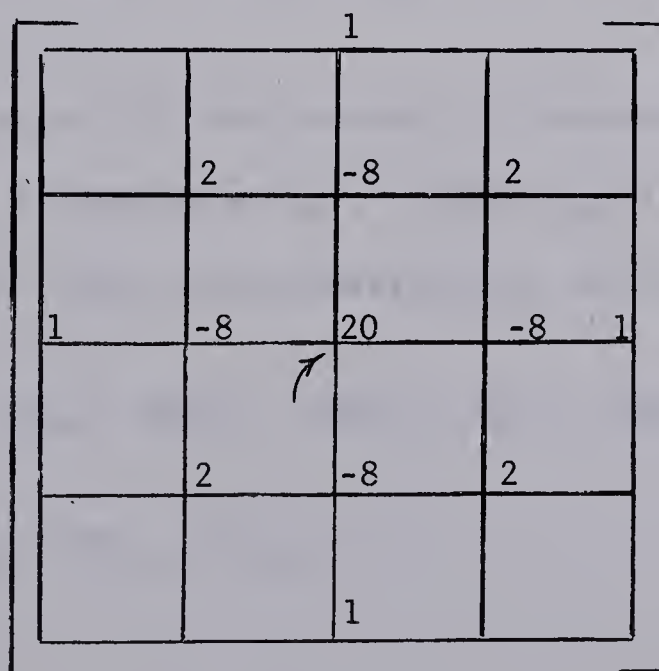


(2.4)

For the symmetric loading considered in this study, 60 difference operators were required to cover all cases of yielding combinations that could occur. The underlying assumptions and techniques of deriving these operators are similar and so, for reasons of space, only a few typical examples are derived and presented in detail.

(i) Difference Operator for General Interior Point

The operator form of the equilibrium equation for an interior point in the elastic range is derived in Reference (12), using Newmark's plate analog. It is reproduced below for ready reference.



$$w = \frac{Qh^2}{N}$$

(2.5)

It is observed that the above pattern is identical to that obtained from finite differences applied to the plate equation.

(ii) Difference Operator for Point "o" with Yield Hinge (TYPE III) at "g"

From FIGURE 2.2, equilibrium equation for forces in vertical direction for grid point "o" can be written as:

$$\bar{V}_{ocx} - \bar{V}_{oax} + \bar{V}_{oey} - \bar{V}_{ogy} = Q \quad (2.6)$$

Expressing EQUATION (2.6) in terms of moments, we have

$$\begin{aligned} \frac{1}{h} \left(\bar{M}_{ox} - \bar{M}_{cx} + \bar{M}_{Cxy} - \bar{M}_{Dxy} - \bar{M}_{ax} + \bar{M}_{ox} - \bar{M}_{Bxy} \right. \\ \left. + \bar{M}_{Axy} + \bar{M}_{oy} - \bar{M}_{ey} + \bar{M}_{Axy} - \bar{M}_{Dxy} - \bar{M}_{gy} + \bar{M}_{oy} \right. \\ \left. - \bar{M}_{Bxy} + \bar{M}_{Cxy} \right) = Q \end{aligned} \quad (2.7)$$

EQUATION (2.7) may be written as

$$\begin{aligned} 2\bar{M}_{ox} - \bar{M}_{cx} + 2\bar{M}_{Cxy} - 2\bar{M}_{Dxy} - \bar{M}_{ax} - 2\bar{M}_{Bxy} \\ + 2\bar{M}_{Axy} + 2\bar{M}_{oy} - \bar{M}_{ey} - \bar{M}_{gy} = Q \end{aligned} \quad (2.8)$$

Since point "g" has yielded, no increment of moment can take place in the y direction at "g". Thus \bar{M}_{gy} is considered to be zero in EQUATION (2.8). With this substitution, we have,

$$\begin{aligned} 2\bar{M}_{ox} - \bar{M}_{cx} + 2\bar{M}_{Cxy} - 2\bar{M}_{Dxy} - \bar{M}_{ax} - 2\bar{M}_{Bxy} \\ + 2\bar{M}_{Axy} + 2\bar{M}_{oy} - \bar{M}_{ey} = Q \end{aligned} \quad (2.9)$$

The bending and twisting moments in the above equation can be expressed in terms of deflections in accordance with EQUATIONS (2.3) and (2.4). Substituting these, the difference operator is expressed as follows:

		1		
	2	-8	2	
1	-8	19	-8	1
	$2-\mu$	$-6+2\mu$	$2-\mu$	

$w = \frac{Qh^2}{N}$

(2.10)

(iii) Difference Operator for Point "o" with Yield Hinge (TYPE II) at "a"

The yielding at grid point "a" when $|M_{ay}| = |M_p|$ is parallel to the x direction. Thus, at this point, load can be carried in one direction only, and an increment in loading results in an increase in M_{ax} . However, since changes in curvature in the y direction will not affect M_{ax} because of yielding, Poisson's ratio for this point for subsequent increments of loading may be taken as zero.

Expressing the bending and twisting moments in terms of deflections in EQUATION (2.8), and using the operator for M_{ax} with Poisson's ratio = 0, we obtain the difference operator for point "o" as follows:

1				$w = \frac{Qh^2}{N}$	(2.11)
	2	-8	2 - μ		
1	-8	20	-8 + 2 μ		
	2	-8	2 - μ		
		1			

(iv) Difference Operator for Point "o" with Yield Hinge (TYPE III) at "o" and with Yield Hinge (TYPE I) at "e"

For further increment of loading $M_{ox} = 0$, $M_{oy} = 0$, and since yielding has occurred in point "e" parallel to the y direction, the operator for M_{ey} as expressed in EQUATION (2.3) may be used with Poisson's ratio = 0.

Using these conditions and substituting into EQUATION (2.8), we

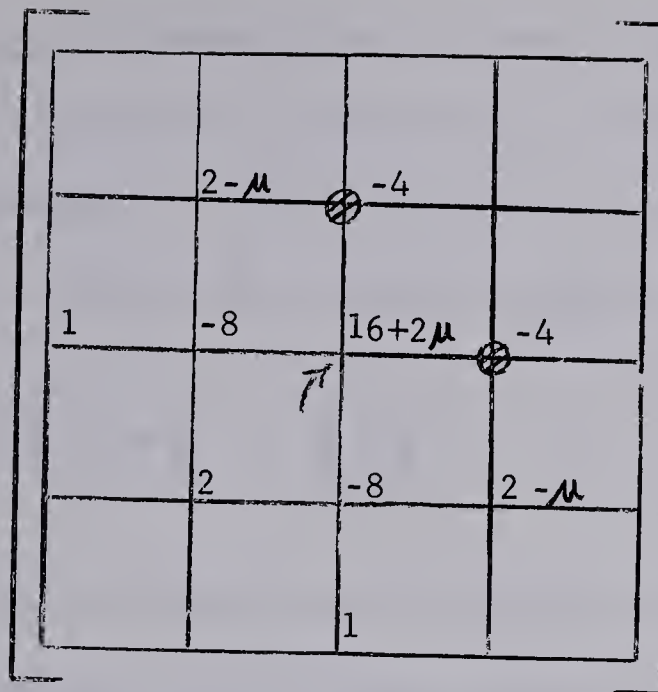
have the operator for point "o" as follows:

$$w = \frac{Qh^2}{N} \quad (2.12)$$

(v) Difference Operator for Point "o" with Yield Hinge (TYPE III) at "a" and Yield Hinge (TYPE III) at "e"

For further increment of loading, $M_{ey} = 0$, and $M_{ax} = 0$. It is also assumed that, since there will be yielding in the panel between point "a" and point "e", $M_{axy} = 0$ for further increment of loading.

Substituting these conditions in EQUATION (2.8), we have the following operator for point "o":



$$w = \frac{Qh^2}{N} \quad (2.13)$$

(vi) Difference Operator for Point "o" with Yield Hinges (TYPE III)
at "o", "a", "c", "e", and "g"

If yielding according to TYPE III occurs at points "o", "a", "c", "e" and "g", all terms on the left hand side of equilibrium equation, EQUATION (2.8) become zero, indicating that the load increment Q for this condition is zero.

This signifies that a local flexural failure has occurred at this point and that the maximum load has been reached.

2.5 Determination of Dimensionless Parameters for Loads and Deflections

When an equation of equilibrium is written for each grid point in the physical analog, the resulting set of linear equations can be written for each increment of loading in matrix form as

$$\frac{N}{h^2} [K] \{ \Delta w \} = \{ \Delta Q \} \quad (2.14)$$

where $[K]$ is the stiffness matrix formed by all the coefficients of the deflections determined from difference operators for a specified increment of loading.

$\{ \Delta w \}$ is a column matrix of incremental deflections at each grid point.

$\{ \Delta Q \}$ is the column matrix of load increments applied at corresponding grid points.

The solution of EQUATION (2.14) may be written as

$$\frac{N}{h^2} \{ \Delta w \} = [F] \{ \Delta Q \} \quad (2.15)$$

where $[F]$ is the flexibility matrix.

Following the procedure mentioned in SECTION (2.3) $\{ \Delta Q \}$ in EQUATION (2.15) is adjusted until the formation of a new yield hinge.

At this stage, the resulting total deflections in terms of N and h of the plate will be as follows:

$$\frac{N}{h^2} \{ w_1 \} + \frac{N}{h^2} \{ \Delta w \} = \frac{N}{h^2} \{ w_2 \} \quad (2.16)$$

The total loads will be

$$\{Q_1\} + \{\Delta Q\} = \{Q_2\} \quad (2.17)$$

where $\frac{N}{h^2} \{w_1\}$ = previously summed up deflections in terms of N and h .

$\{Q_1\}$ = previously summed up loads.

$\frac{N}{h^2} \{w_2\}$ = the new total deflections in terms of N and h .

$\{Q_2\}$ = the new total loads.

For a plate of given aspect ratio and support conditions i.e. given plan geometry, $\frac{N}{h^2} \{w_2\}$ and $\{Q_2\}$ in EQUATIONS (2.16) and (2.17) are directly proportional to the plastic moment M_p .

In practice, it is convenient to consider a plate with a value of plastic moment M_p equal to unity, which will be denoted by M_{pI} . For this condition, $\frac{N}{h^2} \{w_2\}$ and $\{Q_2\}$ in EQUATIONS (2.16) and (2.17) are designated by $\frac{N_I}{h_I^2} \{w_2\}$ and $\{Q_2\}$ respectively. Thus for any plate with similar plan geometry, the load and deflection for any particular value of M_p may be determined as follows:

$$\{Q\} = \frac{M_p}{M_{pI}} \{Q_2\} \quad (2.18)$$

$$\frac{N}{h^2} \{w\} = \frac{M_p}{M_{pI}} \frac{N_I}{h_I^2} \{w_2\}$$

where $\{Q\}$ = the total load for a plate with given M_p
 $\frac{N}{h^2} \{w\}$ = the total deflections in terms of N and h
 for a plate with given M_p .

Relationships similar to EQUATION (2.18) can be obtained for every stage of yielding for this plate. Using these, it is possible to plot the load-deflection curves for the plate if M_p and N are known. Obviously, it will be advantageous to express the load-deflection characteristics by dimensionless parameters that are independent of plate properties such as thickness and material. The derivations of these parameters are shown below.

Consider a uniformly distributed loading case

Let $rh = b$

From EQUATION (2.18) ,

$$\{q\} = \frac{1}{h^2} \{Q\} = \frac{M_p}{M_{pI} h^2} \{Q_2\} = \frac{M_{pr}^2}{M_{pI} b^2} \{Q_2\} \quad (2.19)$$

We can define $\{K_L\}$, for any stage of yielding, as the dimensionless coefficient relating the load to the plastic moment M_p and the shorter span of the plate (b) as follows.

$$\{q\} = \frac{M_p}{b^2} \{K_L\} \quad (2.20)$$

Equating the values of $\{q\}$ from EQUATIONS (2.19) and (2.20),
 we have

$$\frac{M_p}{M_{pI} b^2} \{Q_2\} = \frac{M_p}{b^2} \{K_L\} \quad (2.21)$$

$$\therefore \{K_L\} = \frac{r^2}{M_{pI}} \{Q_2\} \quad (2.21)$$

It should be emphasized that EQUATION (2.20) represents the load at any grid point on the plate, and as such represents a set of algebraic equations that can be used separately. For a uniformly distributed load, K_L is constant for all the grid points.

From EQUATION (2.18),

$$\frac{N}{h^2} \{w\} = \frac{M_P}{M_{pI}} \frac{N_I}{h_I^2} \{w_2\} \quad (2.22)$$

$$\{w\} = \frac{M_P}{M_{pI}} \frac{N_I}{N} \frac{h^2}{h_I^2} \{w_2\}$$

For any particular point the deflection can be expressed in terms of the plate properties and loading as

$$w = \frac{qb^4}{N} K'_D \quad (2.23)$$

where K'_D is the deflection coefficient.

From EQUATIONS (2.22) and (2.23), for a particular point, we have

$$\frac{qb^4}{N} K'_D = \frac{M_P}{M_{pI}} \frac{N_I}{N} \frac{h^2}{h_I^2} w_2$$

But, from EQUATION (2.20),

$$q = \frac{M_P}{b^2} K_L$$

$$\therefore \frac{M_p K_L b^4}{b^2 N} K'_D = \frac{M_p}{M_{pI}} \frac{N_I}{N} \frac{h^2}{h_I^2} w_2$$

Since $rh = b$, we have

$$K'_D = \frac{N_I w_2}{M_{pI} h_I^2 r^2 K_L} \quad (2.24)$$

At any increment of yielding the value of q will change. It is more convenient to have the expression for deflections in such a way that only one term varies. This can be accomplished by defining a new coefficient K_D as $K_D = K'_D \frac{q}{q_y}$ where q_y is the load at first yield.

The load parameter K_L and deflection parameter K_D can now be used to obtain plots that are representatives of load-deflection curves for any given plan geometry of the plate, i.e. given aspect ratio and support conditions, but is independent of plate properties such as M_p and N .

To obtain true load-deflection curves for a given plate, they are computed from the following relationships.

$$q = K_L \frac{M_p}{b^2} \quad (2.25)$$

$$w = K_D \frac{q_y b^4}{N}$$

For any other kind of loading, similar procedure as outlined above can be followed to obtain the dimensionless parameters for load and deflection.

CHAPTER III

LIMITATIONS OF METHOD OF ANALYSIS

3.1 General Limitations

The method of analysis is based on the ordinary theory of flexure of plates, where the effects of stresses normal to the plane of the plate and the resultant stresses in the plane of the plate are neglected. Thus it is subjected to all inherent limitations of this theory in the elastic regions. In addition, the material in the yielded regions is assumed to behave in a purely plastic manner, and therefore, the method of analysis should not be applied to materials where strains may be such as to permit strain hardening.

3.2 Tolerances Used in Establishing the Yielding of Grid Points

In applying the method of analysis to various plates, it was necessary to derive the appropriate operators, solve the resulting simultaneous equations for deflections, compute the stress resultants at each grid point, and trace the progression of yielding for every increment of loading until the formation of a collapse mechanism. For this, an extensive program was written to make use of the digital computer IBM 7040.

Although it is possible to establish the yielding in the plate one grid point at a time, the amount of computation is considerable, and it was felt desirable to place some restriction on the computation consistent with the accuracy that may be expected. For this reason, it was assumed that a grid point had yielded if the principal bending moment of

that grid point was within $\pm 1\%$ of the plastic moment of the plate. In actual applications, because of this tolerance, there were cases where two or even three grid points yielded at the same time. However, this did not affect the ultimate load or the final yield patterns.

The average running time for each problem was approximately one-half hour.

3.3 Grid Spacing

Newmark's plate analog approximates the behavior of a plate, and in general, a finer grid spacing will give more accurate solutions in the elastic range. However, in extending the use of this model into the plastic range, the condition mentioned in SECTION 2.4 (vi) should not, for most cases, be realised at any time prior to the formation of a collapse mechanism in the plate. Therefore, to obtain the collapse mechanism, and to use the assumption that the principal action of the plate is mainly flexure, a limit had to be placed on the fineness of the grid spacing.

In this study, for the single panel rectangular plates subjected to symmetrical loading, the square grid spacing used was one sixth of the shorter span. This was the minimum grid spacing permitted to obtain a collapse mechanism in the plate.

Because of the approximate nature of this analysis, the actual stress conditions within the square grids between the discrete points could only be estimated.

CHAPTER IV

OUTLINE OF INVESTIGATION

4.1 General Remarks

In this study, using the method of analysis described in CHAPTERS II and III, an attempt was made to investigate some of the effects certain parameters would have on the strength and behavior of single panel rectangular plates.

The parameters considered are the aspect ratio ($\frac{b}{a}$), the support conditions, the loading pattern, and Poisson's ratio (μ). The variation of each parameter are tabulated, for convenience in TABLE 4.1.

Since this investigation was intended to give a better understanding of the strength and behavior of structural slabs in buildings, only the loadings and shapes most frequently encountered in practice were investigated. The range of the parameters considered in this study are discussed in detail below.

4.2 Aspect Ratio ($\frac{b}{a}$)

Four aspect ratios of 0.5, 0.6, 0.75 and 1.0 were investigated as approximating the entire range of rectangular plates. Plates with aspect ratios smaller than 0.5 can be assumed to behave essentially as one-way plates, and therefore 0.5 was taken as a lower limit. The upper limit of $\frac{b}{a}$ is 1.0 and corresponds to a square plate. Two intermediate values of aspect ratios, 0.6 and 0.75, were considered to study conditions

between these limits.

4.3 Support Conditions

A fixed edge plate represents approximately a typical interior panel supported on rigid beams of a building floor when all panels are uniformly loaded. However, if only one panel of a building floor is loaded, it might be approximated by a simply supported or hinged plate. The two support conditions (fixed edge and simply supported) also offer advantages of symmetry in obtaining the solutions in this study. For the above reasons these two support conditions were taken into consideration.

4.4 Loading Pattern

The types of loading most frequently considered for the design of building slabs are uniform load, symmetrical line load, and concentrated load at the center. Most of the solutions obtained were for the plates with uniform loading, as it was felt that these solutions would be more useful for design purposes than the other types of loading.

4.5 Poisson's Ratio

Since it was felt that general conclusions regarding the influence of Poisson's ratio on the ultimate strength and behavior of plates could be drawn from the case of uniform loading only, variation in the value of Poisson's ratio was restricted to this loading case. Four values of Poisson's ratio, namely 0.0, 0.1, 0.2 and 0.3 were considered. Solutions for the other types of loading considered were obtained for a value of Poisson's ratio equal to zero.

The various combinations of parameters investigated in this study are summarized in TABLE 4.1.

PLATES CONSIDERED IN THIS INVESTIGATION

No.	Aspect Ratio b/a	Poisson's Ratio	Loading Condition	Support Condition
1	0.5	0	Uniform	Simply supported
2	0.5	0.1	Uniform	Simply supported
3	0.5	0.2	Uniform	Simply supported
4	0.5	0.3	Uniform	Simply supported
5	0.5	0	Uniform	Fixed edge
6	0.6	0	Uniform	Simply supported
7	0.6	0.1	Uniform	Simply supported
8	0.6	0.2	Uniform	Simply supported
9	0.6	0.3	Uniform	Simply supported
10	0.6	0	Uniform	Fixed edge
11	0.6	0.3	Uniform	Fixed edge
12	0.75	0	Uniform	Simply supported
13	0.75	0.3	Uniform	Simply supported
14	0.75	0	Uniform	Fixed edge
15	1.0	0	Uniform	Simply supported
16	1.0	0.1	Uniform	Simply supported
17	1.0	0.2	Uniform	Simply supported
18	1.0	0.3	Uniform	Simply supported
19	1.0	0	Uniform	Fixed edge
20	1.0	0.3	Uniform	Fixed edge
21	0.6	0	Line load on long axis of symmetry	Simply supported
22	0.6	0	Line load on long axis of symmetry	Fixed edge
23	0.6	0	Line load on short axis of symmetry	Simply supported
24	0.6	0	Line load on short axis of symmetry	Fixed edge
25	1.0	0	Line load on axis of symmetry	Simply supported
26	1.0	0	Line load on axis of symmetry	Fixed edge
27	0.5	0	Concentrated load at the center	Simply supported
28	0.5	0	Concentrated load at the center	Fixed edge
29	1.0	0	Concentrated load at the center	Simply supported
30	1.0	0	Concentrated load at the center	Fixed edge

CHAPTER V

PRESENTATION AND DISCUSSION OF RESULTS

5.1 Introduction

From the analyses, the actual deflections at every grid point were obtained for each stage of yielding until the formation of a collapse mechanism. From these, the yield patterns, and the bending and twisting moments at each location were determined.

For each plate the dimensionless load parameter was plotted against the dimensionless maximum deflection parameter for every increment of yielding. (See FIGURES 5.1 through 5.20, 5.30 through 5.35 and 5.43 through 5.46). For convenience and clarity these plots also contain a plan view of the plate showing the progression of yielding, and the ultimate load as obtained from the "yield line theory".

As a plate is loaded beyond the load required for first yield there is a definite zone or area in which yielding occurs. After a study of the distribution of principal bending moments, the extent of this yielded zone or area for square and rectangular plates for the three types of loading considered were determined and are presented in FIGURES 5.21, 5.36 and 5.47.

To study the effect of Poisson's ratio (μ), actual load-deflection plots were made for some specific plates of assumed dimensions subjected to uniform loading. These were plotted in FIGURES 5.22 through 5.25 for the values of Poisson's ratio considered.

To obtain some idea of the distribution of deflections and bending moments in typical plates, these values were plotted along the axes of symmetry for loads corresponding to first yield and ultimate in FIGURES 5.26 through 5.29, 5.37 through 5.42 and 5.48 through 5.51.

In addition to the FIGURES mentioned above, a few TABLES are also presented in this CHAPTER. TABLES 5.1, 5.3, 5.5 and 5.7 show the comparison of deflections and moments obtained in this study for some plates with those from available elastic solutions. Loads at first yield and at ultimate for various plates subjected to three types of loading are tabulated in TABLES 5.2, 5.4, 5.9 and 5.10 whereas TABLES 5.6, 5.8 and 5.11 through 5.14 indicate the maximum deflections at first yield and at ultimate for these same plates.

5.2 Uniform Load

(i) Behavior and yield patterns

Simply supported plates

Inspection of FIGURES 5.1 through 5.4, 5.6 through 5.9 and 5.12 through 5.13 indicates that for the rectangular plates ($\frac{b}{a} = 0.5$, $\frac{b}{a} = 0.6$, $\frac{b}{a} = 0.75$), the position of first yield is at the center for all values of Poisson's ratio considered. As the load is increased, the yielding proceeds along the axis of symmetry in the long or x-direction until the length of yielding is about one half of the long span ($\frac{a}{2}$), at which time the yielding has become a band whose width is about one third of the short span ($\frac{b}{3}$). Yielding then progresses towards the corners of the plate. It is seen that the grid points nearest to the corners are the last points to yield prior to the formation of the collapse mechanism

except for one case for which $\frac{b}{a} = 0.75$ and $\mu = 0$. For this case, grid points located on the diagonals and two grid spacings from the edges are the last points to yield as indicated in FIGURE 5.12. This behavior is due to the large contribution of twisting moment to the yielding of the corner grid points for the case of Poisson's ratio equal to zero and near square plan dimensions.

Final yield patterns obtained from the analyses agree with the patterns assumed in the yield line theory except that instead of yield lines we have yield bands. From examination of FIGURE 5.21 it may be concluded that for a particular simply supported plate, greater values of Poisson's ratio result in greater widths of yield bands. For plates of homogeneous material such as steel plates, one could expect yielding throughout the yielded zone prior to the formation of collapse mechanism. However, for non-homogeneous plates such as reinforced concrete slabs, one would expect yielding in the form of fracture lines with non-yielded parts between them randomly spaced within the yielded zone.

FIGURES 5.4, 5.9 and 5.13 show that the centers of the rectangular plates with $\frac{b}{a} = 0.5$, $\frac{b}{a} = 0.6$, $\frac{b}{a} = 0.75$ and $\mu = 0.3$ have yielded in both directions before the formation of collapse mechanisms, whereas with $\mu = 0$ the centers of these plates have yielded only in the short or y-direction.

For simply supported square plates, FIGURES 5.15 through 5.18 show that Poisson's ratio has a significant influence in the position of first yield as well as in the progression of yielding. For $\mu = 0$, the positions of first yield are at the corner grid points from which, as the load is increased, the yielding progresses diagonally towards the center

until the collapse mechanism is formed. For $\mu = 0.1$, all points along the diagonals yield simultaneously (FIGURE 5.16) for the tolerances of $\pm 1\%$ used in establishing the yielding of the grid points as described in CHAPTER III. For $\mu = 0.2$, FIGURE 5.17 indicates that the plate behaves just the opposite of the plate for $\mu = 0$. For this case ($\mu = 0.2$), the yielding starts at the center and progresses diagonally towards the corners. For $\mu = 0.3$, the plate behaves the same as the plate for $\mu = 0.2$ except that the yield zone around the center is slightly wider. The difference in behavior of plates for different values of Poisson's ratio can be explained as follows:

From the basic expressions for bending and twisting moments, it is seen that an increase in Poisson's ratio increases the magnitude of bending moment and decreases the magnitude of twisting moment. For a square plate, the principal moments at points near the corners are mainly due to the twisting moments. Thus for $\mu = 0$ the yielding occurs first at the corners where the twisting moments are large, whereas for

$\mu = 0.2$ or $\mu = 0.3$ yielding occurs first the center where the bending moments are large, and where the principal moments are mainly due to the bending moments. For $\mu = 0.1$, the principal moments at the corners and at the center are approximately the same and so yielding occurs simultaneously along the diagonals. From the above discussion it can be said that there are three different kinds of behavior of square plates depending on the value of Poisson's ratio. The plate with $\mu = 0.1$ can be looked upon as the border case for the two distinct and opposite manners of behavior with regard to first yield and progression of yielding.

As in the case of rectangular plates ($\frac{b}{a} = 0.5$, $\frac{b}{a} = 0.6$, $\frac{b}{a} = 0.75$) the greater values of Poisson's ratio give the larger widths of yield bands in the square plates. (See FIGURE 5.21).

Fixed edge plates

FIGURES 5.5, 5.10, 5.11 and 5.14 show how the fixed edge rectangular plates ($\frac{b}{a} = 0.5$, $\frac{b}{a} = 0.6$ and $\frac{b}{a} = 0.75$) behave under uniform loading. For a typical rectangular plate, yielding takes place first at the mid-points of the longer fixed edges, and then progresses along these edges until yielding commences at the mid-points of shorter fixed edges. Yielding then proceeds along both fixed edges until yielding begins at the center of the plate. As seen in these FIGURES, the yielding then continues simultaneously along the fixed edges and along the x axis of symmetry until the length of yielding along this axis is about $\frac{a}{2}$. Just before or about the time the yielding at the center spreads to a band width of about $\frac{b}{3}$, the fixed edges become completely yielded. Then the yielding progresses from the ends of the center yield band towards the corners until the formation of a collapse mechanism. For fixed edge plates as for simply supported plates, greater values of Poisson's ratio give greater widths of yield bands and the yield patterns agree with the patterns from yield line theory. From FIGURE 5.21 the width of yield band at the center of the fixed edge plate appear to be narrower than the width of yield band at the center of the simply supported plate for corresponding value of Poisson's ratio since points one grid removed from the center on the y axis of symmetry have not yielded in the former case. This significant difference can be explained by the fact that for the grid points

adjacent to the center point on the short or y axis of symmetry, the influence of negative curvatures from the long fixed edges has to be overcome before positive yielding can take place in the y direction.

In general FIGURES 5.10, 5.11 and 5.14 indicate that yielding occurs in both directions at the centers of the fixed edge rectangular plates before the ultimate loads are reached. However, for the fixed edge rectangular plate with $\frac{b}{a} = 0.5$ and $\mu = 0$, the center yields in the short direction only, since there is more or less one way action in the y direction. Also, for $\mu = 0$ there is a relative decrease in the magnitude of bending moment at the center of this plate in the long or x direction.

Fixed edge square plates subjected to uniform loading behave slightly differently from the rectangular plates ($\frac{b}{a} = 0.5$, $\frac{b}{a} = 0.6$, $\frac{b}{a} = 0.75$) as seen from FIGURES 5.19 and 5.20. For $\mu = 0$, the positions of first yield are at the mid-points of the fixed edges and the yielding progresses along the fixed edges until the fixed edges are essentially completely yielded. (See FIGURE 5.19). Then yielding begins at the center of the plate and proceeds diagonally towards the corners. About the time the ultimate load is reached the yielded zone at the center has spread to a width about one-third of the plate span. However, for

$\mu = 0.3$, the center of the plate yields just before the fixed edges are completely yielded as indicated in FIGURE 5.20. Then the yielding at the center spreads out and progresses towards the corners. The difference in the behavior of these two plates is due to the influence of Poisson's ratio on the magnitudes of bending and twisting moments. As in simply

supported square plates, greater values of Poisson's ratio result in greater widths of yield bands in fixed edge square plates, and the final yield patterns agree with the patterns from yield line theory.

For fixed edge plates, it is interesting to note that the first grid points in from the corners have not yielded at ultimate loads when $\mu = 0.3$ but they have yielded when $\mu = 0$. (See FIGURES 5.10, 5.11, 5.19, and 5.20). Thus, it would appear that for larger values of μ the non-yielded regions in the corners extend further into the plate. There must, however exist (by elastic theory) large negative moments across the corners for both simply supported and fixed edge plates which, at ultimate load, will cause yielding in the corner regions. This kind of yielding has been observed in tests reported on page 91 of Reference (5); but due to the limitation of the grid spacing, the negative yield lines cannot be accurately located in the corner regions from this study.

(ii) Ultimate Load

Simply supported plates

To determine whether the grid spacing chosen was sufficiently fine for accuracy, values obtained in the elastic range were compared with accepted published values by Westergaard and Timoshenko. This comparison is tabulated in TABLE 5.1. Inspection of this TABLE suggests that for practical purposes the coefficients are close enough to their corresponding values to justify use of the grid spacing in this study. Although the elastic functions for one Poisson's ratio can be transformed to corresponding functions for different Poisson's ratio, the plates presented in TABLE 5.1 are restricted to those where comparisons can be made

TABLE 5.1

Comparison of Moments from Analyses and Moments
from Westergaard or Timoshenko in Elastic Range
Simply Supported Plates, Uniform Loading

Plates Considered	M_y (CENTER) = $\beta_1 q b^2$			M_x (CENTER) = $\beta q b^2$		
	β_1 from Analyses	β_1 from Westergaard*	β_1 from Timoshenko**	β from Analyses	β from Westergaard*	β from Timoshenko**
1. $\frac{b}{a} = 0.5$ and $\mu = 0$	0.0951	0.0964		0.0178	0.0174	
2. $\frac{b}{a} = 0.6$ and $\mu = 0$	0.0808	0.0822		0.0245	0.0243	
3. $\frac{b}{a} = 0.75$ and $\mu = 0$	0.0606	0.0620		0.0316	0.0315	
4. $\frac{b}{a} = 1.0$ and $\mu = 0$	0.0361	0.0369		0.0361	0.0369	
5. $\frac{b}{a} = 0.5$ and $\mu = 0.3$	0.1007		0.1017	0.0463		0.0464
6. $\frac{b}{a} = 1.0$ and $\mu = 0.3$	0.0469		0.0479	0.0469		0.0479

* Taken from H.M. Westergaard and W.A. Slater, Proc. ACI Vol. 17, 1921
** Taken from "Theory of Plates and Shells" by Timoshenko and Woinowsky-Krieger

directly. Since the loads, moments and span lengths are interrelated by a dimensionless coefficient, a good check on moment values can also be taken as a good check on load values in the elastic range.

The ultimate loads of simply supported rectangular and square plates under uniform loading compare very well with the corresponding values from the yield line theory. (See TABLE 5.2). Agreement with the yield line theory values are within 5% except for the square plate with $\mu = 0$ in which case the computed ultimate load is 15% higher. These slight differences should be expected as the values from analyses are the results of the yield bands and not of the yield lines as assumed in the yield line theory. Also in this study, considerations were given to the energy absorbed by the elastic bending of the unyielded portions and to the twisting moments, which are neglected in the yield line theory. Some differences from the yield line theory may be expected from assumption that yielding occurs along a series of discrete points instead of along a continuous line.

For simply supported rectangular plates with $\frac{b}{a} = 0.5$ and $\frac{b}{a} = 0.6$, where the positions of first yield are at the centers, higher values of Poisson's ratio tend to lower the first yield loads and slightly increase the ultimate loads. (See TABLE 5.2). For simply supported plates with square and near square dimensions ($\frac{b}{a} = 1.0$ and $\mu = 0.2$, $\frac{b}{a} = 1.0$ and $\mu = 0.3$, $\frac{b}{a} = 0.75$ and $\mu = 0$, $\frac{b}{a} = 0.75$ and $\mu = 0.3$) where the positions of first yield are at the centers, higher values of Poisson's ratio decrease the magnitudes of first yield loads and slightly decrease the ultimate loads. However, for square plates with $\frac{b}{a} = 1.0$ and $\mu = 0$, $\frac{b}{a} = 1.0$ and $\mu = 0.1$, where we have different behaviors of yielding no

TABLE 5.2

Comparison of Ultimate Loads from Analyses
and Ultimate Loads from Yield Line Theory
Simply Supported Plates, Uniform Loading

Plates Considered	$q = K_L \frac{M_p}{b^2}$			$\frac{\text{Load at first yield}}{\text{Ultimate Load}} \%$
	K_L at first yield	K_L at Ultimate	K_L from yield line theory	
1. $\frac{b}{a} = 0.5$ and $\mu = 0$	10.512	14.472	14.200	73%
2. $\frac{b}{a} = 0.5$ and $\mu = 0.1$	10.296	14.472	14.200	71%
3. $\frac{b}{a} = 0.5$ and $\mu = 0.2$	10.116	14.652	14.200	69%
4. $\frac{b}{a} = 0.5$ and $\mu = 0.3$	9.936	14.652	14.200	68%
5. $\frac{b}{a} = 0.6$ and $\mu = 0$	12.384	16.092	15.810	77%
6. $\frac{b}{a} = 0.6$ and $\mu = 0.1$	12.024	16.200	15.810	74%
7. $\frac{b}{a} = 0.6$ and $\mu = 0.2$	11.700	16.272	15.810	72%
8. $\frac{b}{a} = 0.6$ and $\mu = 0.3$	11.340	16.560	15.810	69%
9. $\frac{b}{a} = 0.75$ and $\mu = 0$	16.488	19.512	18.650	84%

TABLE 5.2 (Continued)
Comparison of Ultimate Loads from Analyses
and Ultimate Loads from Yield Line Theory
Simply Supported Plates, Uniform Loading

Plates Considered	$q = K_L \frac{M_p}{b^2}$			Load at first yield % $\frac{\text{Ultimate load}}{\text{Yield load}}$
	K_L at first yield	K_L at Ultimate	K_L from yield line theory	
10. $\frac{b}{a} = 0.75$ and $\mu = 0.3$	14.256	19.332	18.650	74%
11. $\frac{b}{a} = 1.0$ and $\mu = 0$	24.264	27.648	24.000	88%
12. $\frac{b}{a} = 1.0$ and $\mu = 0.1$	24.984	24.984	24.000	100%
13. $\frac{b}{a} = 1.0$ and $\mu = 0.2$	23.112	25.344	24.000	91%
14. $\frac{b}{a} = 1.0$ and $\mu = 0.3$	21.348	25.308	24.000	84%

conclusions can be drawn with respect to first yield loads and ultimate loads. In general, for a typical simply supported plate, one can say that larger value of Poisson's ratio will tend to lower the first yield load if the position of first yield is at the center, and the magnitude of Poisson's ratio has little or no influence on the ultimate load.

An examination of TABLE 5.2 in which first yield loads are tabulated as percentages of ultimate loads indicates that higher reserve strengths exist for plates with smaller values of $\frac{b}{a}$. For example, a simply supported plate with $\frac{b}{a} = 0.5$, $\mu = 0.3$ has a maximum reserve strength of 32%. As the plate becomes more square i.e. for larger values of $\frac{b}{a}$, the reserve strength after first yield decreases and becomes zero for a square plate with $\mu = 0.1$. With the exception of the square plate with $\mu = 0$, it may be concluded that plates with higher Poisson's ratio will have higher reserve strengths after first yield.

Fixed edge plates

TABLE 5.3 shows the comparison of the elastic solutions obtained for fixed edge plates with those of the corresponding values published by Westergaard and Timoshenko. Again the agreement of values is sufficiently close to justify the grid spacing used in the analyses.

Inspection of TABLE 5.4 indicates that the ultimate loads from the analyses are, generally speaking, within $\pm 5\%$ of the corresponding values from the yield line theory. Reasons for these slight differences have already been given in the discussion of the ultimate loads for simply supported plates.

First yield loads expressed as percentages of ultimate loads are given in TABLE 5.4; it is immediately noted that the reserve strength for

TABLE 5.3

41.

COMPARISON OF MOMENTS FROM ANALYSES AND MOMENTS

FROM WESTERGAARD OR TIMOSHENKO IN ELASTIC RANGE

FIXED EDGE PLATES, UNIFORM LOADING

Plates Considered	M_y (CENTER) $= \beta qb^2$		M_x (CENTER) $= \beta qb^2$	
	β from Analyses	β from Westergaard or Timoshenko	β from Analyses	β from Westergaard or Timoshenko
1. $\frac{b}{a} = 0.5$ and $\mu = 0$	0.0414	0.038*	0.00487	0.004*
2. $\frac{b}{a} = 0.6$ and $\mu = 0$	0.0376	0.036*	0.00895	0.007*
3. $\frac{b}{a} = 0.75$ and $\mu = 0$	0.0302	0.030*	0.0143	0.013*
4. $\frac{b}{a} = 1.0$ and $\mu = 0$	0.0183	0.0177*	0.0183	0.0177*
5. $\frac{b}{a} = 1.0$ and $\mu = 0.3$	0.0238	0.0231**	0.0238	0.0231**

* Taken from H.M. Westergaard and W.A. Slater, Proc. ACI Vol. 17, 1921.

** Taken from "Theory of Plates and Shells" by Timoshenko and Woinowsky-Krieger.

TABLE 5.3 (Continued)

Plates Considered	M_y (at mid-point of a) $= \beta qb^2$		M_x (at mid-point of b) $= \beta qb^2$	
	β from Analyses	β from Westergaard or Timoshenko	β from Analyses	β from Westergaard or Timoshenko
1. $\frac{b}{a} = 0.5$ and $\mu = 0$	-0.0791	-0.0829*	-0.052	-0.057*
2. $\frac{b}{a} = 0.6$ and $\mu = 0$	-0.0744	-0.0780*	-0.0516	-0.0565*
3. $\frac{b}{a} = 0.75$ and $\mu = 0$	-0.0637	-0.0680*	-0.0506	-0.0560*
4. $\frac{b}{a} = 1.0$ and $\mu = 0$	-0.0450	-0.0513*	-0.045	-0.0513*
5. $\frac{b}{a} = 1.0$ and $\mu = 0.3$	-0.0450	-0.0513**	-0.045	-0.0513**

* Taken from H.M. Westergaard and W.A. Slater, Proc. ACI Vol. 17, 1921.

** Taken from "Theory of Plates and Shells" by Timoshenko and Woinowsky-Krieger.

TABLE 5.4

Comparison of Ultimate Loads from Analyses
and Ultimate Loads from Yield Line Theory

Fixed Edge Plates, Uniform Loading

Plates Considered	$q = K_L \frac{M_P}{b^2}$			Load at first yield Ultimate Load (%)
	K_L at first yield	K_L at Ultimate	K_L from Yield line theory	
1. $\frac{b}{a} = 0.5$ and $\mu = 0$	12.636	28.044	28.40	45%
2. $\frac{b}{a} = 0.6$ and $\mu = 0$	13.428	31.212	31.62	43%
3. $\frac{b}{a} = 0.6$ and $\mu = 0.3$	13.428	32.040	31.62	42%
4. $\frac{b}{a} = 0.75$ and $\mu = 0$	15.660	37.404	37.300	42%
5. $\frac{b}{a} = 1.0$ and $\mu = 0$	22.356	47.088	48.00	47%
6. $\frac{b}{a} = 1.0$ and $\mu = 0.3$	22.356	45.576	48.00	49%

a fixed edge plate is significantly greater than the reserve strength for a simply supported plate, and ranges from 51% to 58% of the ultimate load. The greater reserve strength for the fixed edge plate is due to its greater degree of redundancy. In the same TABLE it is seen that the first yield load for a fixed edge plate, unlike a simply supported plate, is independent of Poisson's ratio. This is because yielding takes place first at the mid-points of the longer fixed edges, where Poisson's ratio does not have an influence on the magnitude of bending moment. As for simply supported plates, the Poisson's ratio has little or no influence on the ultimate loads for fixed edge plates, which justifies the neglect of Poisson's ratio effect in the yield line theory.

(iii) Deflections

Simply supported plates

The elastic deflections obtained in this study are compared with corresponding deflections obtained from classical solutions in TABLE 5.5. An examination of these values shows that the grid spacing used is also satisfactory for deflections with a maximum variation of approximately 1%.

TABLE 5.6 gives the maximum deflections at ultimate in comparison with maximum deflections at first yield for various simply supported plates. For plates with $\frac{b}{a} = 0.5$, the ratio of maximum deflection at ultimate to maximum deflection at first yield is 1.8 to 2.9. For plates with $\frac{b}{a} = 0.6$ this ratio is 1.5 to 2.3, for plates with $\frac{b}{a} = 0.75$ it is 1.2 to 1.9, and for plates with $\frac{b}{a} = 1.0$ it is 1.0 to 1.5. The lower values of this ratio correspond to lower values of Poisson's ratio for the same plate. With same value of Poisson's ratio, the plates with smaller aspect ratio ($\frac{b}{a}$)

TABLE 5.5
COMPARISON OF DEFLECTIONS FROM ANALYSES
AND DEFLECTIONS FROM TIMOSHENKO
SIMPLY SUPPORTED PLATES, UNIFORM LOADING

Plates Considered	Deflection (CENTER) = $K_D \frac{qb^4}{N}$	
	K_D from Analyses	K_D from Timoshenko*
1. $\frac{b}{a} = 0.5$ and $\mu = 0.3$	0.01022	0.01013
2. $\frac{b}{a} = 1.0$ and $\mu = 0.3$	0.00405	0.00406

*From "Theory of Plates and Shells" by Timoshenko and Woinowsky-Krieger

TABLE 5.6
COMPARISON OF DEFLECTION AT FIRST
YIELD AND DEFLECTIONS AT ULTIMATE
SIMPLY SUPPORTED PLATES, UNIFORM LOADING

Plates Considered	Deflection (CENTER) = $K_D q_y b^4/N$		$\frac{K_D \text{ at Ultimate}}{K_D \text{ at First Yield}}$
	K_D First Yield	K_D At Ultimate	
1. $\frac{b}{a} = 0.5$ and $\mu = 0$	0.01022	0.01885	1.85
2. $\frac{b}{a} = 0.5$ and $\mu = 0.1$	0.01022	0.02117	2.07
3. $\frac{b}{a} = 0.5$ and $\mu = 0.2$	0.01022	0.02451	2.39
4. $\frac{b}{a} = 0.5$ and $\mu = 0.3$	0.01022	0.02965	2.90
5. $\frac{b}{a} = 0.6$ and $\mu = 0$	0.00872	0.01305	1.50
6. $\frac{b}{a} = 0.6$ and $\mu = 0.1$	0.00872	0.01474	1.69

TABLE 5.6 (Continued)

Plates Considered	Deflection (CENTER) = $K_D q_y b^4 / N$		$\frac{K_D \text{ at Ultimate}}{K_D \text{ at First Yield}}$
	K_D at First Yield	K_D At Ultimate	
7. $\frac{b}{a} = 0.6$ and $\mu = 0.2$	0.00872	0.01645	1.89
8. $\frac{b}{a} = 0.6$ and $\mu = 0.3$	0.00872	0.01987	2.28
9. $\frac{b}{a} = 0.75$ and $\mu = 0$	0.00662	0.00819	1.24
10. $\frac{b}{a} = 0.75$ and $\mu = 0.3$	0.00662	0.01265	1.91
11. $\frac{b}{a} = 1.0$ and $\mu = 0$	0.00405	0.00474	1.17
12. $\frac{b}{a} = 1.0$ and $\mu = 0.1$	0.00405	0.00405	1.00
13. $\frac{b}{a} = 1.0$ and $\mu = 0.2$	0.00405	0.00490	1.21
14. $\frac{b}{a} = 1.0$ and $\mu = 0.3$	0.00405	0.00593	1.46

have larger magnitudes of this ratio.

The deflection parameter (K_D) at first yield for a plate of given shape is the same for all values of Poisson's ratio as indicated in TABLE 5.6. However, the load at first yield (q_y) is not the same for different values of Poisson's ratio; therefore actual deflections will not be the same. To clarify this point the reader is referred to FIGURES 5.22 and 5.24 where actual load-deflection plots are presented for assumed elasto-plastic plates. Here, it is seen that deflections at first yield for a given plate decrease for increasing values of Poisson's ratio. However, at ultimate load the deflections are greatest with the largest values of Poisson's ratio.

FIGURES 5.26 and 5.28 give some indication of how the deflections at first yield and at ultimate are distributed along the axes of symmetry for typical simply supported plates. These FIGURES suggest that except for the slightly larger values of deflection at ultimate, the shape and distribution of these deflections along the axes of symmetry are about the same.

Fixed edge plates

TABLE 5.7 shows that in the elastic range the coefficients for maximum deflections obtained from the analyses appear to be consistently larger than the values from Timoshenko by almost 20%. However, the actual deflections are small, and since the grid spacing used was satisfactory for predicting ultimate strength, it is felt that the deflections obtained would be indicative of the deflections at ultimate load for practical purposes.

The deflection at the center of the plate at loads corresponding to first yield and ultimate are given in TABLE 5.8. In general, for the

TABLE 5-7

COMPARISON OF DEFLECTIONS FROM ANALYSES

AND DEFLECTIONS FROM TIMOSHENKO

FIXED EDGE PLATES, UNIFORM LOADING

Plates Considered	Deflection (CENTER) = $K_D \frac{qb^4}{N}$	
	K_D from Analyses	K_D from Timoshenko*
1. $\frac{b}{a} = 1.0$ and $\mu = 0.3$	0.00153	0.00126
2. $\frac{b}{a} = 0.6$ and $\mu = 0.3$	0.00282	0.00235**

*From "Theory of Plates and Shells" by Timoshenko and Woinowsky-Krieger

**This is an interpolated value. $K_D = 0.00230$ for $\frac{a}{b} = 1.6$ and $K_D = 0.00238$ for $\frac{a}{b} = 1.7$.

TABLE 5-8

COMPARISON OF DEFLECTIONS AT FIRST

YIELD AND DEFLECTIONS AT ULTIMATE

FIXED EDGE PLATES, UNIFORM LOADING

Plates Considered	Deflection (CENTER) = $K_D = \frac{q_y b^4}{N}$		$\frac{K_D \text{ at Ultimate}}{K_D \text{ at First Yield}}$
	K_D at First Yield	K_D At Ultimate	
1. $\frac{b}{a} = 0.5$ and $\mu = 0$	0.00305	0.02570	8.42
2. $\frac{b}{a} = 0.6$ and $\mu = 0$	0.00282	0.01971	6.98
3. $\frac{b}{a} = 0.6$ and $\mu = 0.3$	0.00282	0.02660	9.44
4. $\frac{b}{a} = 0.75$ and $\mu = 0$	0.00234	0.01273	5.45
5. $\frac{b}{a} = 1.0$ and $\mu = 0$	0.00153	0.00617	4.03
6. $\frac{b}{a} = 1.0$ and $\mu = 0.3$	0.00153	0.00817	5.34

fixed edge plates considered, the following statement can be made. The value of the ratio of deflection at ultimate to deflection at first yield decreases with increasing values of aspect ratio ($\frac{b}{a}$) and increases with increasing value of Poisson's ratio. This statement is also true for simply supported plates.

It should be pointed out as in the case of simply supported plates that although the values of deflection parameter (K_D) at first yield are the same for a given fixed edge plate for different values of Poisson's ratio, the actual deflections at first yield will not be the same because of the differences in the magnitudes of first yield load (q_y). FIGURES 5.23 and 5.25 show the actual load-deflection relationships for assumed elasto-plastic plates. Like in simply supported plates these FIGURES indicate that for a given fixed edge plate and for a given applied load, the greater value of Poisson's ratio will give smaller deflection in the elastic range, but will cause greater deflection at ultimate load.

The distribution of the deflections at first yield and at ultimate along the axes of symmetry of typical fixed edge plates are given in FIGURES 5.27 and 5.28. Unlike the simply supported plates, there is large increase in deflection at ultimate compared to deflection at first yield.

The influence of Poisson's ratio on the deflections of both simply supported and fixed edge plates may be explained as follows.

From the discussions on yield patterns and ultimate load it is noted that the ultimate load is independent of Poisson's ratio, and the greater widths of yield bands result from higher values of Poisson's ratio.

A plate with a higher value of Poisson's ratio has more two-way action, and therefore gives smaller deflection in the elastic range. However, a plate with a higher value of Poisson's ratio will also have greater magnitudes of bending moment distributed across the plate. Therefore, at the same ultimate load greater areas of the plate will be yielded. This is the reason why we have greater widths of yield bands and greater ultimate deflections for higher values of Poisson's ratio. Since Poisson's ratio does not effect the magnitude of the yield moment, the ultimate load from considerations of equilibrium, will not change with change in Poisson's ratio. It should be emphasized that the above values and discussions of deflections are for elastic and elasto-plastic behavior only and do not consider time effects such as creep.

(iv) Bending Moments

Simply supported plates

FIGURES 5.26 and 5.28 give the distribution of bending moments along the axes of symmetry for some typical simply supported plates under uniform load. In the regions where the plate is still elastic the bending moment diagrams are similar in shape to the deflection curves. However along the points where yielding has occurred, the moment is constant having a value of M_p and appears as a horizontal straight line. These FIGURES are helpful in determining the limiting boundaries of yielding while plotting the yield patterns. (FIGURE 5.21).

The values of bending moments in the elastic range are compared in TABLE 5.1 with the values from Westergaard and Timoshenko. It is noted that agreement is within 2%.

Fixed edge plates

The distributions of bending moments along the axes of symmetry for the fixed plates subjected to uniform loading are shown in FIGURES 5.27 and 5.29. For a square plate, negative moments are developed in the regions near the fixed edges. As the load is increased, yielding begins at the mid-points of these fixed edges, and progresses along the edges permitting them to rotate. Thus the plate behaves more and more like a simply supported plate resulting in a decrease in the negative moments near the edges and an increase in the positive moment around mid span. Further increase in load results in positive yielding at mid span. A similar behavior occurs in the short span of the rectangular plate. However in the long span the negative moments in the regions near the shorter fixed edges continue to increase in magnitude until yielding occurs at the mid-points of these fixed edges. Further loading results in a decrease in negative moments in the vicinity of these edges.

FIGURES 5.27 and 5.29 are helpful in drawing the yield patterns shown in FIGURE 5.21. Again it is noted that the yield zone at the center in the short span direction of the fixed edge plate is less than that of the simply supported case.

5.3 Line Load

Line loads were placed along the axis of symmetry at midspan in the long (x) direction or the short (y) direction. In the following paragraph the discussion of the line load in the long direction is given firstly followed by the line load in the short direction. Care should be taken to distinguish between the different effects caused

by these two loading patterns.

(i) Behavior and yield patterns

Simply supported plates

The behavior of the simply supported plates under line load placed along the x-axis of symmetry is illustrated in FIGURES 5.30 and 5.34. In these FIGURES it is seen that yielding begins at the center of the plates and then proceeds along the x-axis of symmetry almost to the supports. At this stage of loading the center of the square plate has yielded in both directions and the rectangular plate with $\frac{b}{a} = 0.6$ has yielded only in the short direction. Further loading results in yielding progressing towards the corners until the formation of collapse mechanisms.

The behavior of a simply supported square plate subjected to a line load placed along the y-axis of symmetry is identical, of course, to the behavior of the plate subjected to a line load placed along the x-axis of symmetry. For a rectangular plate with $\frac{b}{a} = 0.6$ under a line load placed along the y-axis of symmetry, the progression of yielding is shown in FIGURE 5.32. The position of first yield is at the center, and yielding proceeds along the y-axis of symmetry until the length of yielding is about $\frac{b}{3}$, at which time it spreads rapidly into the plate until it reaches the longer edges of the plate. It should be pointed out that the region in which yielding has occurred in both directions extends to about one-third the width of the plate along the y-axis of symmetry before yielding fans out towards the supports. In this case there is

local flexure failure in the region near the center of the plate.

Fixed edge plates

From FIGURE 5.31, for the fixed edge plate with $\frac{b}{a} = 0.6$ subjected to line load placed on the x-axis of symmetry, yielding begins simultaneously at mid-points of all fixed edges and at the center. The tolerance used in establishing the yielding of these points is $\pm 1\%$ as described in CHAPTER III. Yielding then alternates between the points on the x-axis of symmetry and the points on the fixed edges until the formation of a collapse mechanism as shown in FIGURE 5.36.

The behavior of fixed edge square plate under line load placed along the x-axis of symmetry can be seen in FIGURE 5.35 where it shows that the positions of first yield are at mid-points of fixed edges where they meet the x-axis of symmetry. The center is the next point of yield, after which yielding alternates between the points on the x-axis of symmetry and the points on the fixed edges. Considerable yielding takes place around the center, and from FIGURE 5.35 it is seen that about one-third the width of the plate along the x-axis of symmetry has yielded in both directions before the formation of a collapse mechanism shown in FIGURE 5.36.

FIGURE 5.33 shows how yielding takes place in the fixed edge rectangular plate with $\frac{b}{a} = 0.6$ subjected to line load placed along the y-axis of symmetry. Yielding starts at the mid-points of the long fixed edges and then proceeds along these edges until the length of yielding on each edge is about $\frac{a}{4}$. Yielding then alternates between the points on the y-axis of symmetry and the points on the long fixed edges until

the yield pattern is formed as shown in FIGURES 5.33 and 5.36. This is the local flexure failure around the region where the symmetrical line load is placed. Inspection of FIGURE 5.33 indicates that the region around the center of the plate has yielded in both x and y directions before the formation of a local flexure failure mechanism.

(ii) Ultimate Load

Simply supported and fixed edge plates

TABLES 5.9 and 5.10 show the first yield loads and the ultimate loads for the simply supported and the fixed edge plates subjected to line load. The reserve strengths after first yield, range from 27% to 41% of the ultimate load for the simply supported plates, and from 46% to 61% of the ultimate load for the fixed edge plates. As expected, the fixed edge plates possess greater reserve strengths than the simply supported plates.

Inspection of TABLE 5.9 indicates that the reserve strengths after first yield, for the simply supported plates considered, are about the same for the same mode of collapse mechanism. However, it can be seen from TABLE 5.10 that for the same mode of collapse mechanism, the fixed edge square plate has higher reserve strength than the fixed edge rectangular plate, the reason being that considerable area of the fixed edge square plate has yielded before the formation of collapse mechanism.

To determine the accuracy of solutions from the analyses, comparisons were made with solutions from elastic analyses using Levy's method. The deflection of the simply supported square plate from the

TABLE 5.9

COMPARISON OF FIRST YIELD LOADS
AND ULTIMATE LOADS FROM ANALYSES
SIMPLY SUPPORTED PLATES, LINE LOAD

Plates considered	$q' = C_L \frac{M_P}{b}$		Load at $\frac{\text{first yield}}{\text{ultimate load}}$ (%)
	C_L at first yield	C_L at ultimate	
1. $\frac{b}{a} = 1.0$ and $\mu = 0$ Line load (x-x)	9.726	16.134	60.2%
2. $\frac{b}{a} = 0.6$ and $\mu = 0$ Line load (x-x)	5.604	9.528	59.0%
3. $\frac{b}{a} = 0.6$ and $\mu = 0$ Line load (y-y)	11.004	15.192	72.6%

TABLE 5.10

COMPARISON OF FIRST YIELD LOADS
AND ULTIMATE LOADS FROM ANALYSES
FIXED EDGE PLATES, LINE LOAD

Plates considered	$q' = C_L \frac{M_P}{b}$		Load at $\frac{\text{first yield}}{\text{ultimate load}}$ (%)
	C_L at first yield	C_L at ultimate	
1. $\frac{b}{a} = 1.0$ and $\mu = 0$ Line load (x-x)	10.014	24.720	40.6%
2. $\frac{b}{a} = 0.6$ and $\mu = 0$ Line load (x-x)	8.844	16.512	53.7%
3. $\frac{b}{a} = 0.6$ and $\mu = 0$ Line load (y-y)	8.220	21.348	38.5%

analyses is within 4% of the deflection from elastic analysis, and the moments are within 2% of the corresponding values from elastic analysis. Thus, the grid spacing used can be assumed to be satisfactory.

(iii) Deflections

Simply supported and fixed edge plates

TABLES 5.11 and 5.12 contain the dimensionless coefficients for maximum deflections at first yield and at ultimate load for simply supported and fixed edge plates respectively, when subjected to line load. The ratios of the deflections at ultimate to deflections at first yield are also shown in these TABLES. For the formation of yield patterns indicated in FIGURE 5.36 these ratios range from 1.8 to 2.6 and 4.7 to 5.2 for the simply supported and the fixed edge plates respectively.

The distributions of deflections along the axes of symmetry for both simply supported and fixed edge plates are given in FIGURES 5.37 through 5.42.

(iv) Bending Moments

Simply supported and fixed edge plates

The distribution of bending moments are shown in FIGURES 5.37 through 5.42 for simply supported and fixed edge plates subjected to line load. FIGURES 5.37 and 5.38 indicate that for the simply supported and fixed edge rectangular plates with $\frac{b}{a} = 0.6$, subjected to line load

TABLE 5.11

COMPARISON OF DEFLECTIONS AT FIRST
YIELD AND DEFLECTIONS AT ULTIMATE
SIMPLY SUPPORTED PLATES, LINE LOAD

Plates considered	Deflection (CENTER) = $C_D q' \frac{b^3}{y_N}$		$\frac{C_D \text{ at ultimate}}{C_D \text{ at first yield}}$
	C_D at first yield	C_D at ultimate	
1. $\frac{b}{a} = 1.0$ and $\mu = 0$ Line load (x-x)	0.00705	0.01465	2.05
2. $\frac{b}{a} = 0.6$ and $\mu = 0$ Line load (x-x)	0.0146	0.03742	2.56
3. $\frac{b}{a} = 0.6$ and $\mu = 0$ Line load (y-y)	0.00982	0.01784	1.82

TABLE 5.12

COMPARISON OF DEFLECTIONS AT FIRST
YIELD AND DEFLECTIONS AT ULTIMATE
FIXED EDGE PLATES, LINE LOAD

Plates considered	Deflection (CENTER) = $C_D q'_y \frac{b^3}{N}$		$\frac{C_D \text{ at ultimate}}{C_D \text{ at first yield}}$
	C_D at first yield	C_D at ultimate	
1. $\frac{b}{a} = 1.0$ and $\mu = 0$ Line load (x-x)	0.00321	0.01516	4.72
2. $\frac{b}{a} = 0.6$ and $\mu = 0$ Line load (x-x)	0.00566	0.02726	4.82
3. $\frac{b}{a} = 0.6$ and $\mu = 0$ Line load (y-y)	0.00416	0.02163	5.20

along the x-axis, there is little change in the distribution and magnitude of M_y along the y-axis of symmetry after first yield. A similar distribution of M_y can be seen in FIGURE 5.41 for simply supported square plate. Another notable feature for simply supported rectangular plate, as indicated in FIGURE 5.39 is the appearance of negative bending moments M_x along the long axis of symmetry when the line load is placed along the short axis of symmetry. By considering a strip of plate along the long axis as a beam subjected to a concentrated load at mid span, it would appear that the ends of this beam are prevented from fully rotating by the unloaded portions of the plate near the ends and thus negative moments are developed. These FIGURES of bending moment distribution are helpful in drawing the yield patterns shown in FIGURE 5.36.

5.4 Concentrated Load

(i) Behavior and yield patterns

Simply supported plates

FIGURE 5.43 shows the behavior of the simply supported rectangular plate with $\frac{b}{a} = 0.5$ subjected to concentrated load at the center. The position of first yield is at the center. After the center has yielded in both directions, yielding fans out along the longer axis of symmetry until the yield zones reach the long edges. The final yield pattern as shown in FIGURE 5.47 agrees with the pattern shown on page 29 of Reference (5), except for a slight difference. The pattern shown in Reference (5) has negative yield lines at the outer boundary of the yield zone, whereas the one from the analyses does not. At the formation of the final yield pattern shown in FIGURE 5.47, a few grid points were found to have lost

their flexural capacities, and the analyses was stopped automatically. However, inspection of FIGURE 5.48 shows that there is considerable magnitude of negative M_x along the x-axis of symmetry and this indicates that if the load is slightly increased there will be negative yielding at the outer boundary of the yield zone. The overall length of the yield zone from the analyses is about the same as that of the yield zone in Reference (5).

For simply supported square plate subjected to concentrated at the center, FIGURE 5.45 shows that yielding starts at the center of the plate. Yielding then spreads out and proceeds towards the corners. The resulting collapse mechanism, as indicated in FIGURE 5.47, is the same as that of the square plate subjected to uniform load. This pattern agrees with the actual pattern obtained from test as shown in Reference (9).

Fixed edge plates

For fixed edge rectangular plate with $\frac{b}{a} = 0.5$, subjected to concentrated load at the center, yielding begins at the center as indicated in FIGURE 5.44. After yielding of the center in both directions yielding alternates between the points inside the plate, and the points on the long fixed edges until the formation of the yield pattern shown in FIGURE 5.47. The extent of this yield zone is about one-third the length of the plate, and the width is about one-third the width of the plate. Inspection of distribution of moments in FIGURE 5.49 suggests that there will be negative yielding at the outer boundary of this yielded zone.

The behavior of a fixed edge square plate subjected to a concentrated load at the center is indicated in FIGURE 5.46. Yielding begins at the center and then alternates between the points inside the plate and the

points on the fixed edges until the formation of the yield pattern shown in FIGURE 5.47. Here also we have negative yielding at the outer boundary. This pattern without the yielding at fixed edges according to Reference (5) is called a conical collapse mode.

(ii) Ultimate Load

Simply supported plates

For simply supported rectangular plate with $\frac{b}{a} = 0.5$ subjected to concentrated load at the center, the magnitude of the ultimate load obtained was $9.591 M_p$ whereas from Reference (5) it is $10.28 M_p$. This difference is probably due to the difference in criterion used to determine the ultimate load. In the analyses, the ultimate load was taken to be the load corresponding to the condition when the yield zone reached the plate boundary. At this load, although the negative moments at the boundary of the yield zone were large, they had not reached the plastic moment of the plate which is the condition assumed in the collapse mechanism in Reference (5). However, the increase in load required to form negative yielding and establish the collapse mechanism would be small.

The first yield load for this simply supported plate is $3.689 M_p$, and therefore the reserve strength after first yield is approximately 62% of the ultimate load.

The ultimate load obtained in the case of simply supported square plate subjected to concentrated load at the center is $9.055 M_p$, and the corresponding value from the yield line theory is $8.0 M_p$ for the similar collapse mechanism. The ultimate load from the analyses is thus about 13% greater than the value from the yield line theory which

corresponds to increase noted for the case of uniformly loaded square plate. This increase in load is expected as the yield pattern in both cases passes through the diagonals at the corners where for $\mu = 0$, the twisting moments are large. The effects of these twisting moments are neglected in the yield line theory. The first yield load is $4.522 M_p$ and therefore the percentage of the ratio of the first yield load to ultimate load in this case is approximately 50%. Therefore the reserve strength of the plate after first yield is also 50% of the ultimate load.

Fixed edge plates

The ultimate load of the fixed edge rectangular plate with $\frac{b}{a} = 0.5$ at the formation of collapse mechanism shown in FIGURE 5.47 is $12.444 M_p$. The load at first yield is $4.778 M_p$. The percentage of the ratio of the first yield load to ultimate load in this case is 38%. The reserve strength is therefore equal to 62% of the ultimate load.

For the fixed edge square plate subjected to concentrated load at the center the ultimate load is $12.666 M_p$. This is slightly higher than the ultimate load from the yield line theory for the conical collapse mode which is $12.56 M_p$. The reason for this slight difference is, in addition to the different assumptions and considerations of the two methods, there is some negative yielding along the fixed edges in the yield pattern obtained from the analyses. The first yield load from the analyses is $5.553 M_p$, and therefore the reserve strength after first yield is approximately 56% of the ultimate load.

From the above discussion, it appears that the reserve strength of plates subjected to concentrated load at the center is independent of the support conditions.

(iii) DeflectionsSimply supported and fixed edge plates

The distribution of the deflections along the axes of symmetry for both simply supported and fixed edge plates are shown in FIGURES 5.49 through 5.51. Inspection of TABLES 5.13 and 5.14 indicates that for the plates considered, the larger ratio of maximum deflection at ultimate to maximum deflection at first yield, will result for plates with smaller $\frac{b}{a}$. This is true for both simply supported and fixed edge plates. For same $\frac{b}{a}$ and same Poisson's ratio, the fixed edge plate will have larger ratio of maximum deflection at ultimate to maximum deflection at first yield than that of the simply supported plate. Incidentally this effect is more pronounced for the plates subjected to uniform loading. (See TABLES 5.6 and 5.8).

(iv) Bending momentsSimply supported and fixed edge plates

The distribution of the bending moments along the axes of symmetry for simply supported and fixed edge plates subjected to concentrated loads are given in FIGURES 5.49 through 5.51. The significance of these diagrams is that negative bending moments occur at some points along the axes of symmetry even for simply supported plates. For these plates, the unloaded parts of the plate do not allow the full rotation of the edges, and thus negative moments are developed along the axes of symmetry.

TABLE 5.13

COMPARISON OF DEFLECTIONS AT FIRST

YIELD AND DEFLECTIONS AT ULTIMATE

SIMPLY SUPPORTED PLATES, CONCENTRATED LOAD AT THE CENTER

Plates Considered	Deflection (Center) = $B_D P_y b^2 / N$		$\frac{B_D \text{ at ultimate}}{B_D \text{ at first yield}}$
	B_D at first yield	B_D at ultimate	
1. $\frac{b}{a} = 1.0$ and $\mu = 0$	0.01277	0.04395	3.44
2. $\frac{b}{a} = 0.5$ and $\mu = 0$	0.01791	0.09986	5.57

TABLE 5.14

COMPARISON OF DEFLECTIONS AT FIRST

YIELD AND DEFLECTIONS AT ULTIMATE

FIXED EDGE PLATES, CONCENTRATED LOAD AT THE CENTER

Plates Considered	Deflection (Center) = $B_D P_y b^2 / N$		$\frac{B_D \text{ at ultimate}}{B_D \text{ at first yield}}$
	B_D at first yield	B_D at ultimate	
1. $\frac{b}{a} = 1.0$ and $\mu = 0$	0.00700	0.03581	5.12
2. $\frac{b}{a} = 0.5$ and $\mu = 0$	0.00889	0.06186	6.96

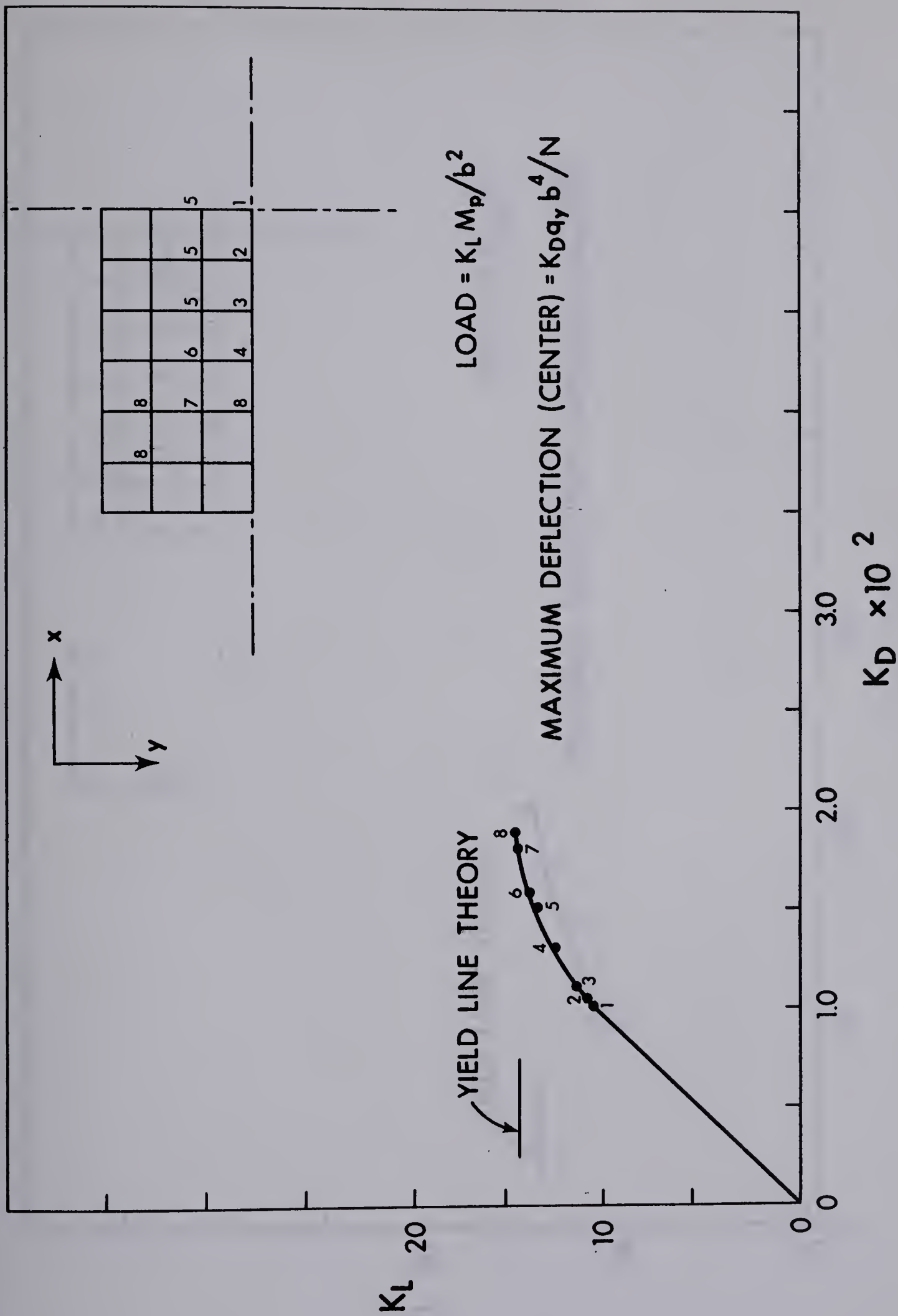


FIGURE 5.1 LOAD-MAXIMUM DEFLECTION CHARACTERISTICS OF SIMPLY SUPPORTED PLATE, $\frac{b}{a} = 0.5$, $\mu = 0$, UNIFORM LOAD

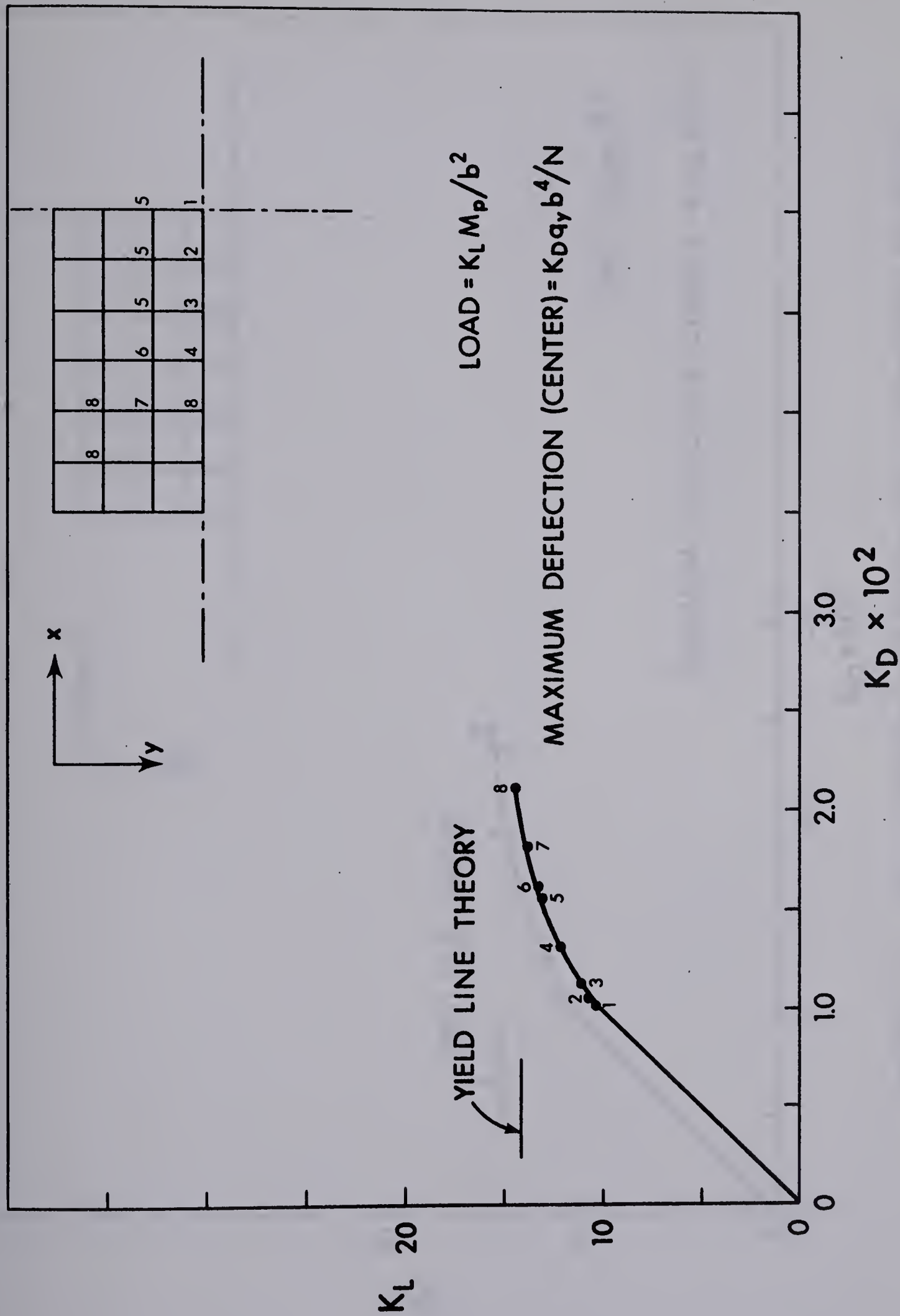


FIGURE 5.2 LOAD-MAXIMUM DEFLECTION CHARACTERISTICS OF SIMPLY SUPPORTED PLATE, $\frac{b}{a} = 0.5$, $\mu = 0.1$, UNIFORM LOAD

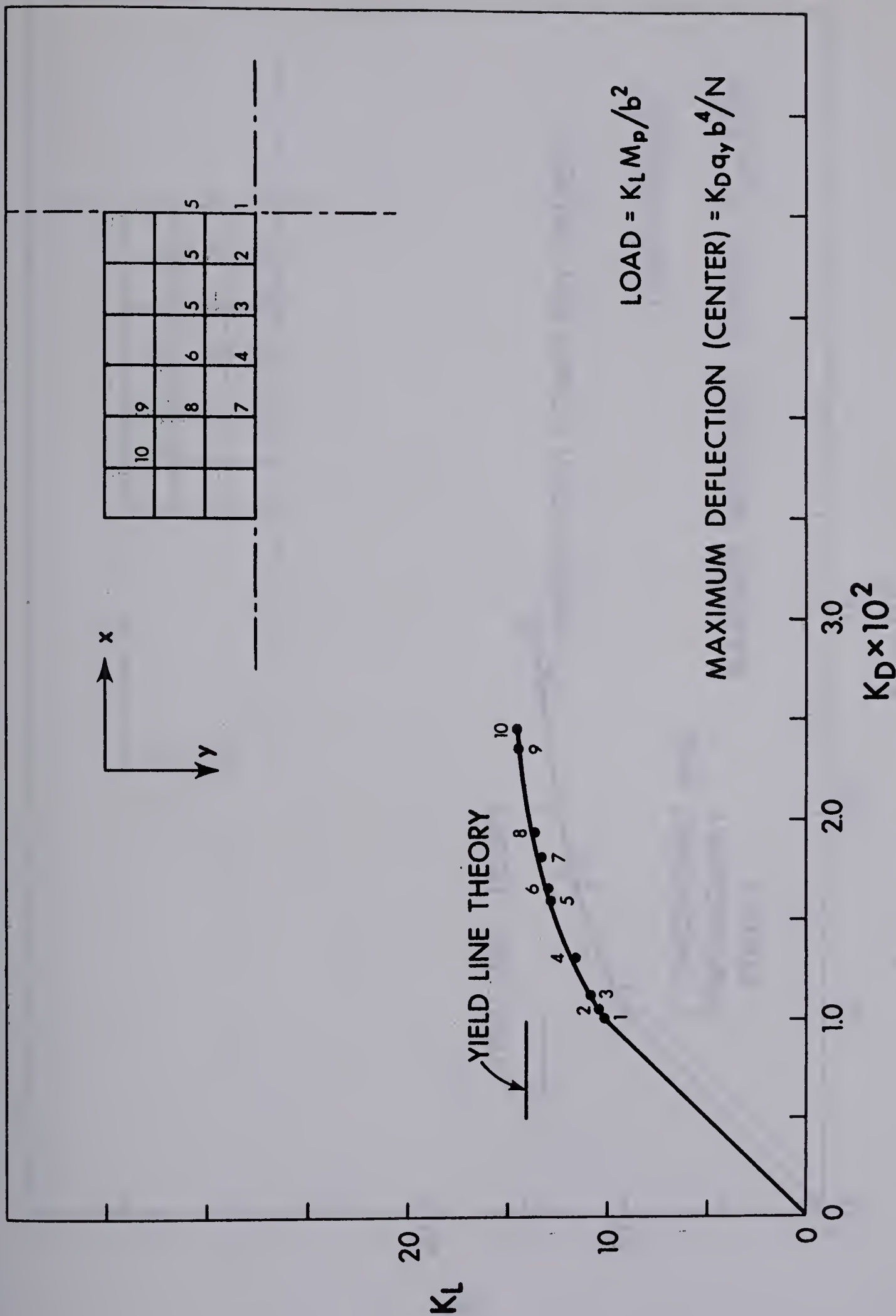


FIGURE 5.3 LOAD-MAXIMUM DEFLECTION CHARACTERISTICS OF SIMPLY SUPPORTED PLATE, $\frac{b}{a} = 0.5$, $\mu = 0.2$, UNIFORM LOAD

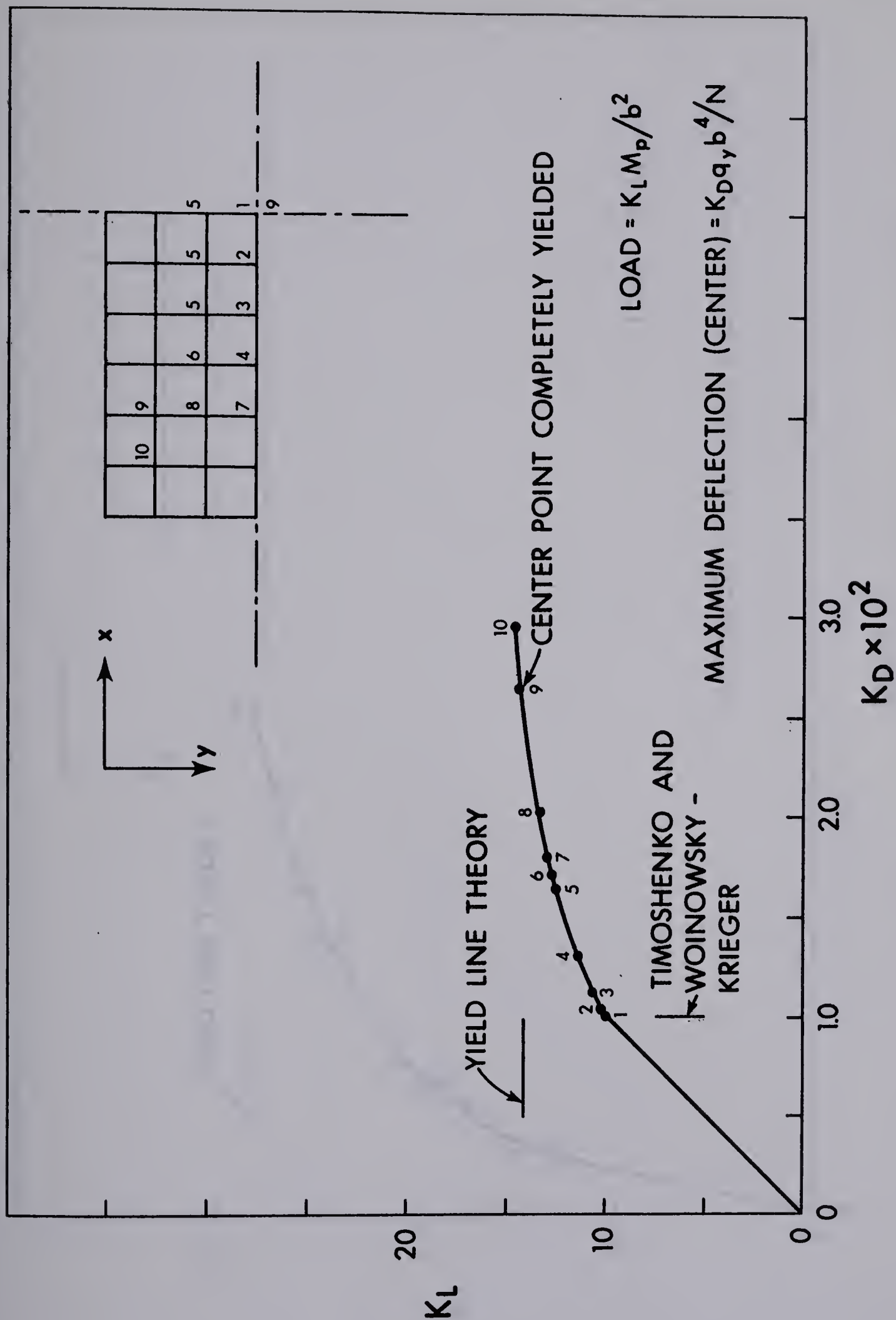


FIGURE 5.4 LOAD-MAXIMUM DEFLECTION CHARACTERISTICS OF SIMPLY SUPPORTED PLATE, $\frac{b}{a} = 0.5$, $\mu = 0.3$, UNIFORM LOAD

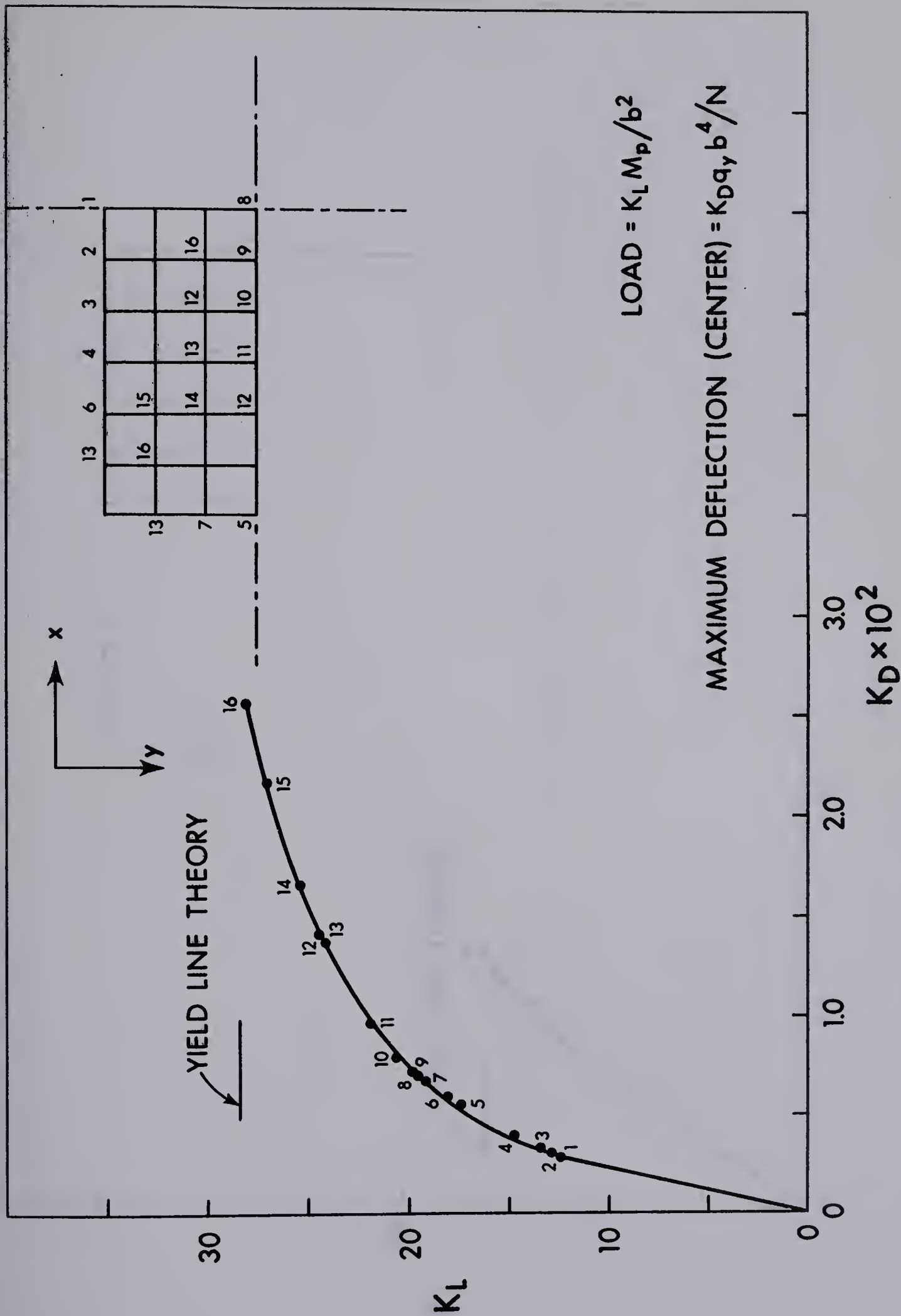


FIGURE 5.5 LOAD-MAXIMUM DEFLECTION CHARACTERISTICS OF FIXED
EDGE PLATE, $\frac{b}{a} = 0.5$, $\mu = 0$, UNIFORM LOAD

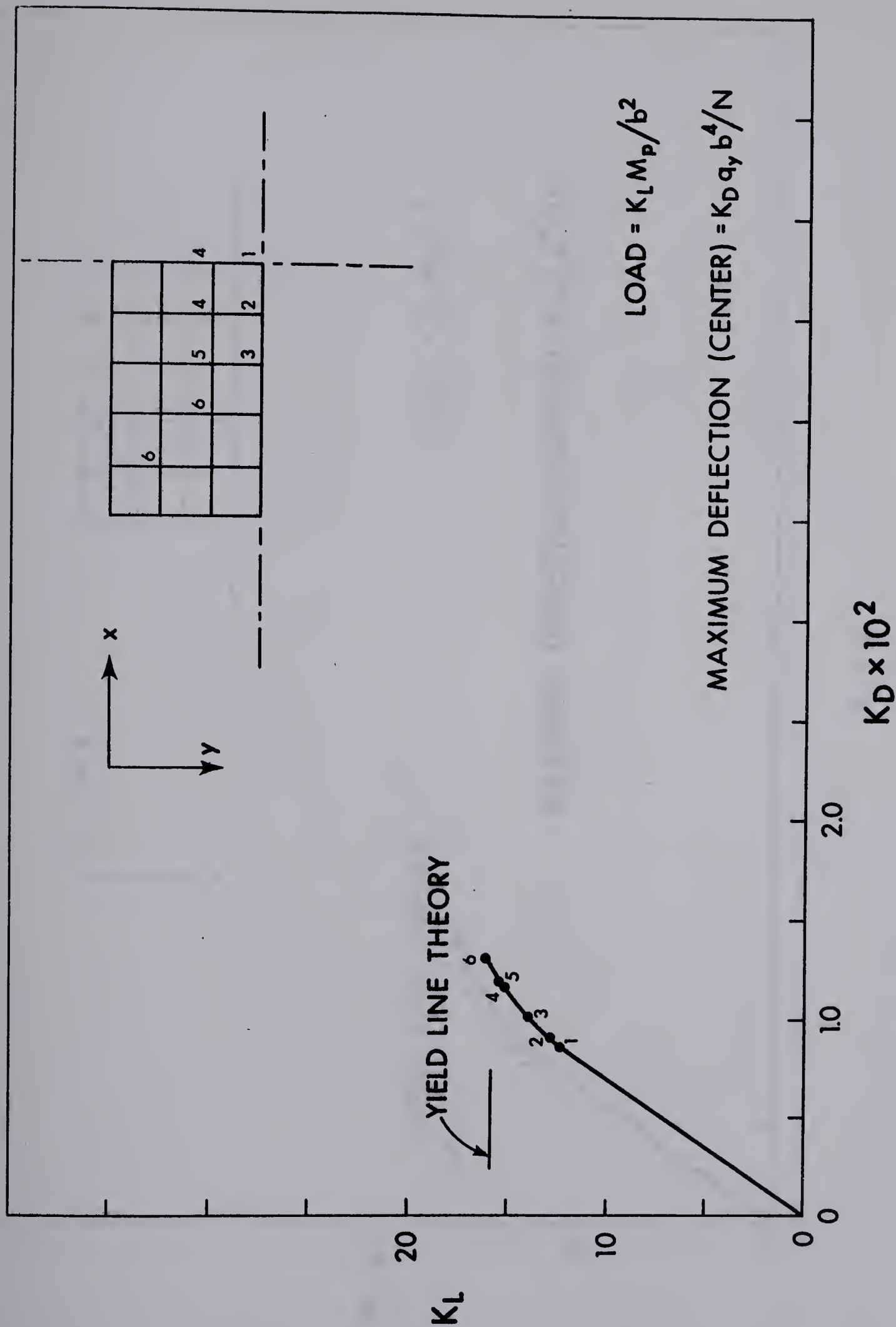


FIGURE 5.6 LOAD-MAXIMUM DEFLECTION CHARACTERISTICS OF SIMPLY SUPPORTED PLATE, $\frac{b}{a} = 0.6$, $\mu = 0$, UNIFORM LOAD

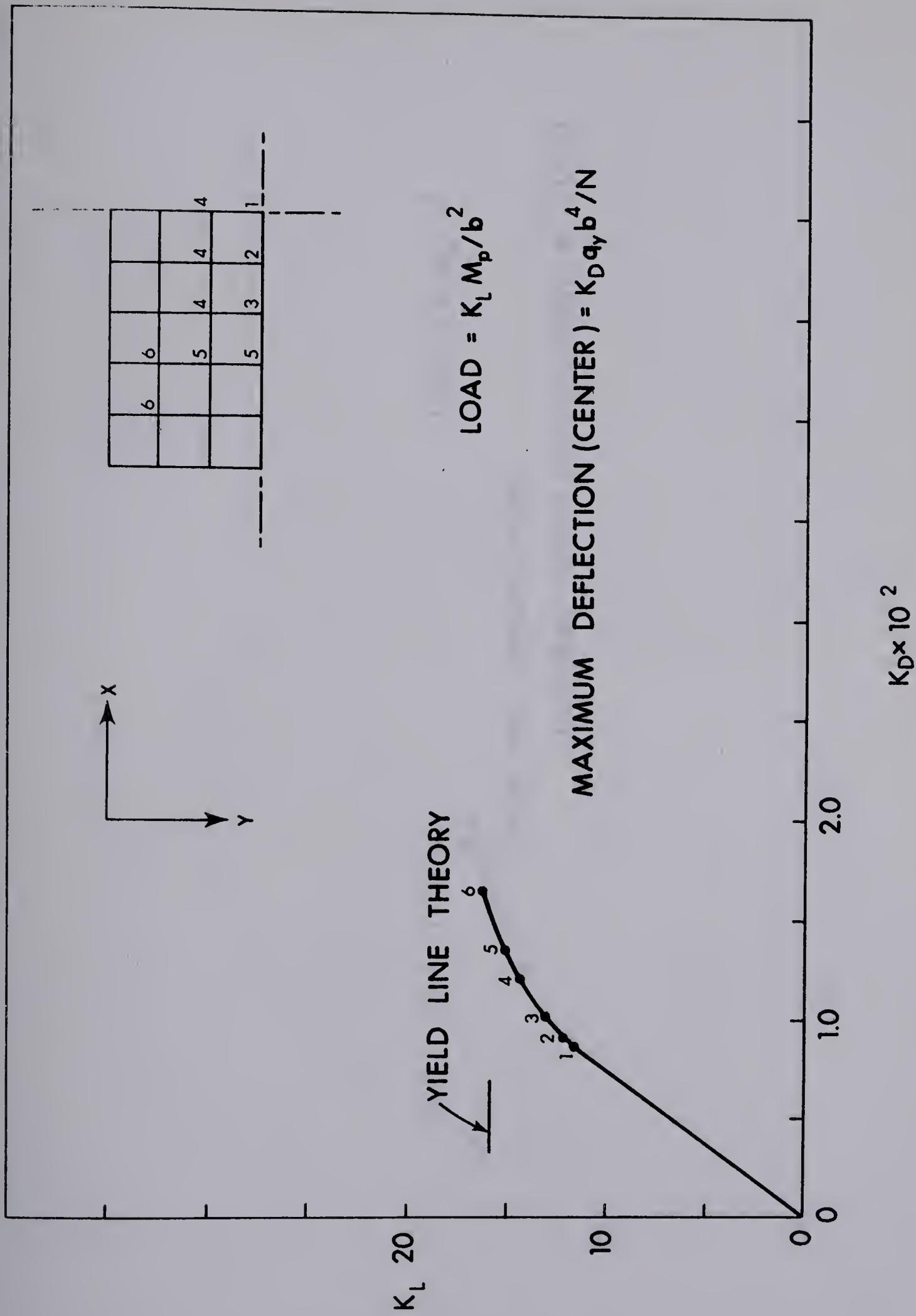


FIGURE 5.8 LOAD-MAXIMUM DEFLECTION CHARACTERISTICS OF SIMPLY SUPPORTED PLATE, $\frac{b}{a} = 0.6$, $\mu = 0.2$, UNIFORM LOAD

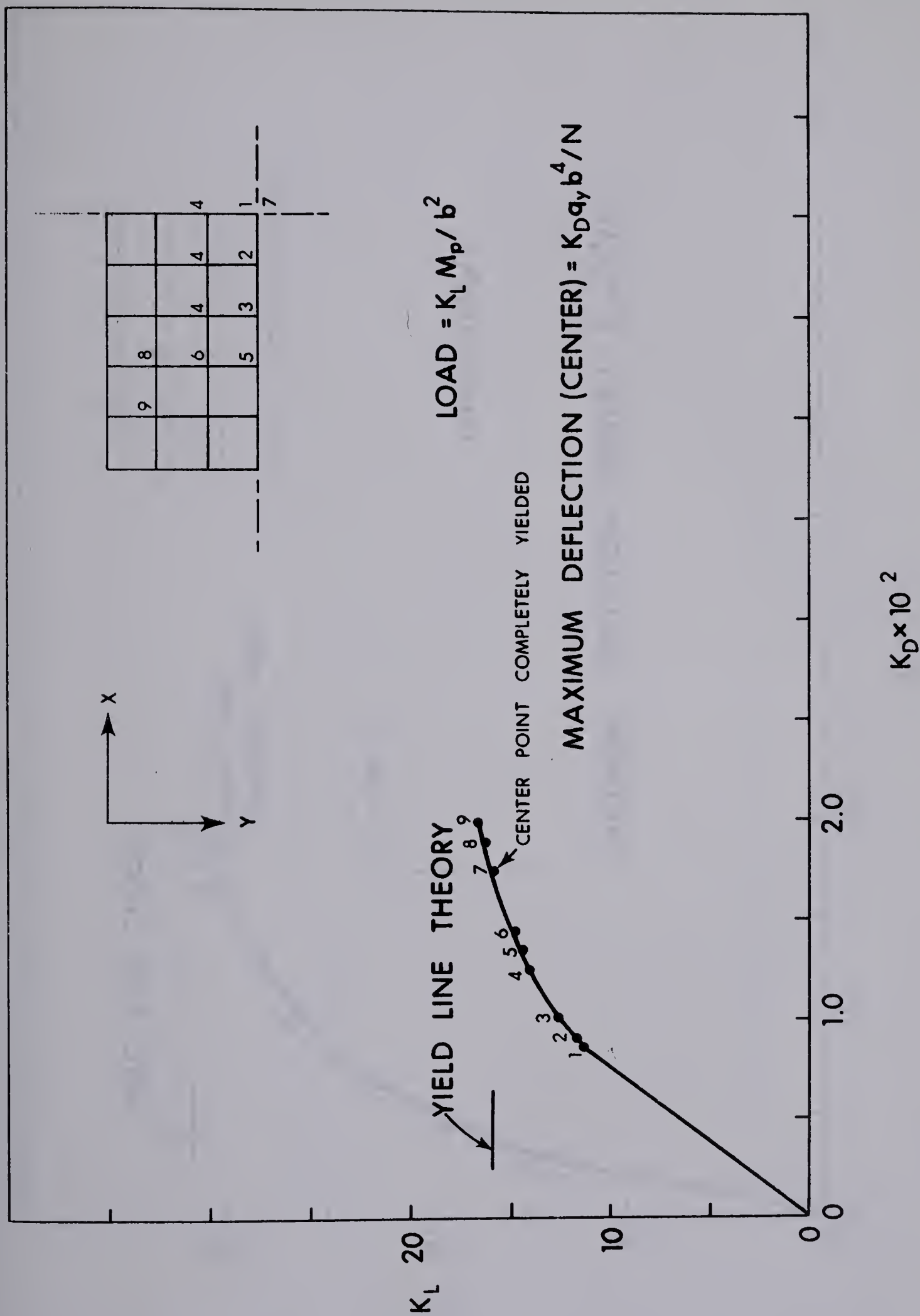


FIGURE 5.9 LOAD-MAXIMUM DEFLECTION CHARACTERISTICS OF SIMPLY SUPPORTED PLATE, $\frac{b}{a} = 0.6$, $\mu = 0.3$, UNIFORM LOAD

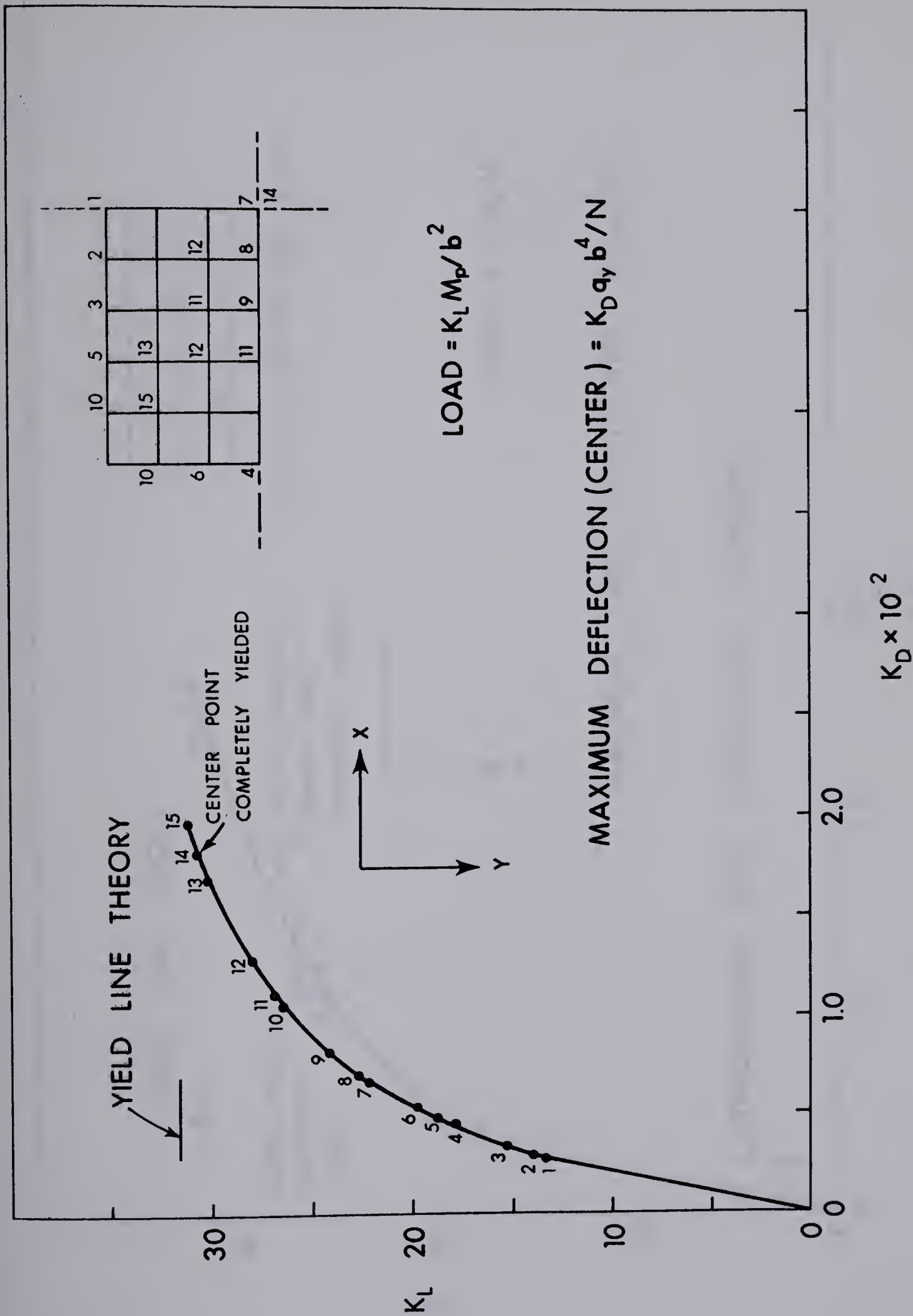


FIGURE 5.10 LOAD-MAXIMUM DEFLECTION CHARACTERISTICS OF FIXED
EDGE PLATE, $\frac{b}{a} = 0.6$, $\mu = 0$, UNIFORM LOAD

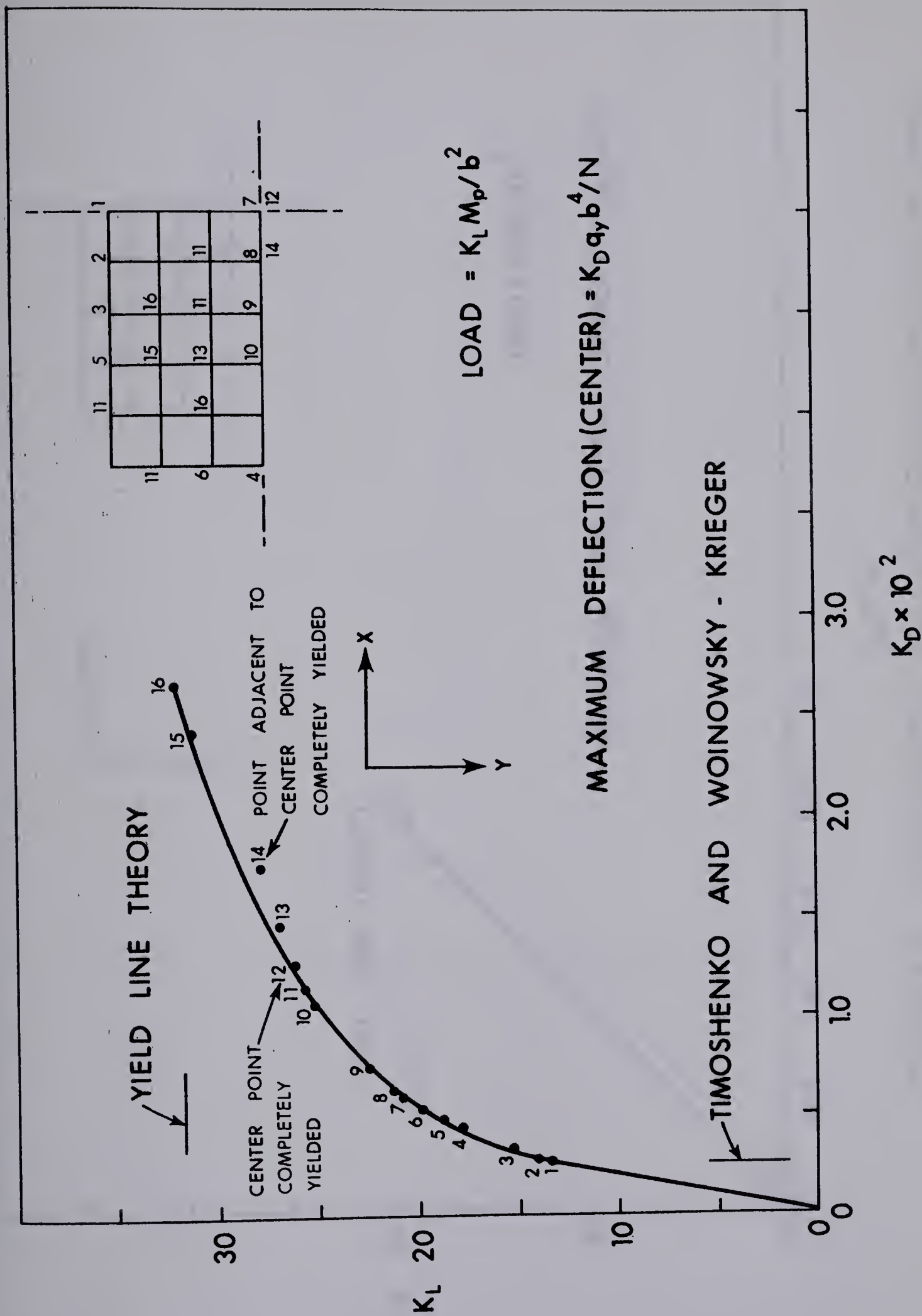


FIGURE 5.11 LOAD-MAXIMUM DEFLECTION CHARACTERISTICS OF FIXED EDGE PLATE, $\frac{b}{a} = 0.6$, $\mu = 0$, UNIFORM LOAD

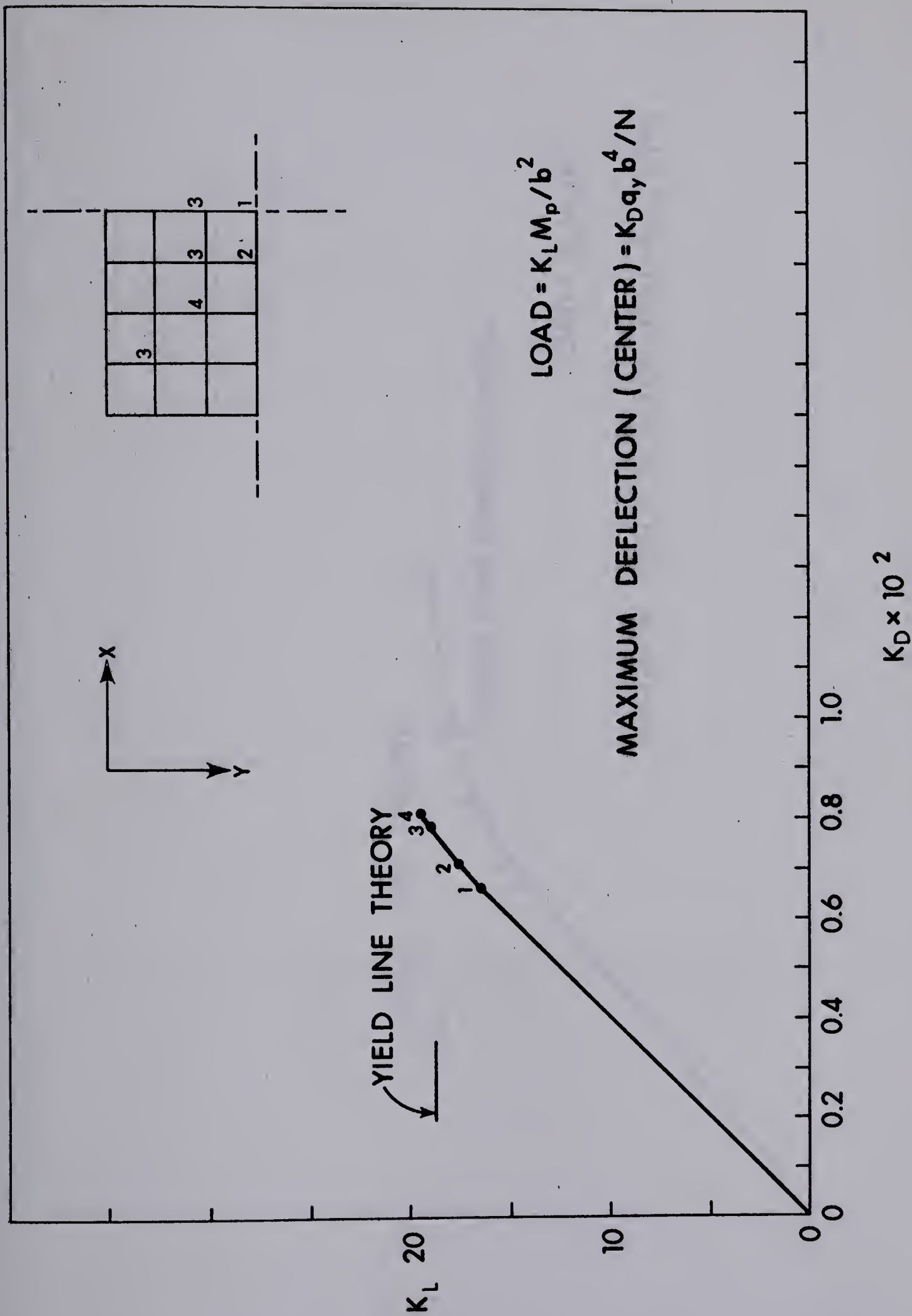


FIGURE 5.12 LOAD-MAXIMUM DEFLECTION CHARACTERISTICS OF SIMPLY SUPPORTED PLATE, $\frac{b}{a} = 0.75$, $\mu = 0$, UNIFORM LOAD

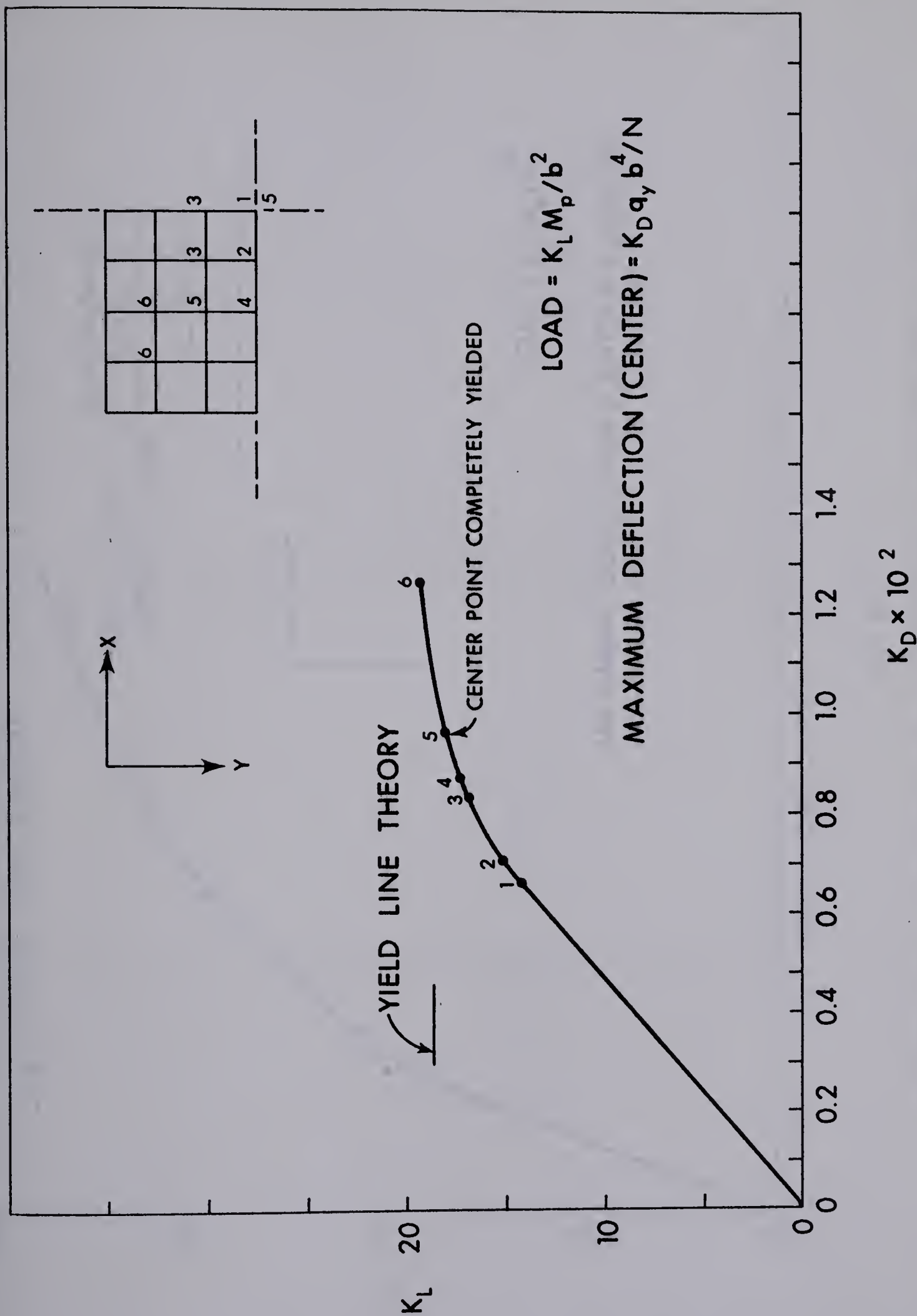


FIGURE 5.13 LOAD-MAXIMUM DEFLECTION CHARACTERISTICS OF SIMPLY SUPPORTED PLATE, $\frac{b}{a} = 0.75$, $\mu = 0.3$, UNIFORM LOAD

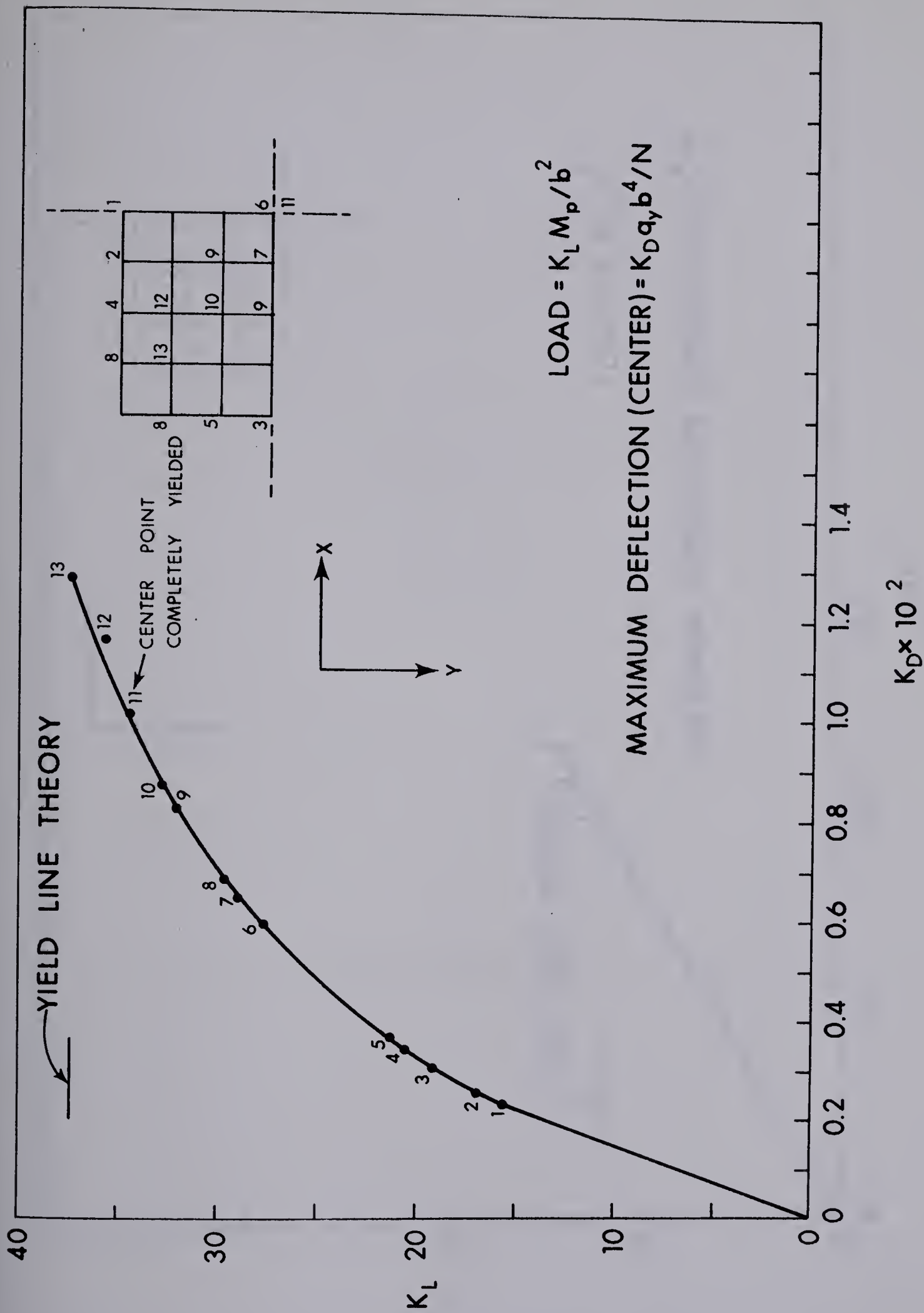


FIGURE 5.14 LOAD-MAXIMUM DEFLECTION CHARACTERISTICS OF FIXED
EDGE PLATE, $\frac{b}{a} = 0.75$, $\mu = 0$, UNIFORM LOAD

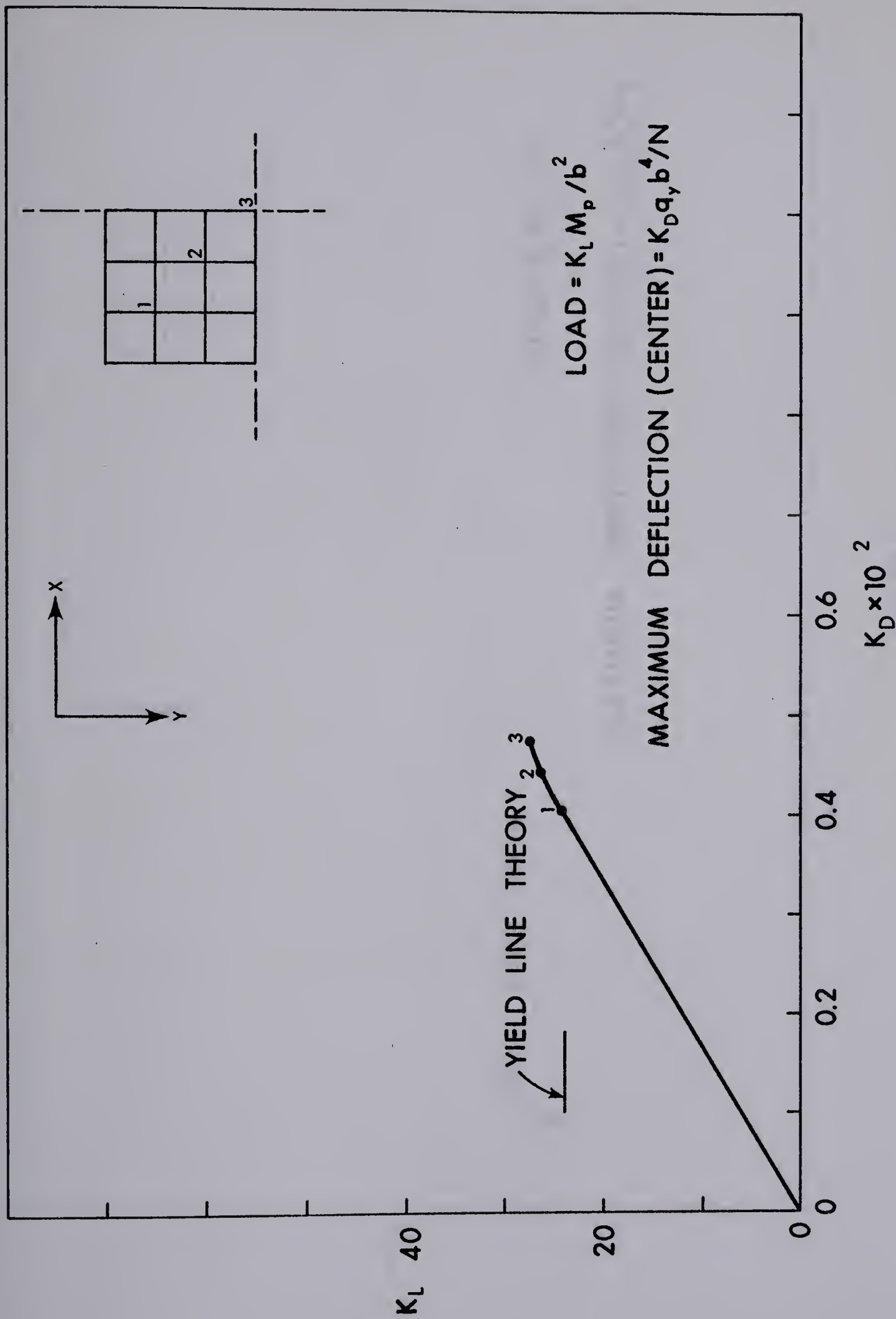


FIGURE 5.15 LOAD-MAXIMUM DEFLECTION CHARACTERISTICS OF SIMPLY SUPPORTED PLATE, $\frac{b}{a} = 1.0$, $\mu = 0$, UNIFORM LOAD

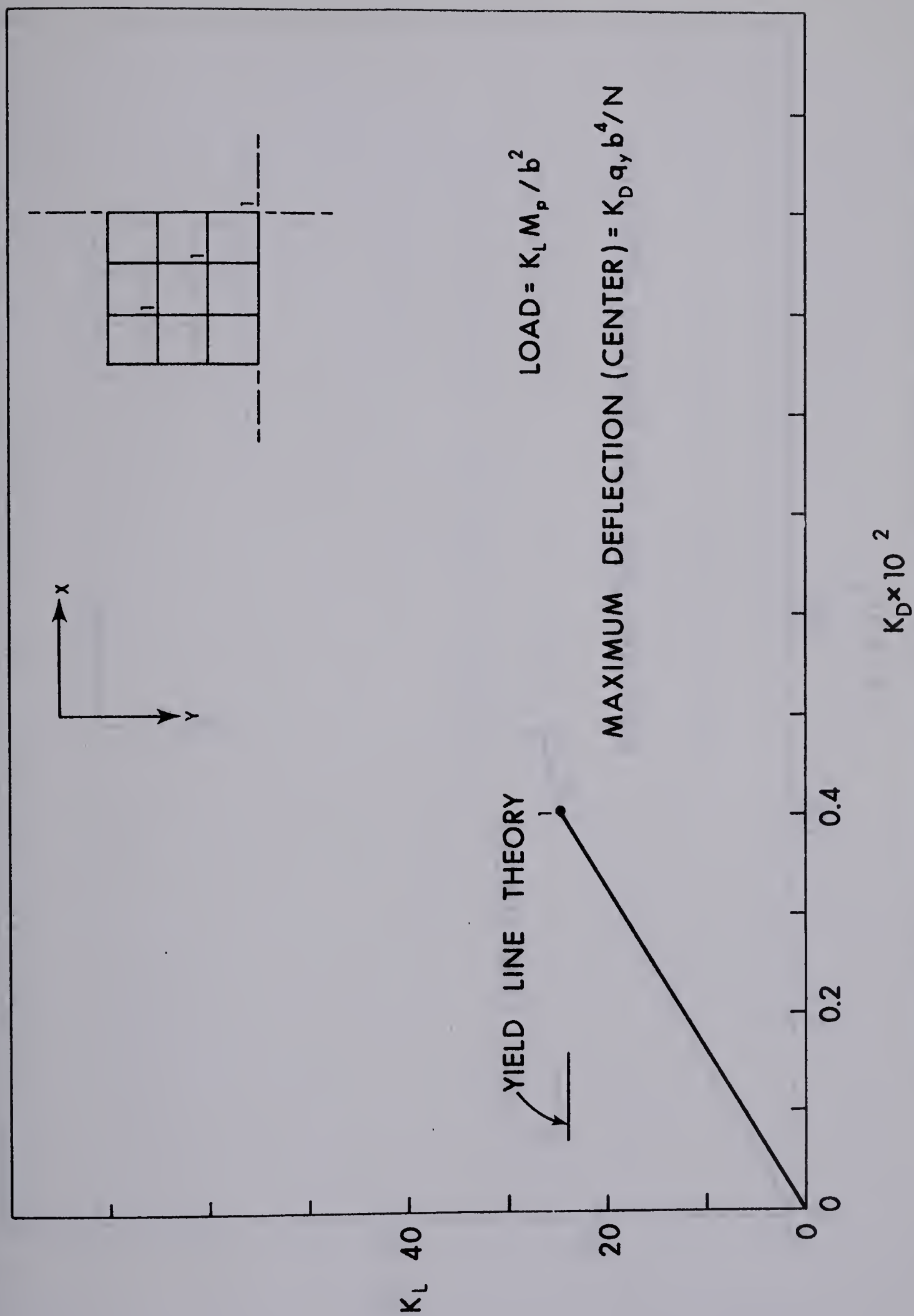


FIGURE 5.16 LOAD-MAXIMUM DEFLECTION CHARACTERISTICS OF SIMPLY SUPPORTED PLATE, $\frac{b}{a} = 1.0$, $\mu = 0.1$, UNIFORM LOAD

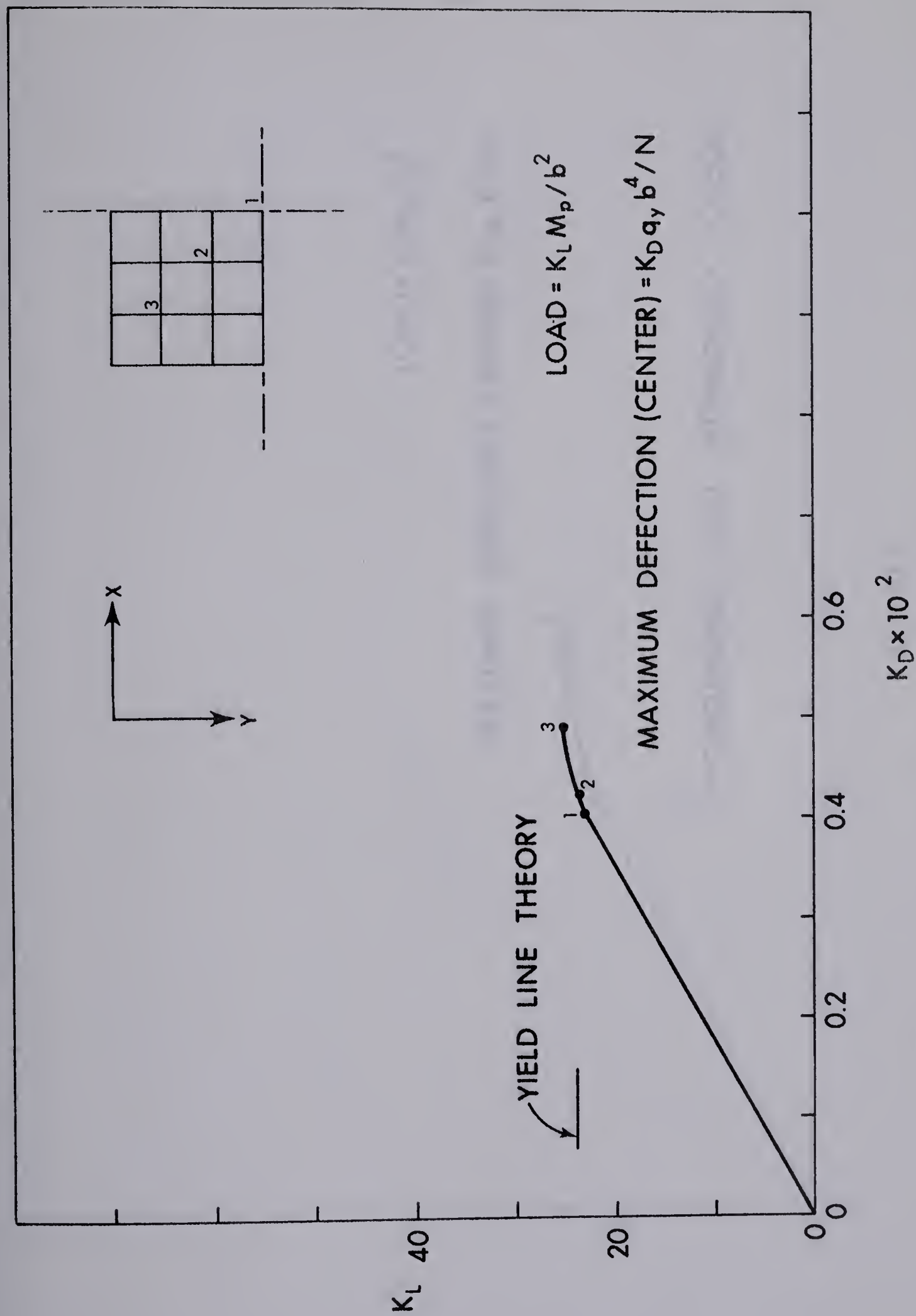


FIGURE 5.17 LOAD-MAXIMUM DEFLECTION CHARACTERISTICS OF SIMPLY SUPPORTED PLATE, $\frac{b}{a} = 1.0$, $\mu = 0.2$, UNIFORM LOAD

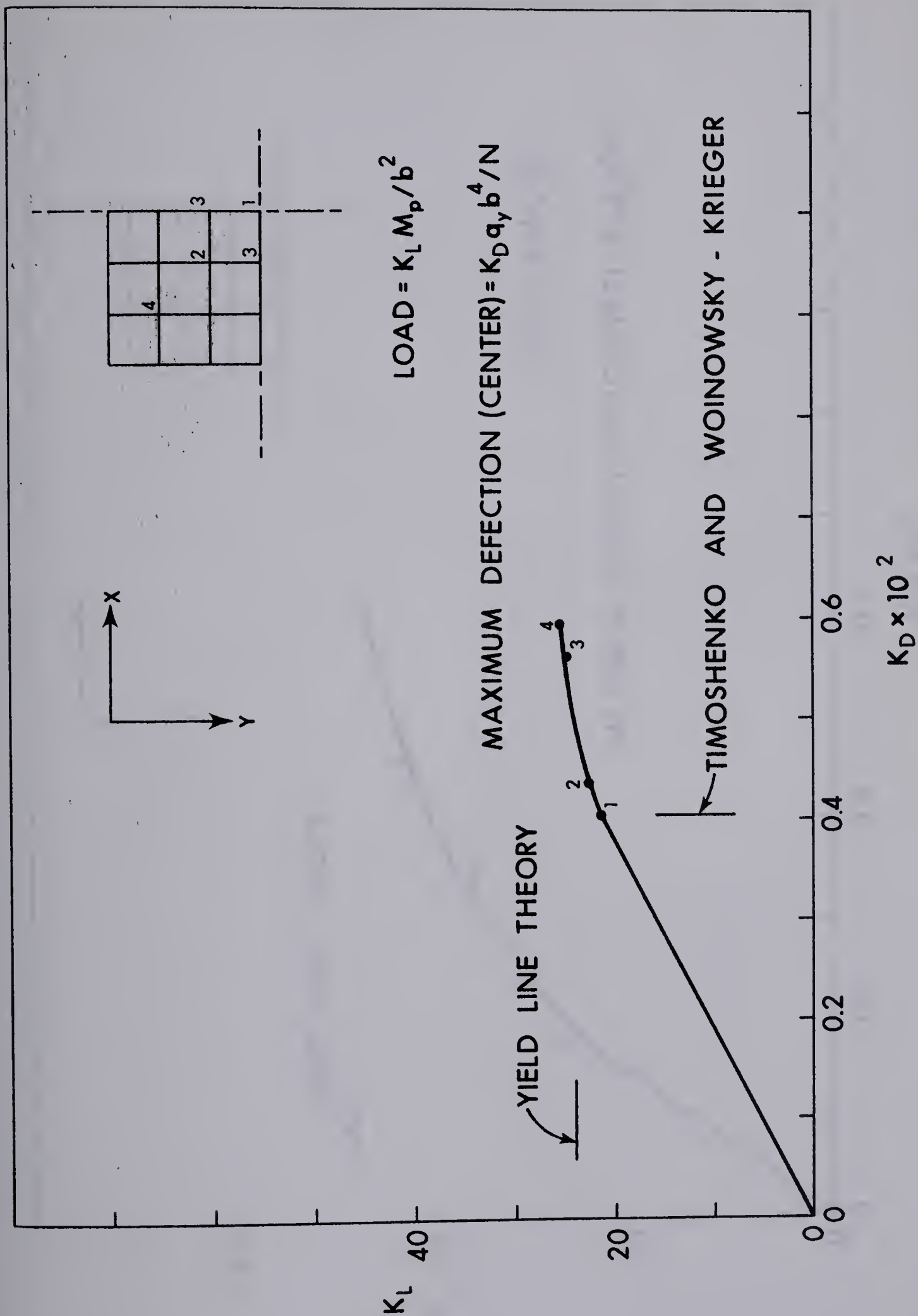


FIGURE 5.18 LOAD-MAXIMUM DEFLECTION CHARACTERISTICS OF SIMPLY SUPPORTED PLATE, $\frac{b}{a} = 1.0$, $\mu = 0.3$, UNIFORM LOAD

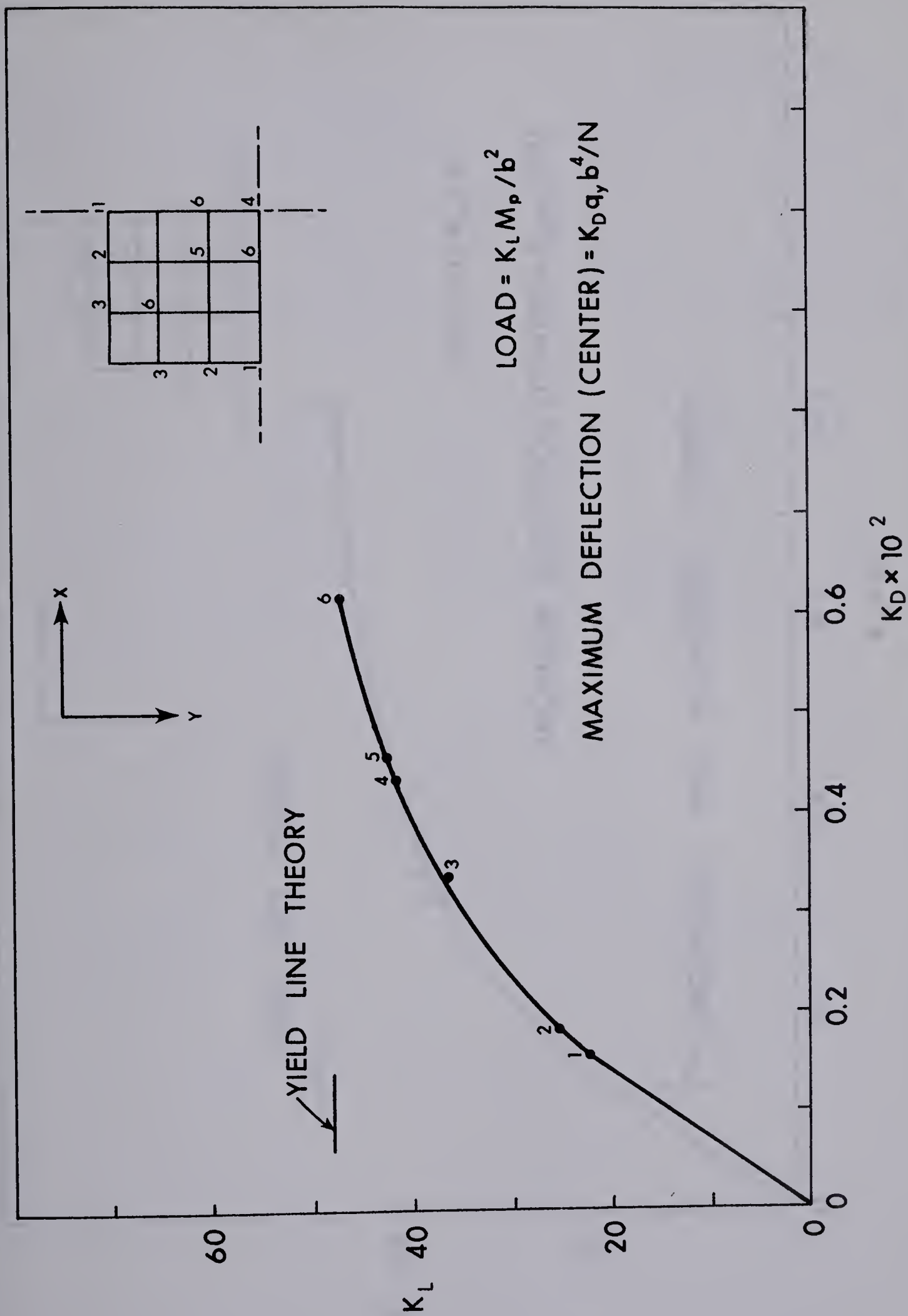


FIGURE 5.19 LOAD-MAXIMUM DEFLECTION CHARACTERISTICS OF FIXED
EDGE PLATE, $\frac{b}{a} = 1.0$, $\mu = 0$, UNIFORM LOAD

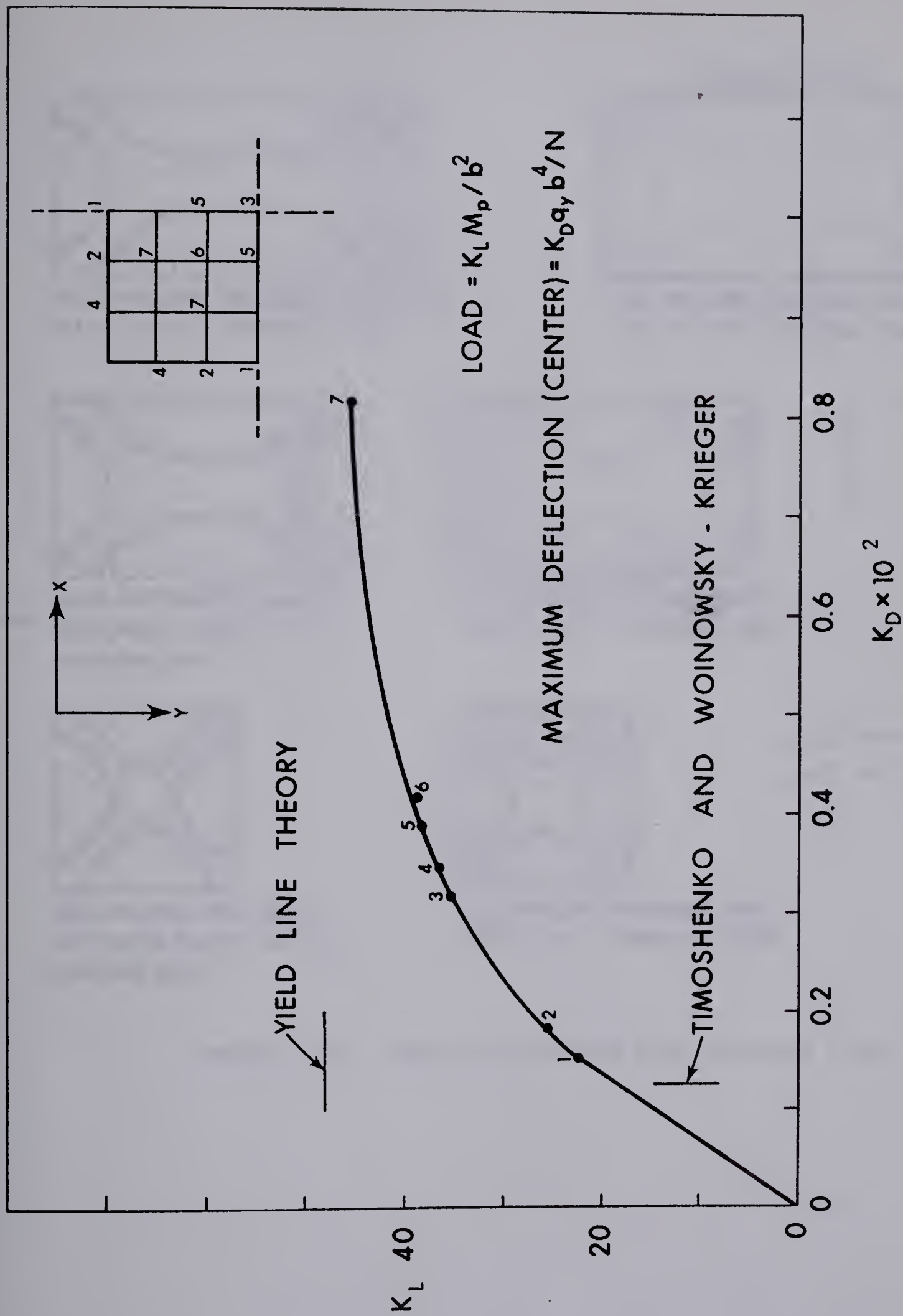
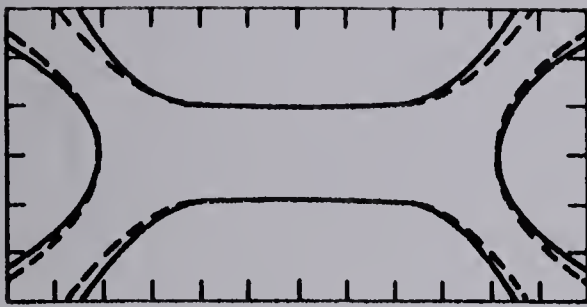
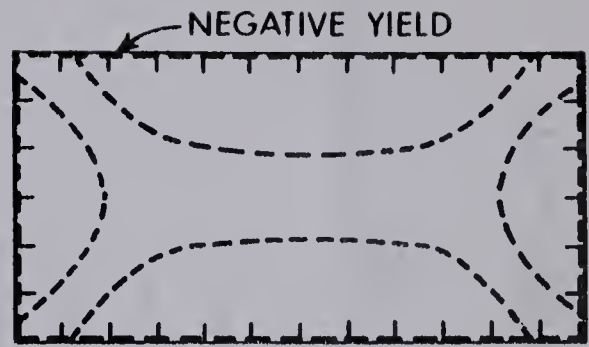


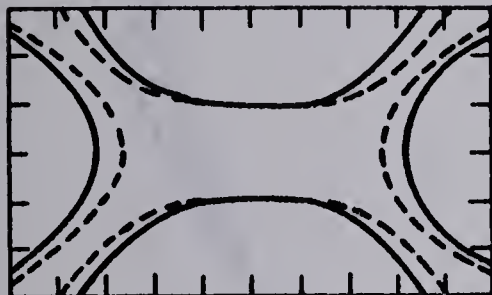
FIGURE 5.20 LOAD-MAXIMUM DEFLECTION CHARACTERISTICS OF FIXED EDGE PLATE, $\frac{b}{a} = 1.0$, $\mu = 0.3$, UNIFORM LOAD



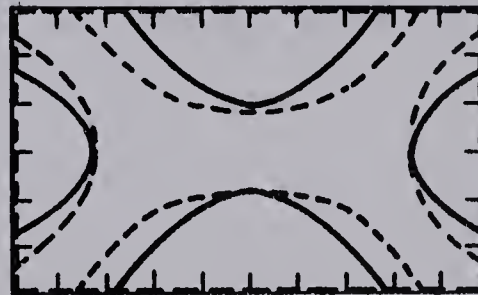
YIELD PATTERN FOR SIMPLY SUPPORTED PLATE, $b/a=0.5$, UNIFORM LOAD



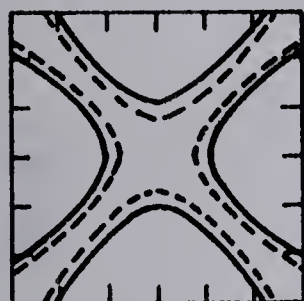
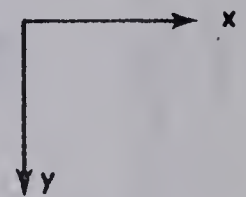
YIELD PATTERN FOR FIXED EDGE PLATE, $b/a=0.5$, UNIFORM LOAD



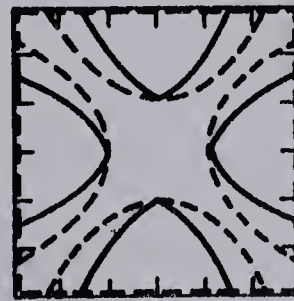
YIELD PATTERN FOR SIMPLY SUPPORTED PLATE, $b/a=0.6$, UNIFORM LOAD



YIELD PATTERN FOR FIXED EDGE PLATE, $b/a=0.6$, UNIFORM LOAD



YIELD PATTERN FOR SIMPLY SUPPORTED PLATE, $b/a=1.0$, UNIFORM LOAD



YIELD PATTERN FOR FIXED EDGE PLATE, $b/a=1.0$, UNIFORM LOAD

$\mu=0.3$ ———
 $\mu=0$ - - - - -

FIGURE 5.21 YIELD PATTERNS FOR UNIFORM LOAD

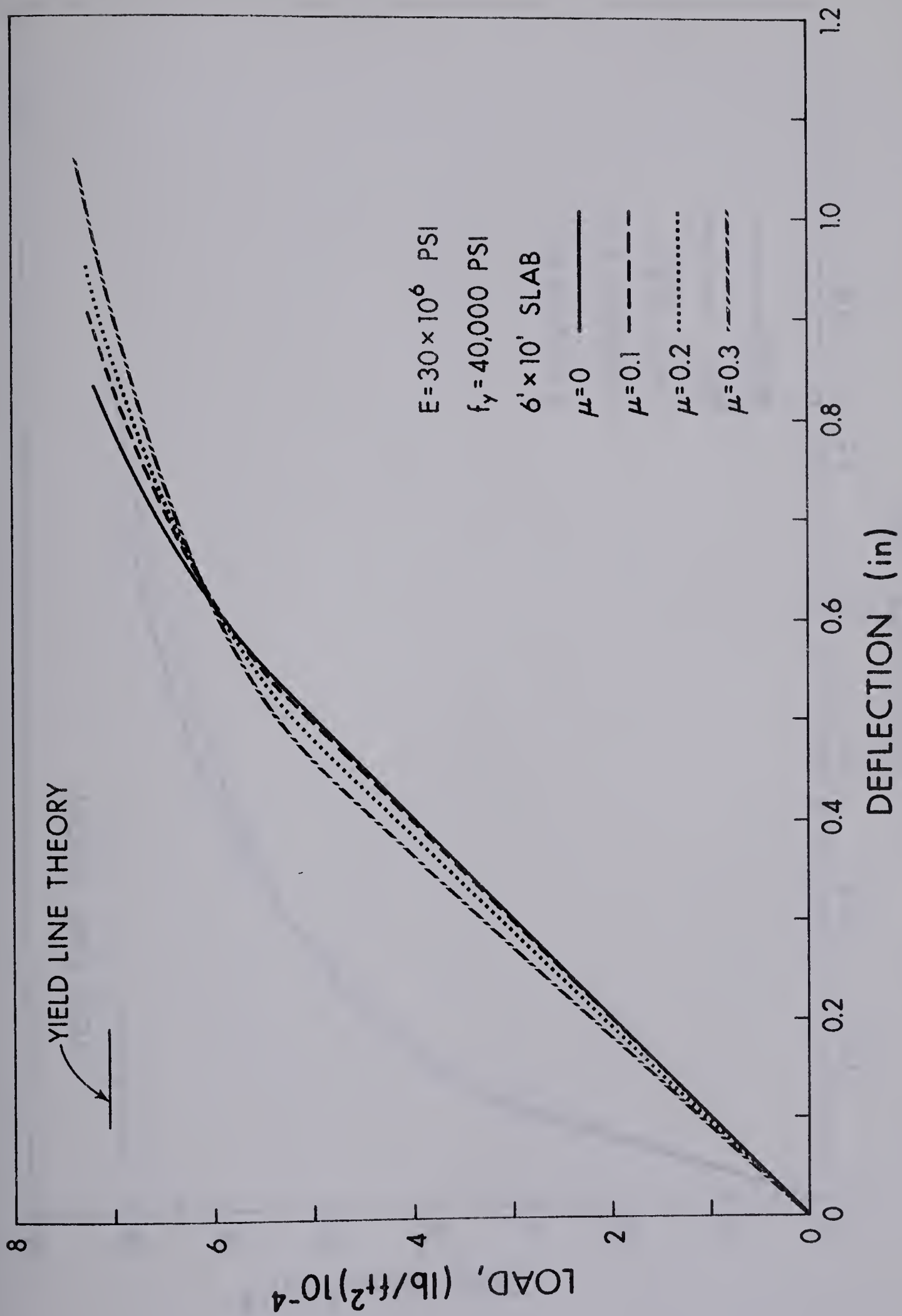


FIGURE 5.22 LOAD-DEFLECTION PLOT FOR SIMPLY SUPPORTED 4 IN. THICK ELASTO-PLASTIC PLATE, $\frac{b}{a} = 0.6$, UNIFORM LOAD

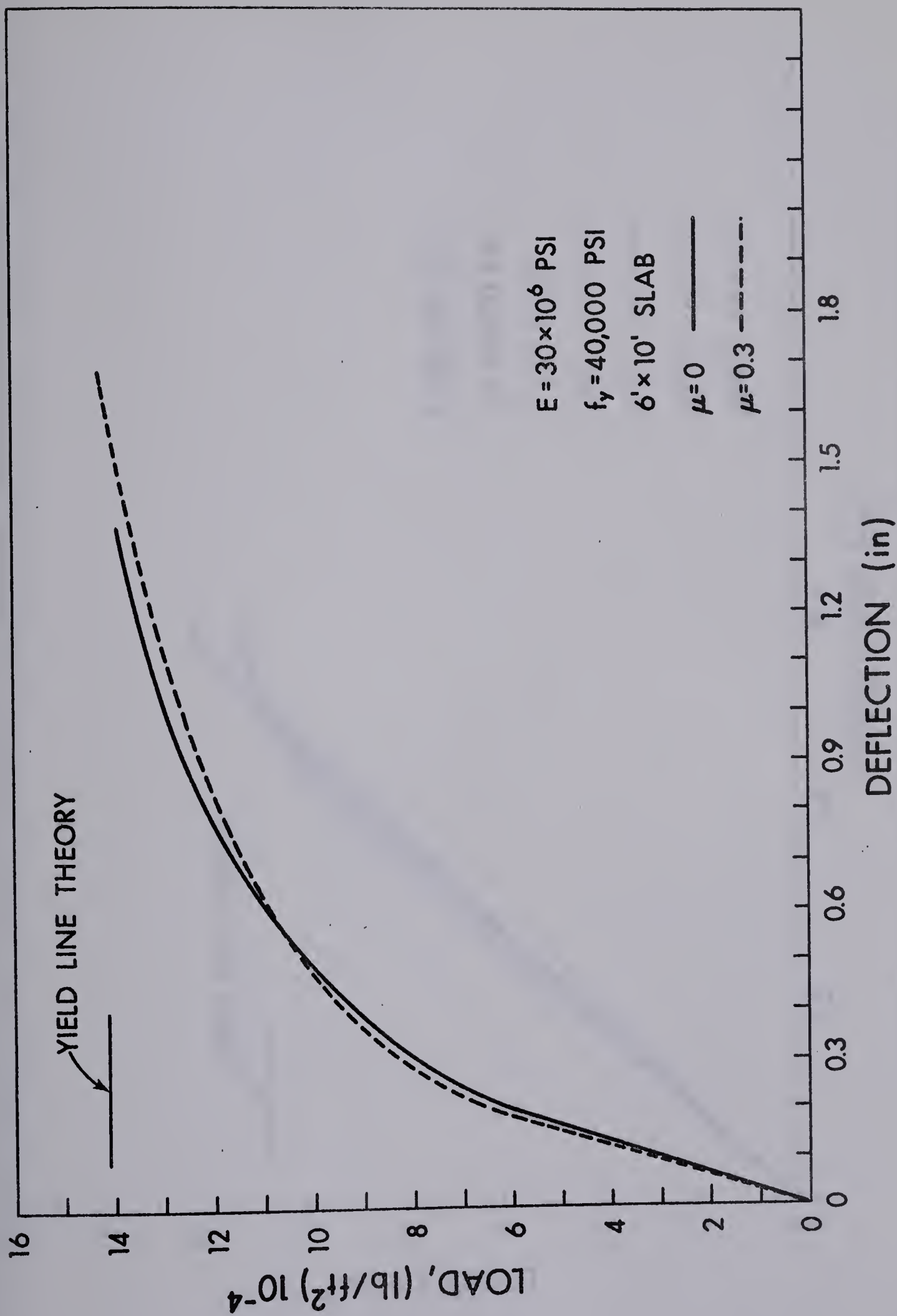


FIGURE 5.23 LOAD-DEFLECTION PLOT FOR FIXED EDGE 4 IN. THICK ELASTO-PLASTIC PLATE, $\frac{b}{a} = 0.6$, UNIFORM LOAD

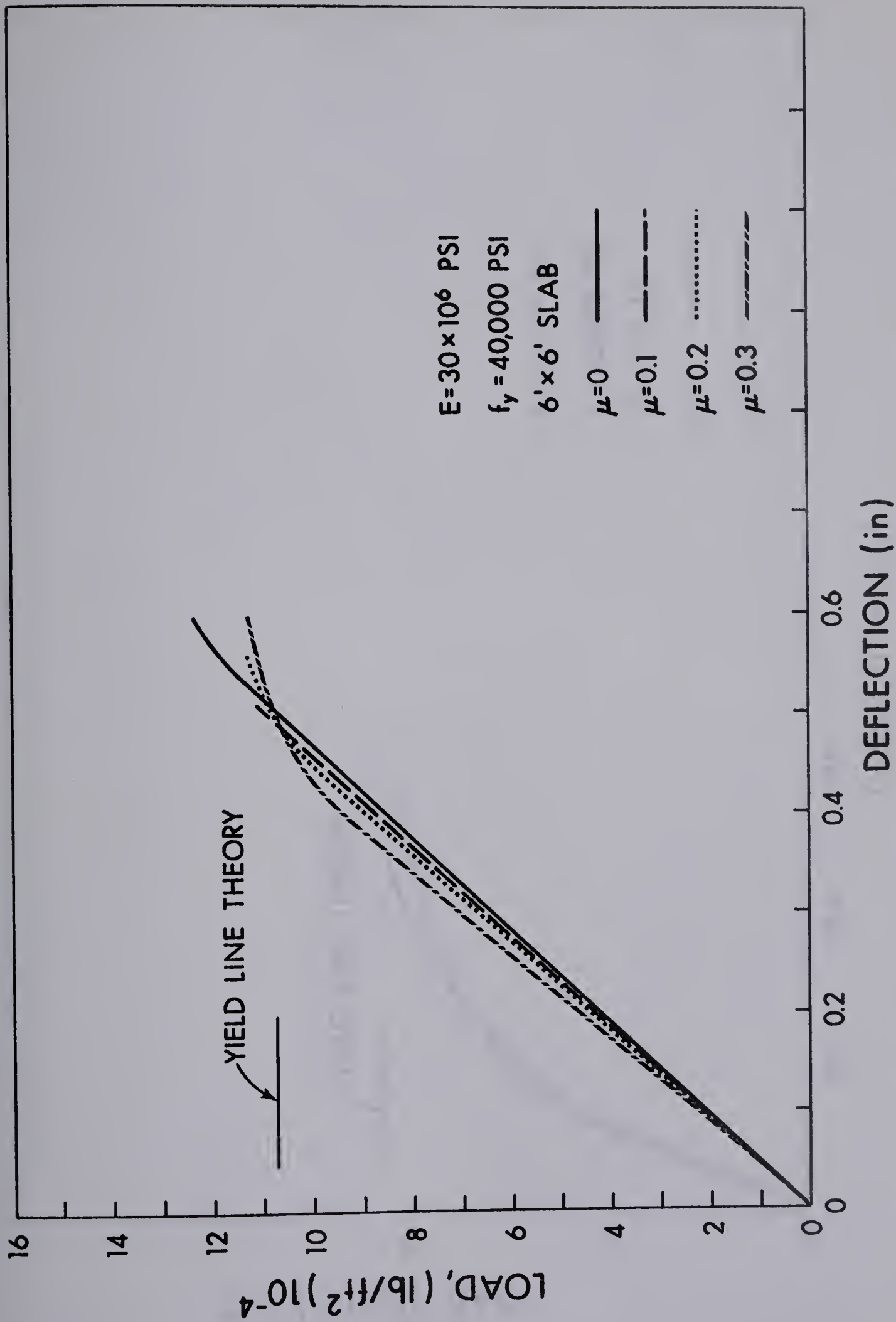


FIGURE 5.24 LOAD-DEFLECTION PLOT FOR SIMPLY SUPPORTED 4 IN. THICK ELASTO-PLASTIC PLATE, $\frac{b}{a} = 1.0$, UNIFORM LOAD

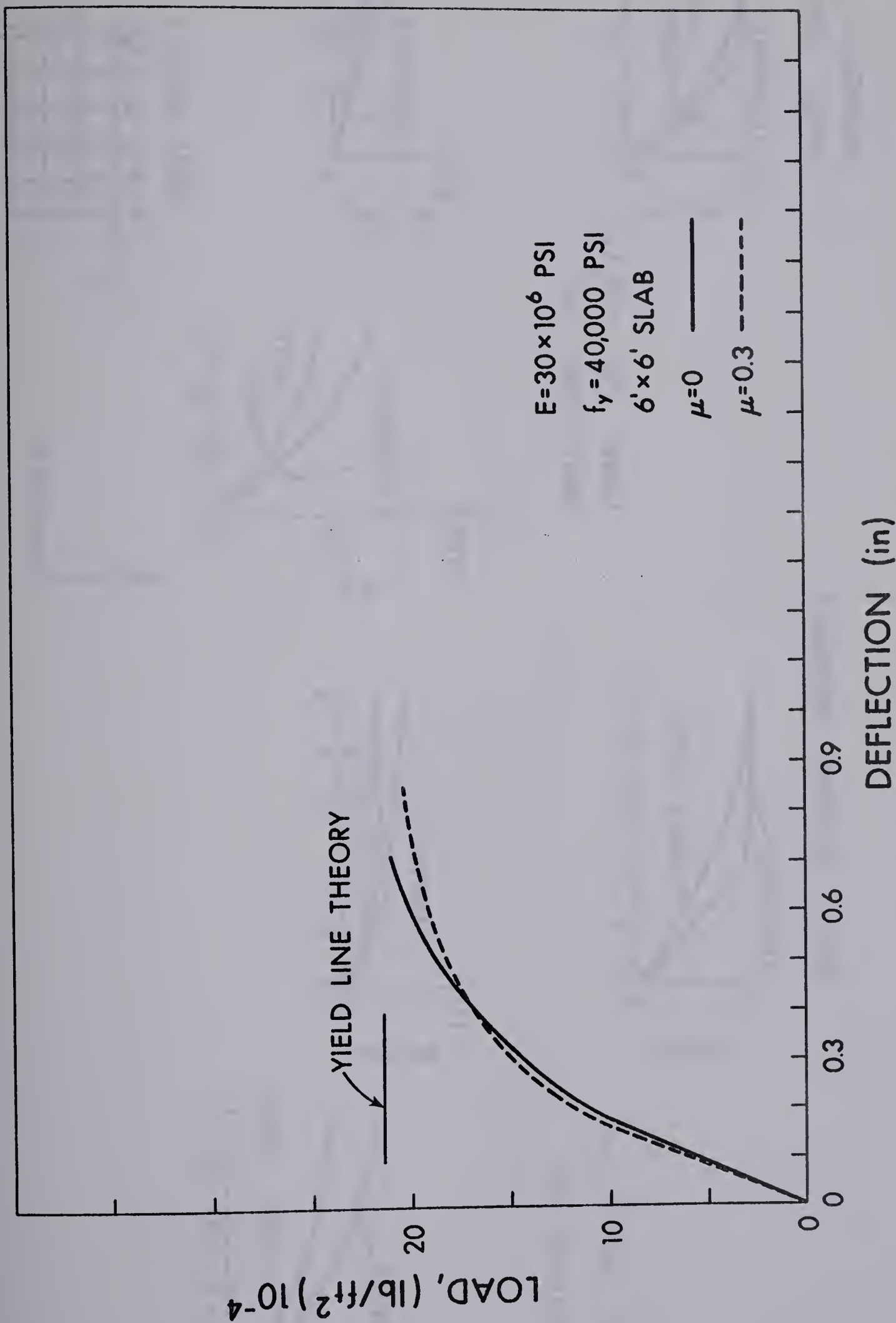


FIGURE 5.25 LOAD-DEFLECTION PLOT FOR FIXED EDGE 4 IN. THICK ELASTO-PLASTIC PLATE, $\frac{b}{a} = 1.0$, UNIFORM LOAD

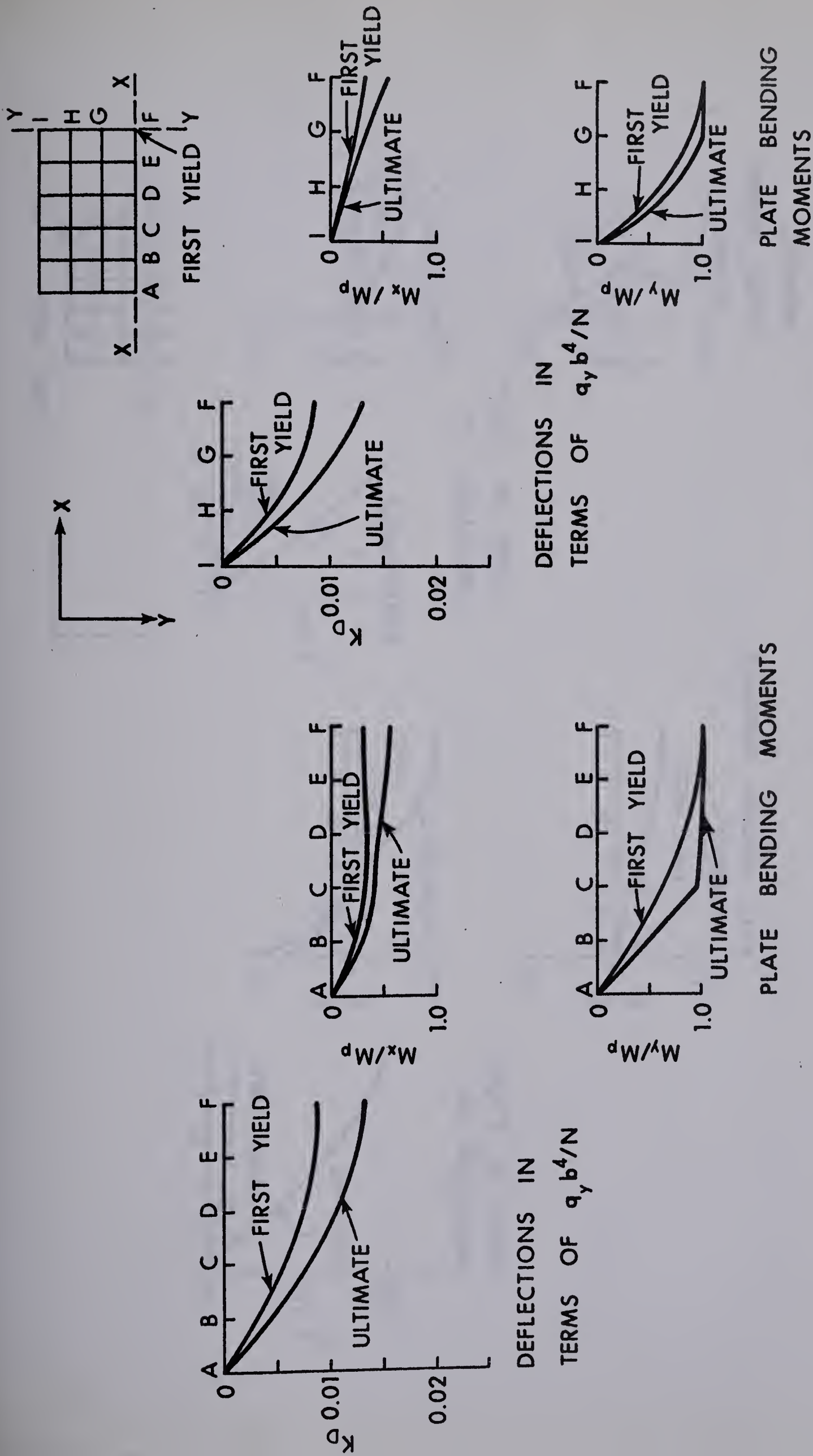


FIGURE 5.26 DEFLECTIONS AND BENDING MOMENTS ALONG LINES X-X AND Y-Y OF SIMPLY SUPPORTED PLATE, $\frac{b}{a} = 0.6$, $\mu = 0$, UNIFORM LOAD

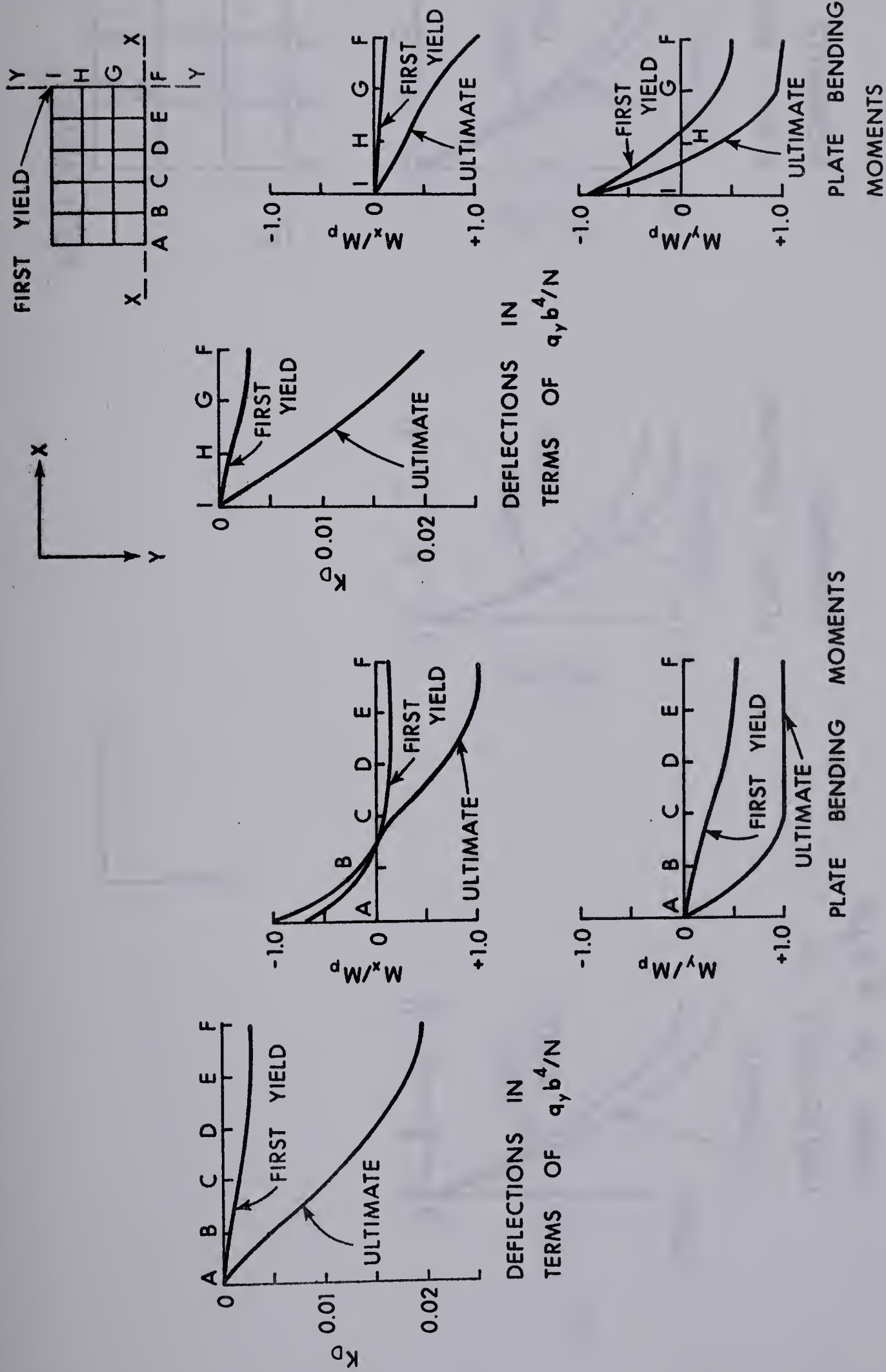
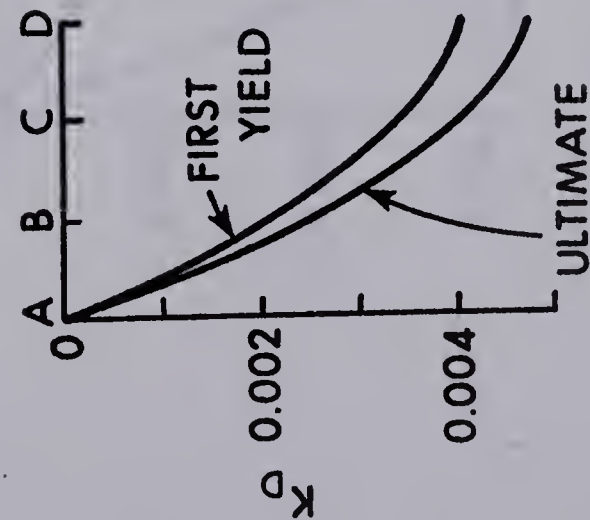
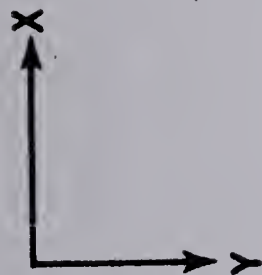
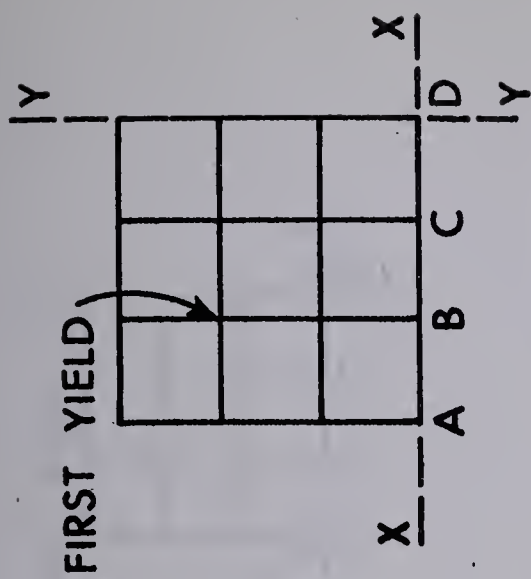


FIGURE 5.27 DEFLECTIONS AND BENDING MOMENTS ALONG LINES X-X AND Y-Y OF FIXED EDGE PLATE, $\frac{b}{a} = 0.6$, $\mu = 0$, UNIFORM LOAD



DEFLECTIONS IN
TERMS OF $q_y b^4/N$

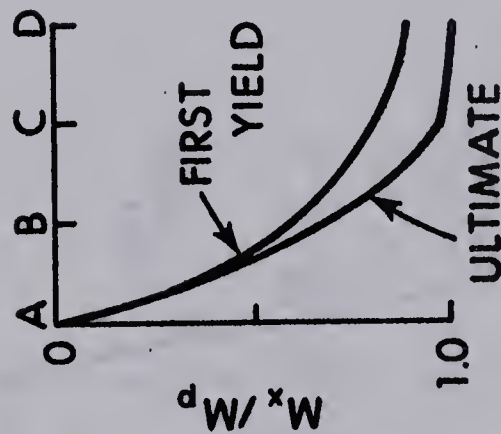


PLATE BENDING
MOMENTS

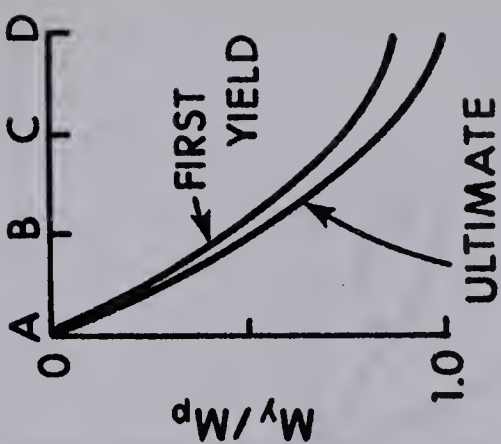


PLATE BENDING
MOMENTS

FIGURE 5.28 DEFLECTIONS AND BENDING MOMENTS ALONG LINE X-X OF
SIMPLY SUPPORTED PLATE, $\frac{b}{a} = 1.0$, $\mu = 0$, UNIFORM LOAD

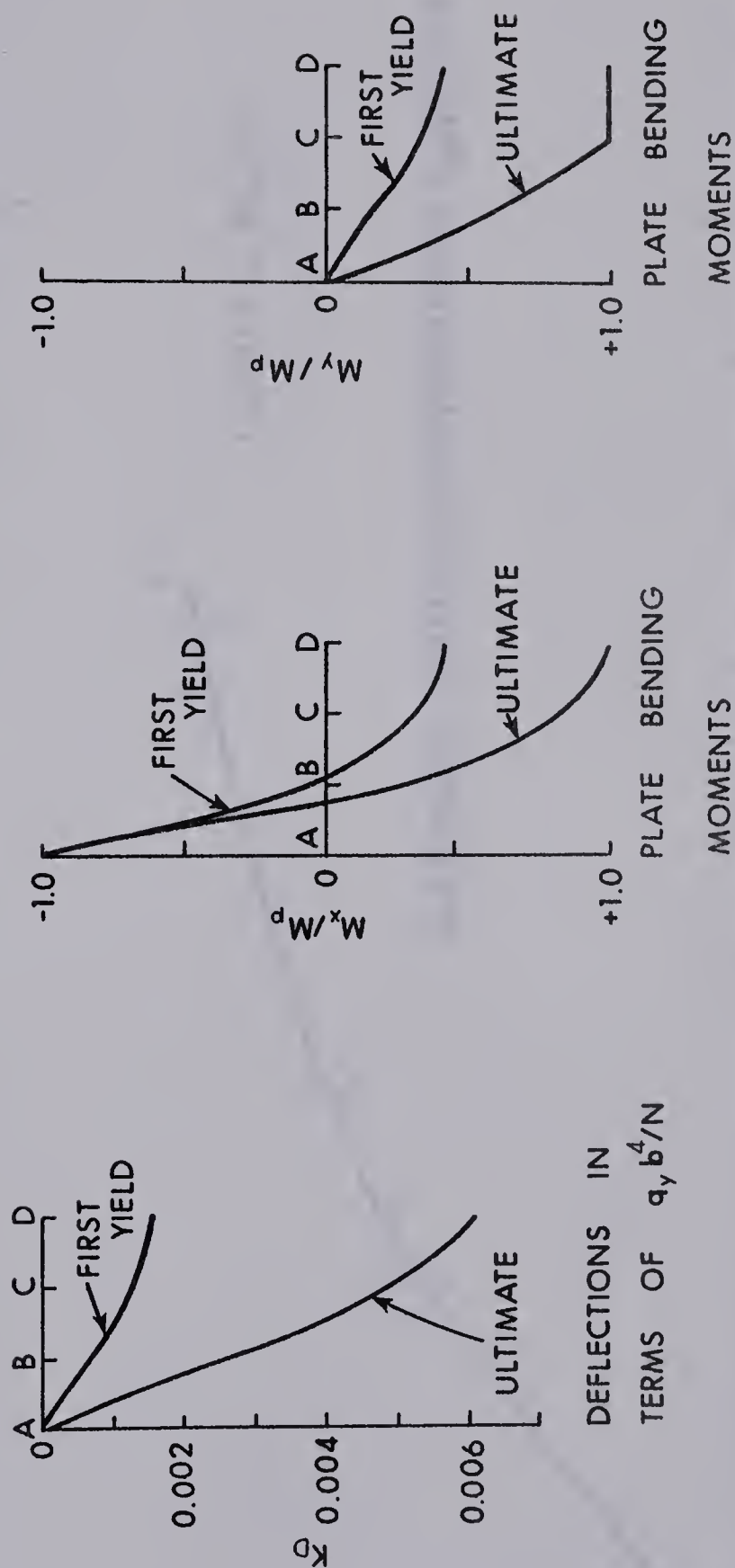
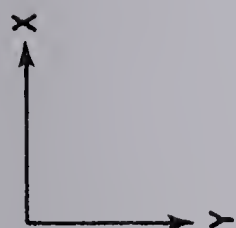
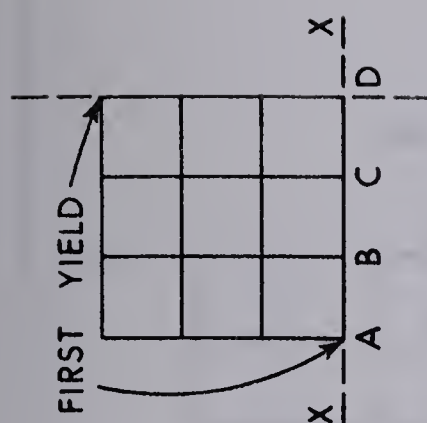


FIGURE 5.29 DEFLECTIONS AND BENDING MOMENTS ALONG LINE X-X OF
FIXED EDGE PLATE, $\frac{b}{a} = 1.0$, $\mu = 0$, UNIFORM LOAD

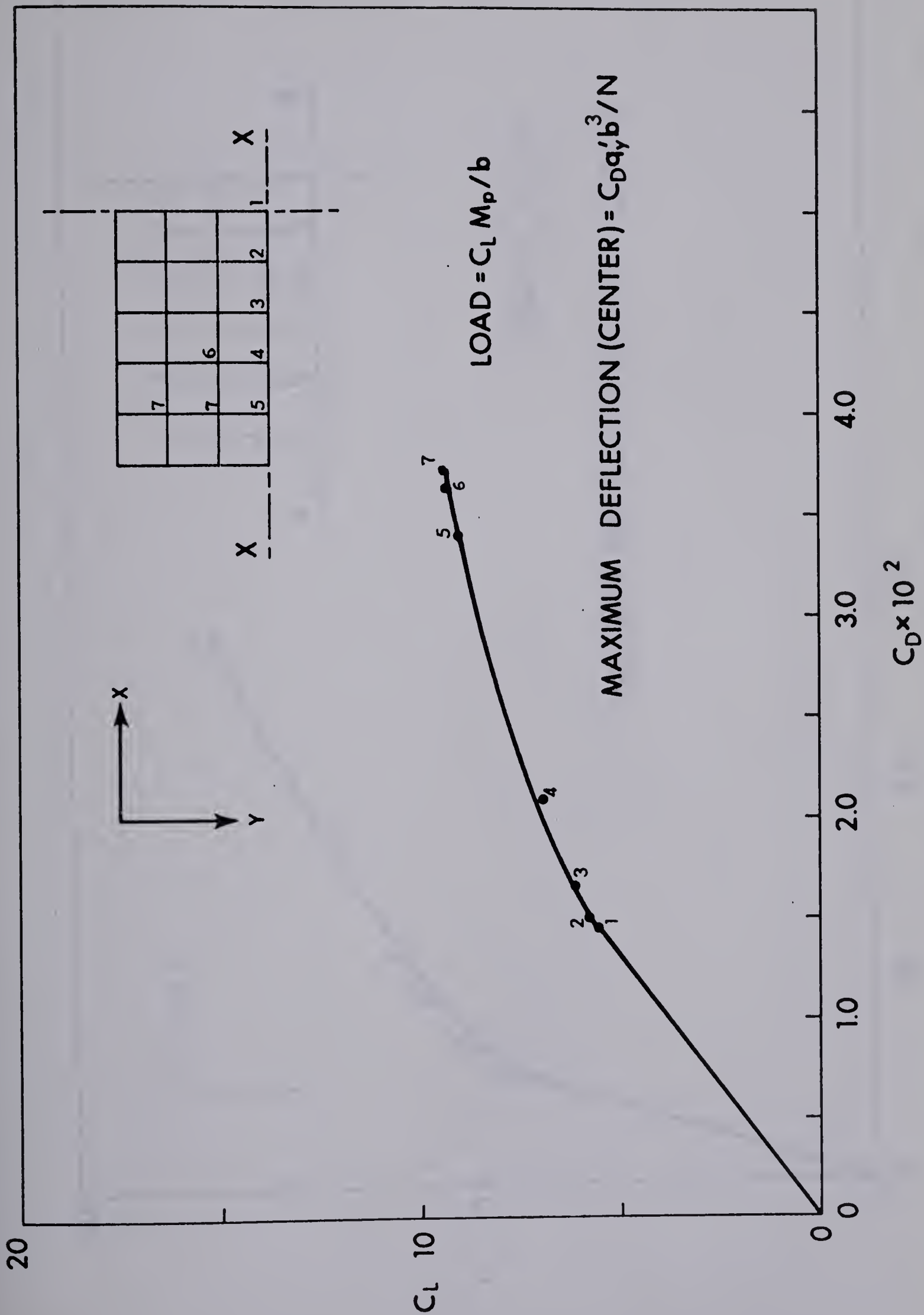


FIGURE 5.30 LOAD-MAXIMUM DEFLECTION CHARACTERISTICS OF SIMPLY SUPPORTED PLATE, $\frac{b}{a} = 0.6$, $\mu = 0$, LINE LOAD [X-X]

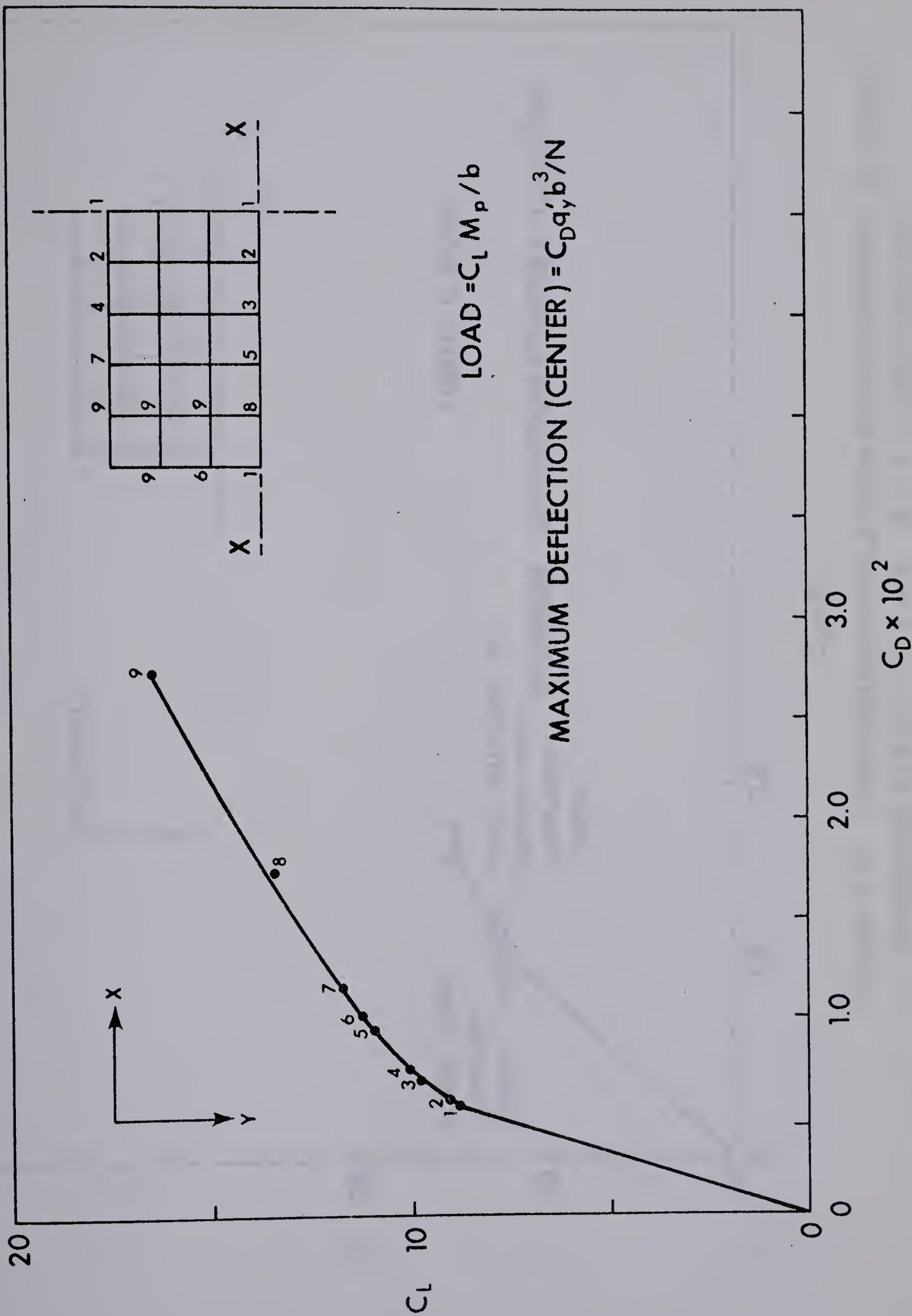


FIGURE 5.31 LOAD-MAXIMUM DEFLECTION CHARACTERISTICS OF FIXED EDGE PLATE, $\frac{b}{a} = 0.6$, $\mu = 0$, LINE LOAD [X-X']

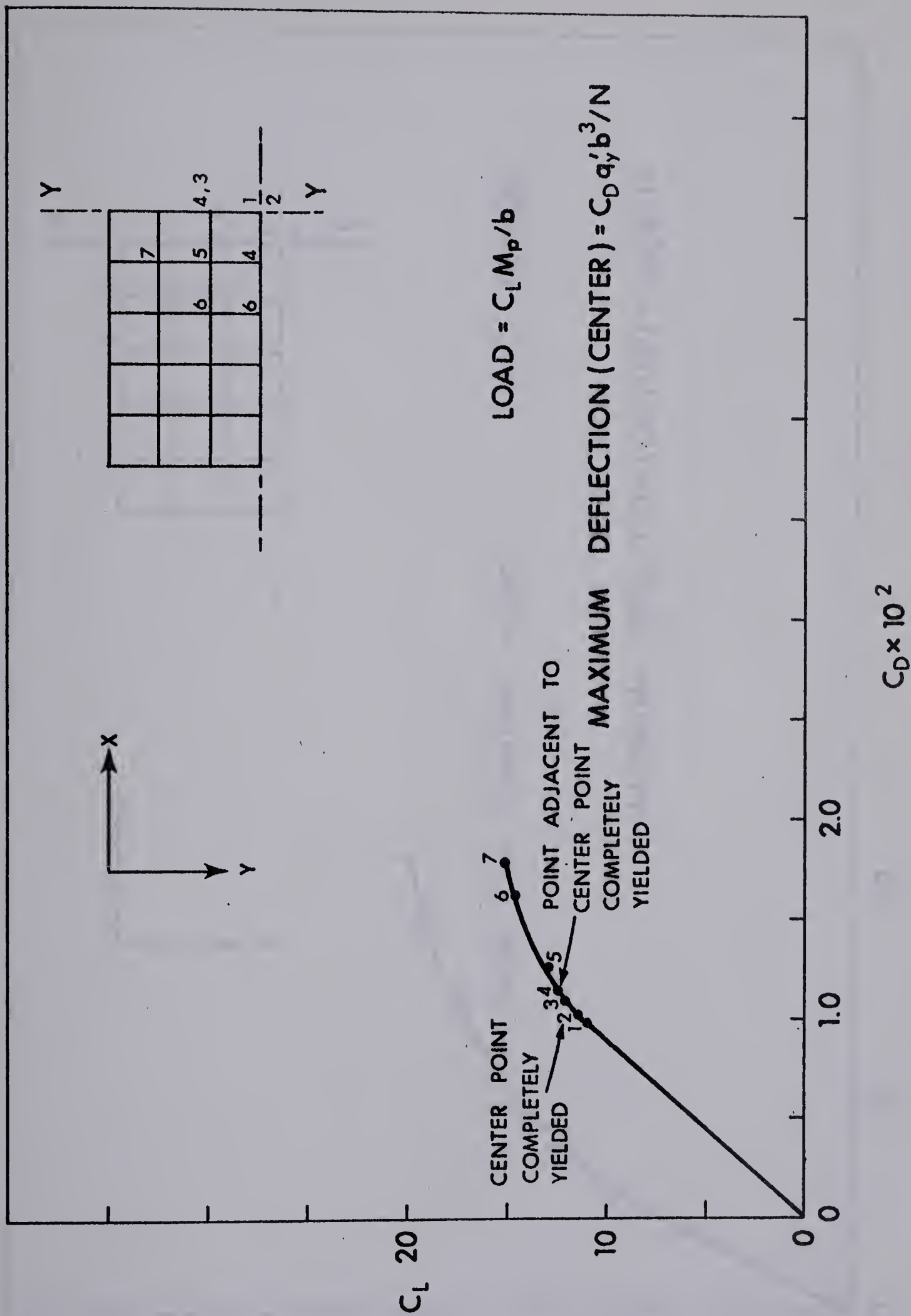


FIGURE 5.32 LOAD-MAXIMUM DEFLECTION CHARACTERISTICS OF SIMPLY SUPPORTED PLATE, $\frac{b}{a} = 0.6$, $\lambda = 0$, LINE LOAD $[Y-Y]$

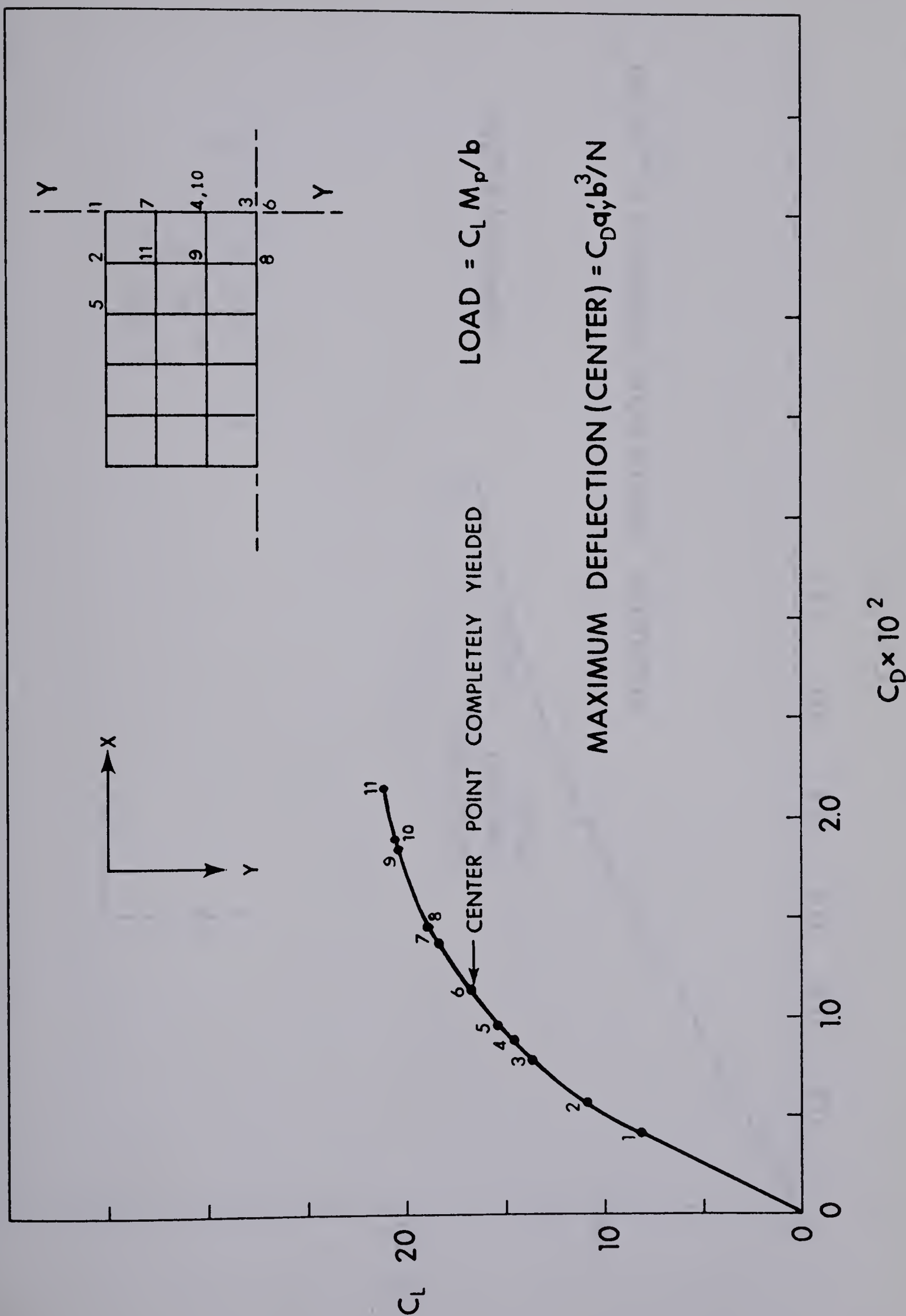


FIGURE 5.33 LOAD-MAXIMUM DEFLECTION CHARACTERISTICS OF FIXED EDGE PLATE, $\frac{b}{a} = 0.6$, $\mu = 0$, LINE LOAD [Y-Y]

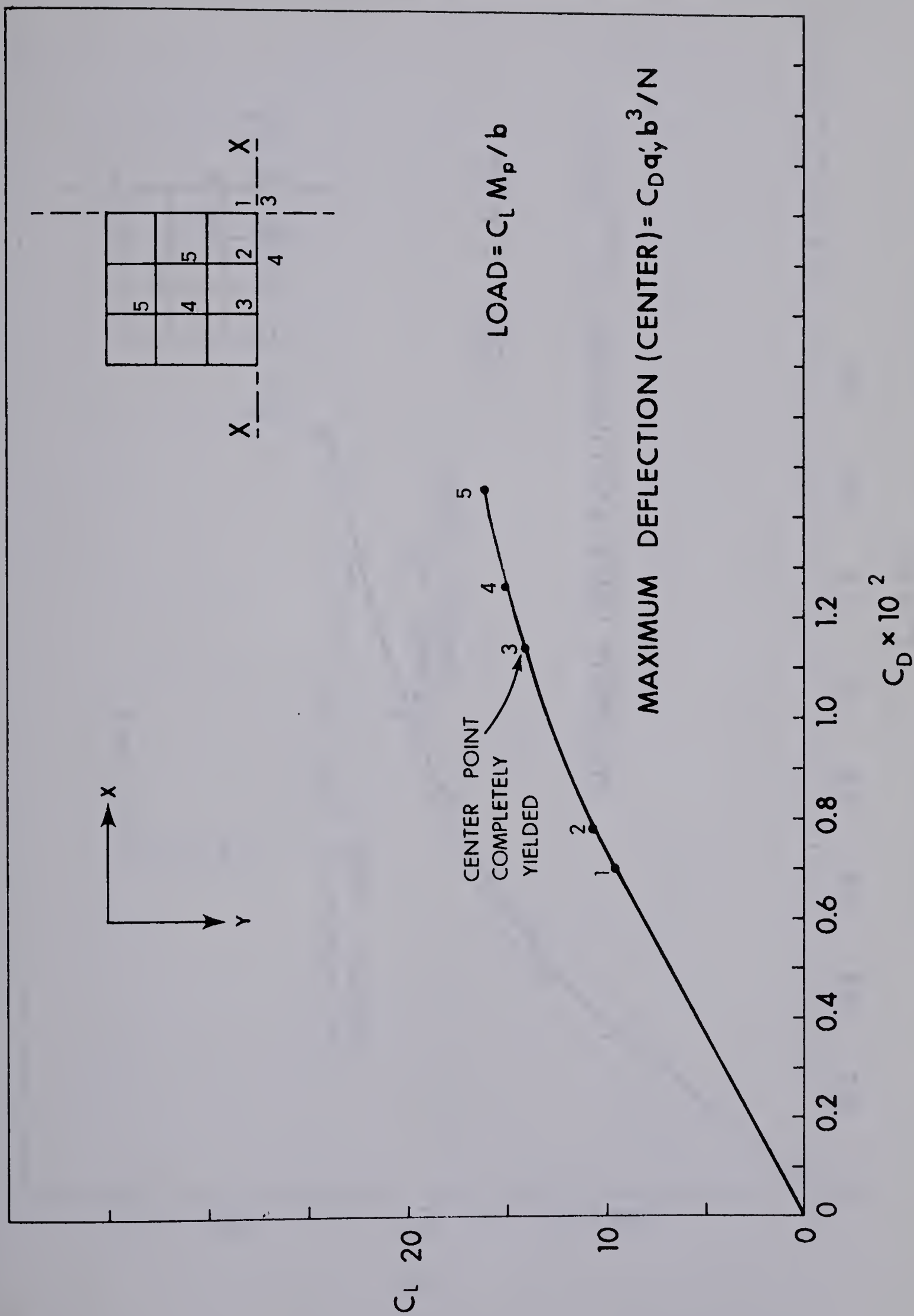


FIGURE 5.34 LOAD-MAXIMUM DEFLECTION CHARACTERISTICS OF SIMPLY SUPPORTED PLATE, $\frac{b}{a} = 1.0$, $\mu = 0$, LINE LOAD $[X-X]$

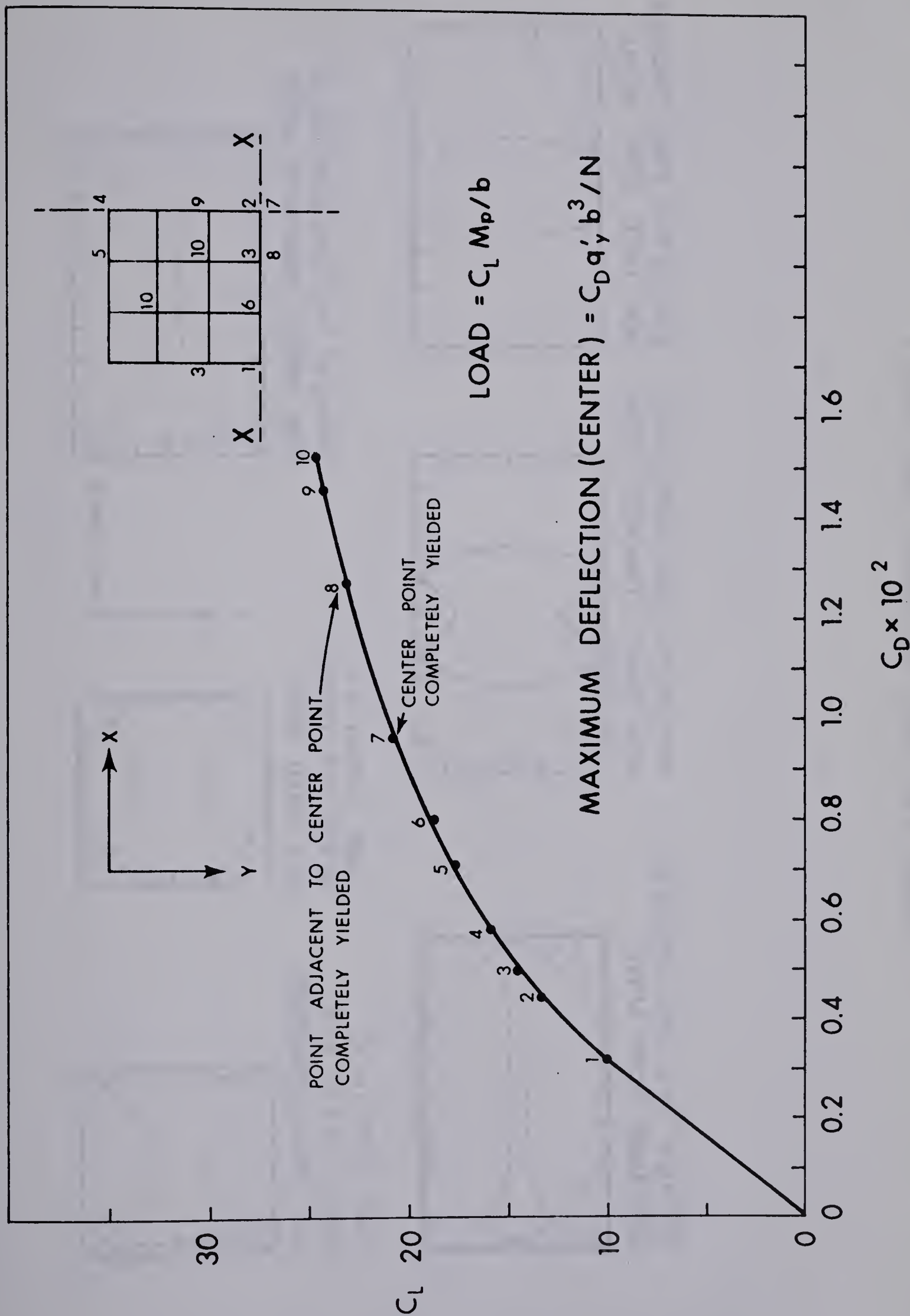


FIGURE 5.35 LOAD-MAXIMUM DEFLECTION CHARACTERISTICS OF FIXED EDGE PLATE, $\frac{b}{a} = 1.0$, $\mu = 0$, LINE LOAD [X-X]

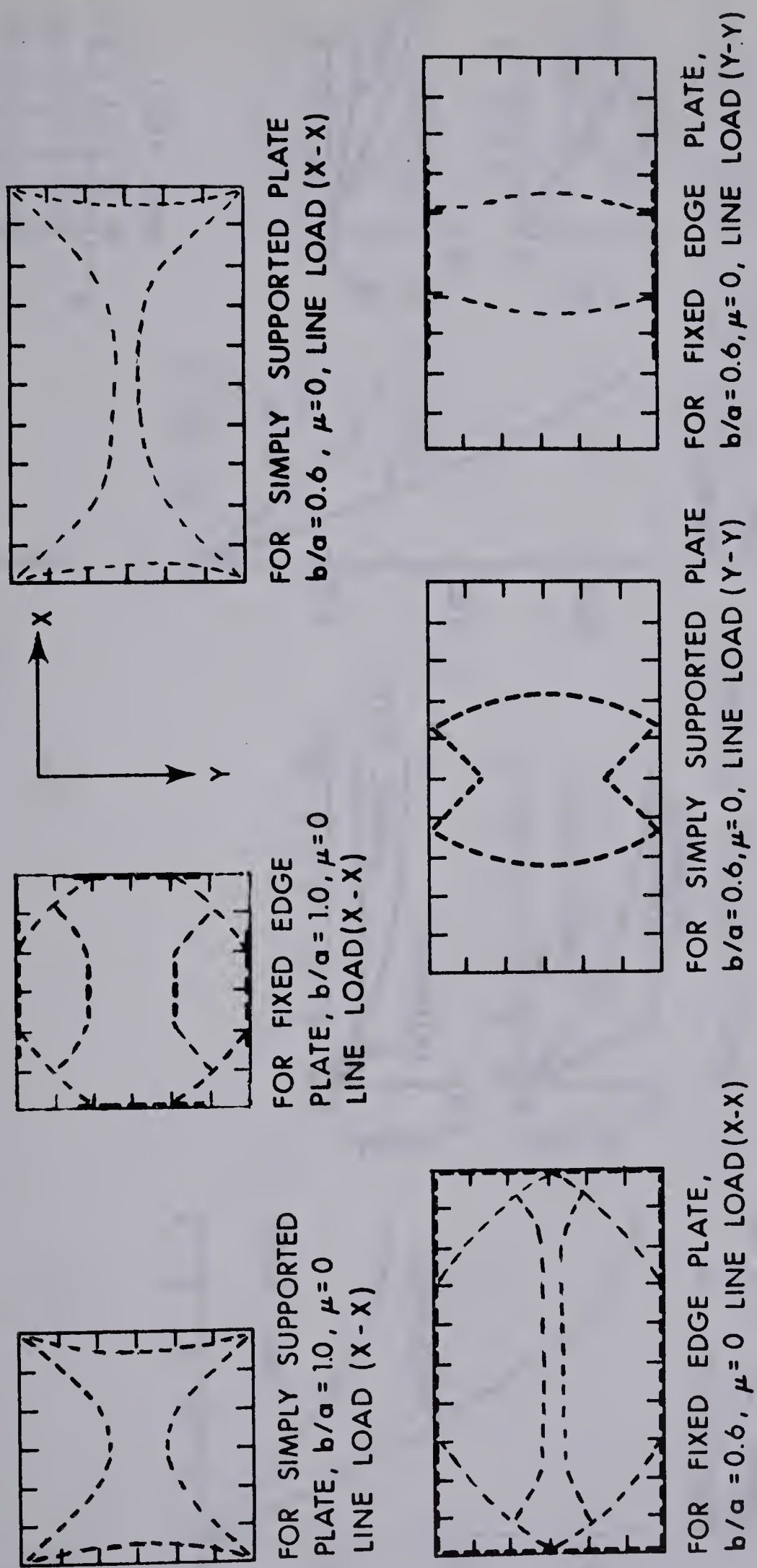


FIGURE 5.36 YIELD PATTERNS [LINE LOAD]

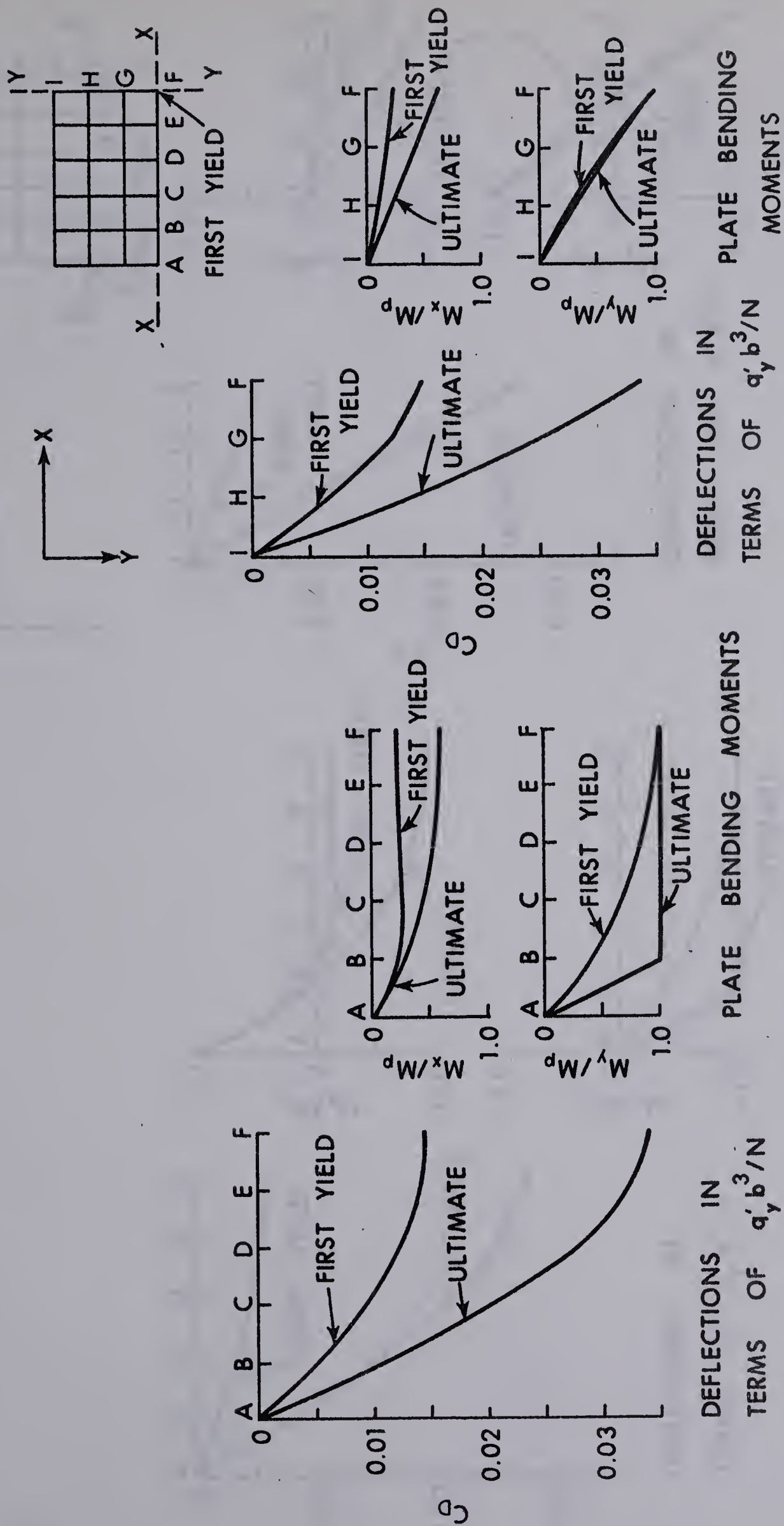


FIGURE 5.37 DEFLECTIONS AND BENDING MOMENTS ALONG LINES X-X AND Y-Y OF SIMPLY SUPPORTED PLATE, $\frac{b}{a} = 0.6$, $\mu = 0$, LINE LOAD [X-X]

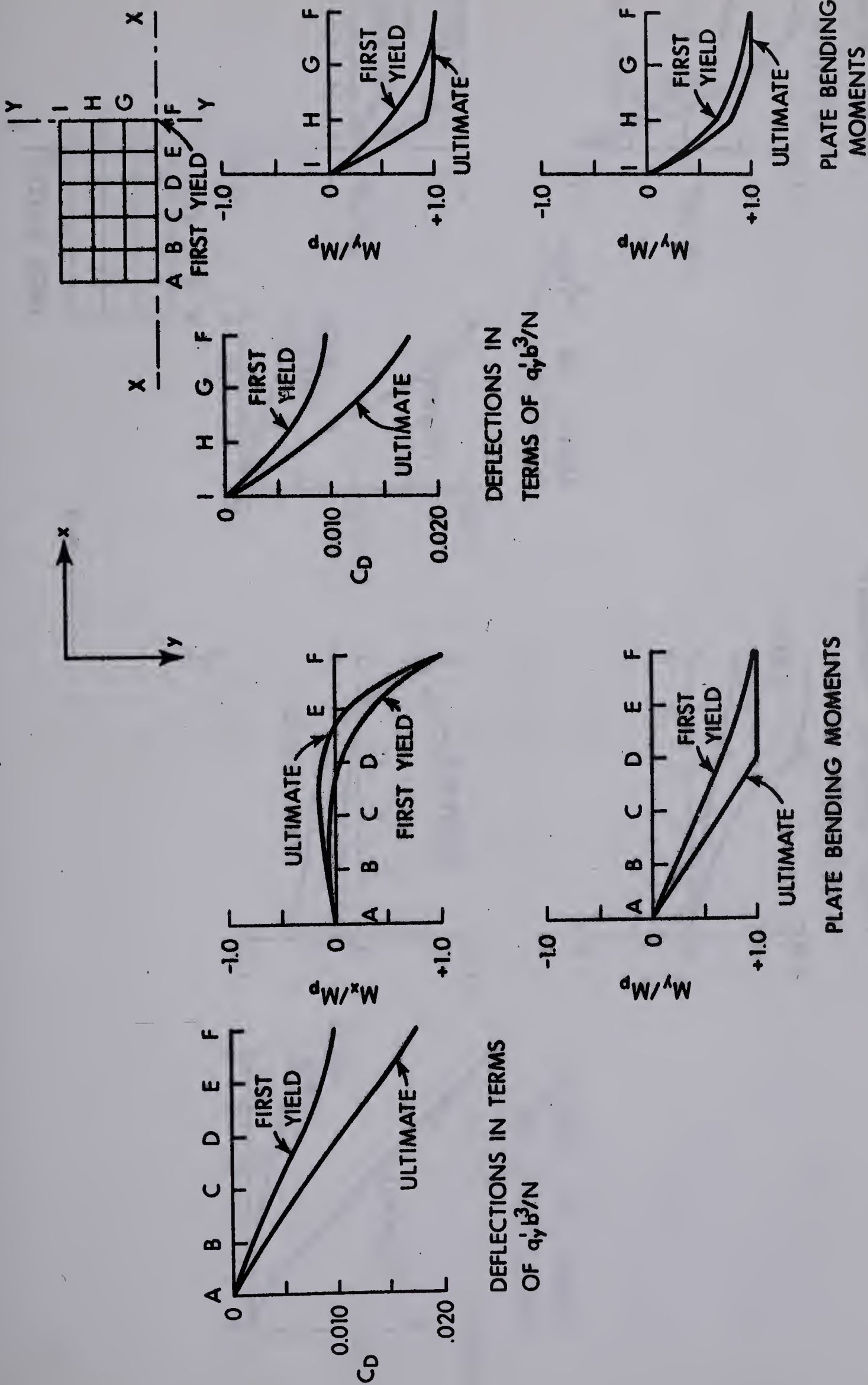


FIGURE 5.39 DEFLECTIONS AND BENDING MOMENTS ALONG LINES X-X AND Y-Y OF SIMPLY SUPPORTED PLATE, $\frac{b}{a} = 0.6$, $\mu = 0$, LINE LOAD [Y=Y]

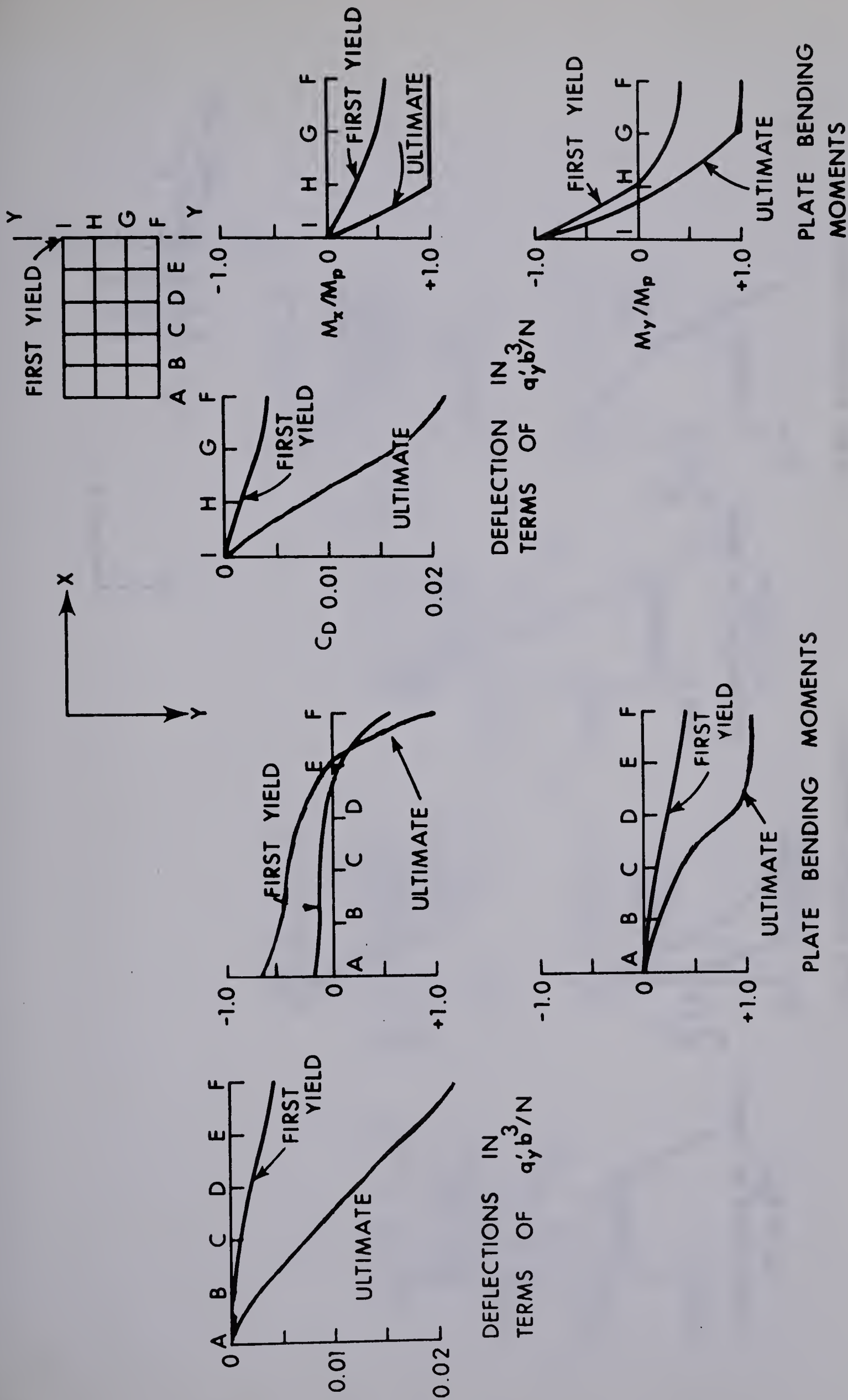


FIGURE 5.40 DEFLECTIONS AND BENDING MOMENTS ALONG LINES X-X AND Y-Y OF
FIXED EDGE PLATE, $\frac{b}{a} = 0.6$, $\mu = 0$, LINE LOAD [Y-Y]

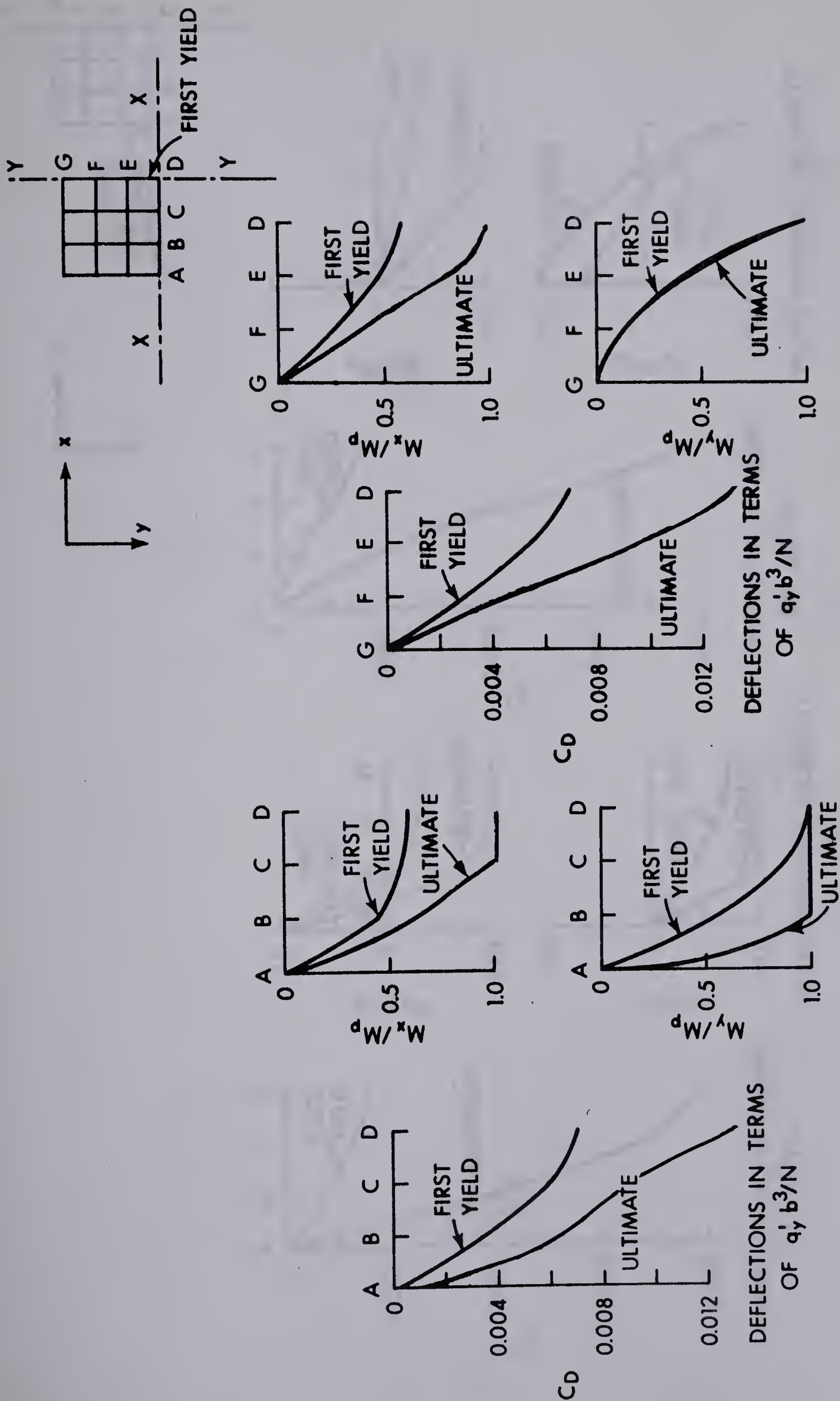


PLATE BENDING MOMENTS

PLATE BENDING MOMENTS

FIGURE 5.41 DEFLECTIONS AND BENDING MOMENTS ALONG LINES X-X AND Y-Y OF SIMPLY SUPPORTED PLATE, $\frac{b}{a} = 1.0$, $\mu = 0$, LINE LOAD [X-X]

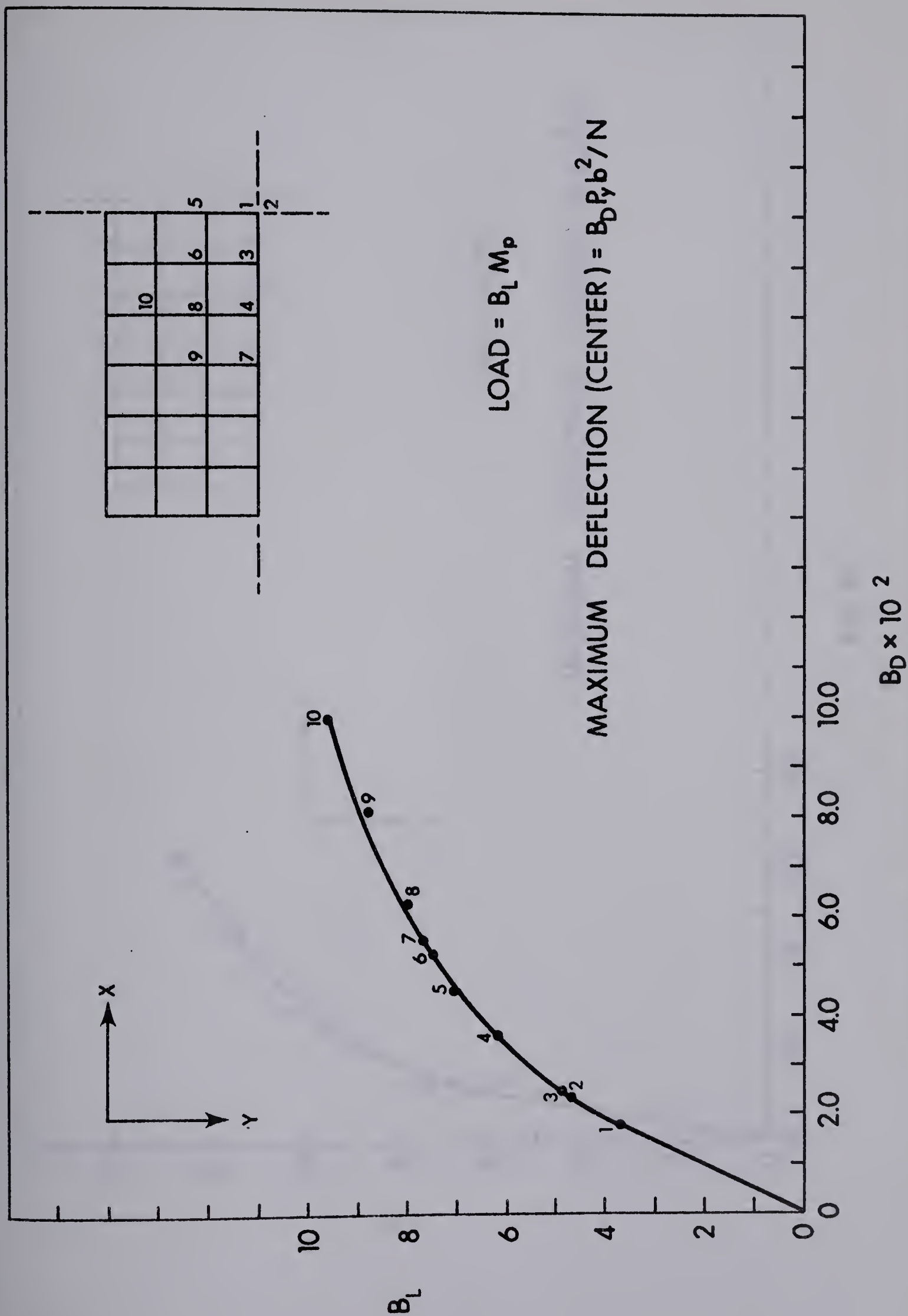


FIGURE 5.43 LOAD-MAXIMUM DEFLECTION CHARACTERISTICS OF SIMPLY SUPPORTED PLATE; $\frac{b}{a} = 0.5$, $\mu = 0$, CONCENTRATED LOAD AT CENTER

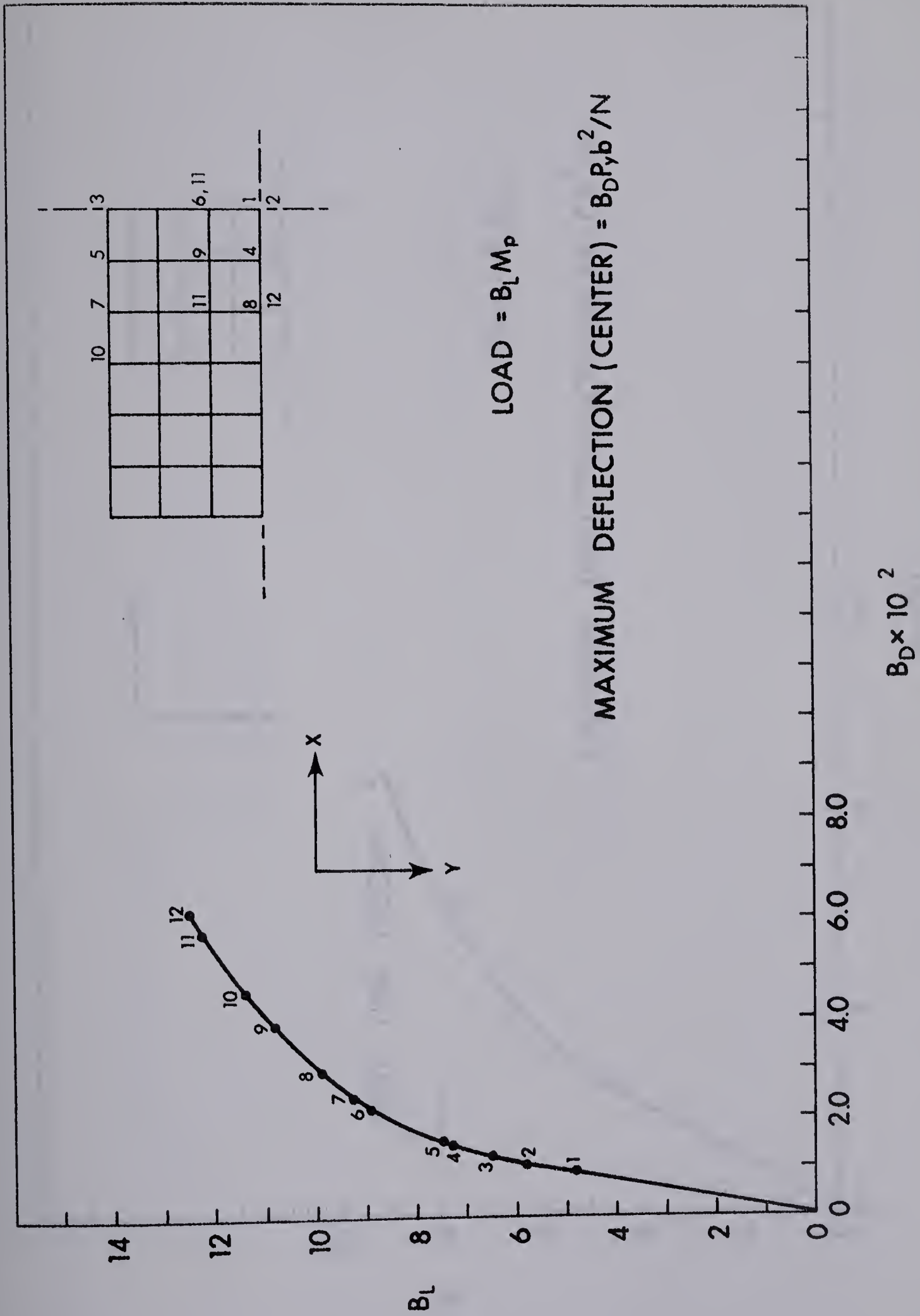


FIGURE 5.44 LOAD-MAXIMUM DEFLECTION CHARACTERISTICS OF FIXED EDGE PLATE, $\frac{b}{a} = 0.5$, $\mu = 0$, CONCENTRATED LOAD AT CENTER

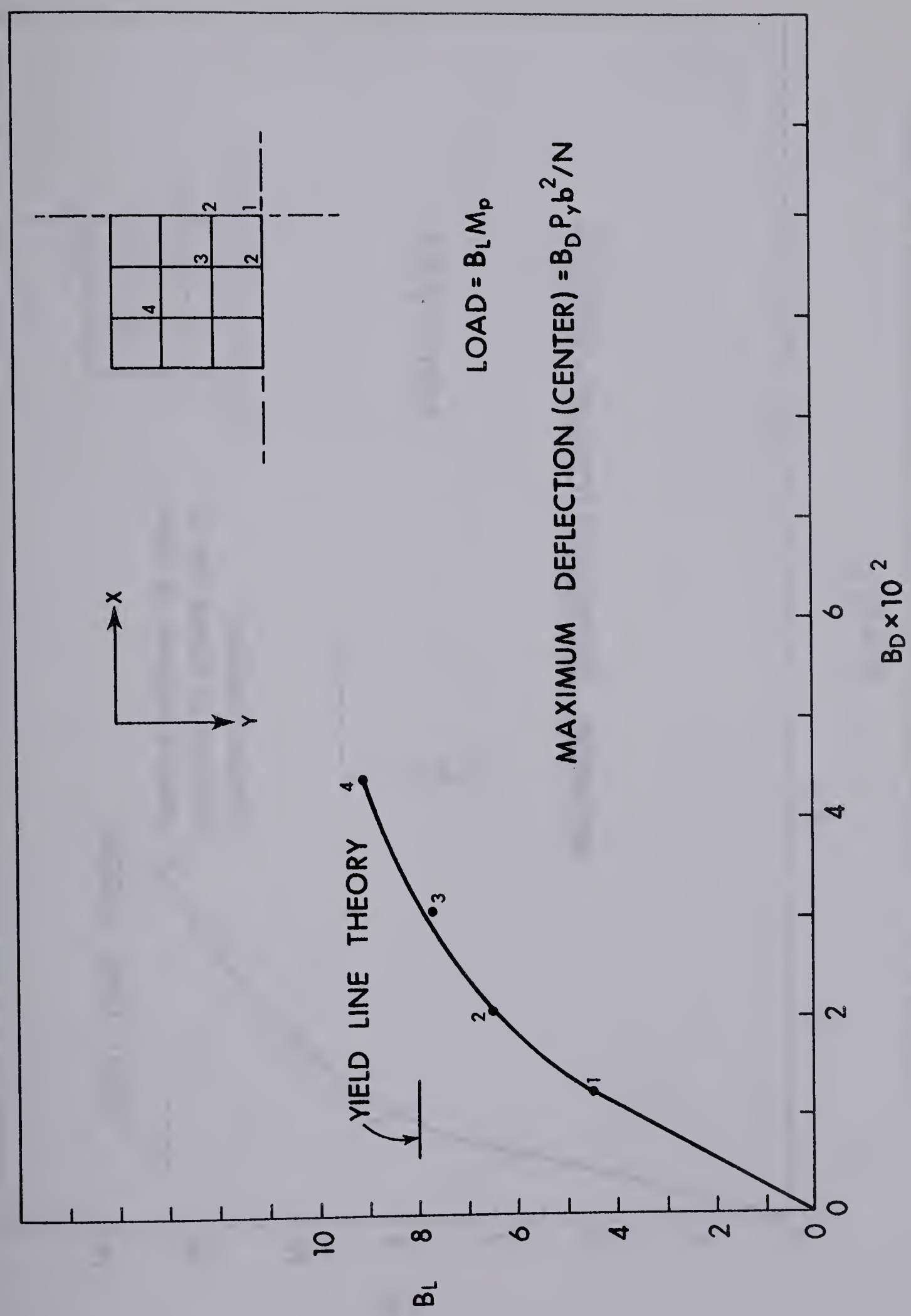


FIGURE 5.45 LOAD-MAXIMUM DEFLECTION CHARACTERISTICS OF SIMPLY SUPPORTED PLATE, $\frac{b}{a} = 1.0$, $\mu = 0$, CONCENTRATED LOAD AT CENTER

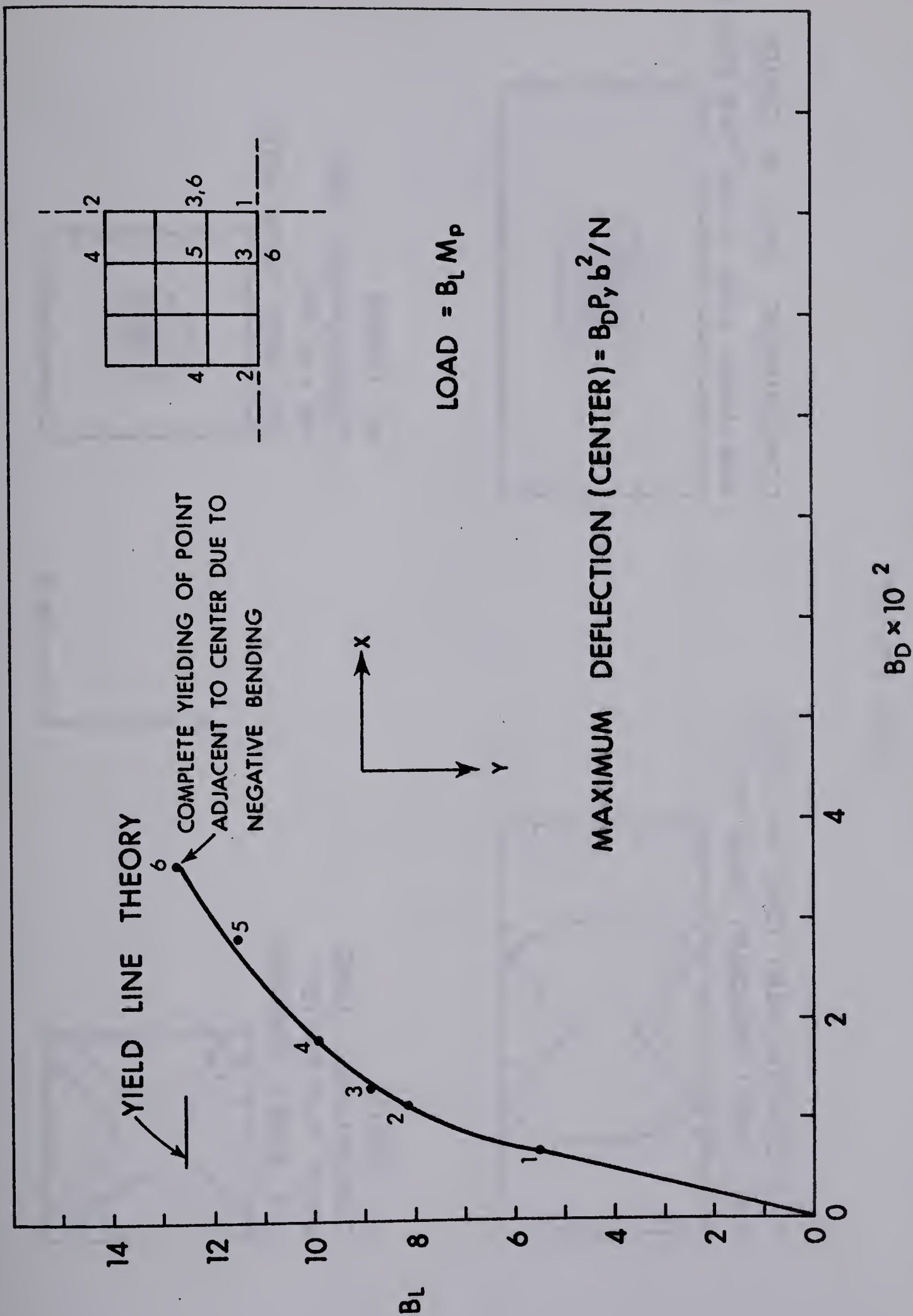
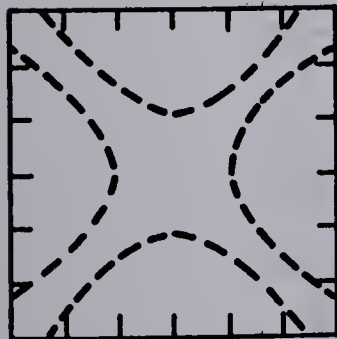
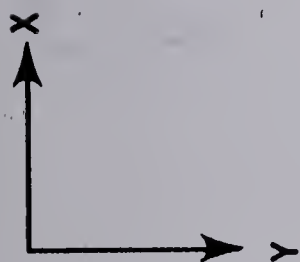
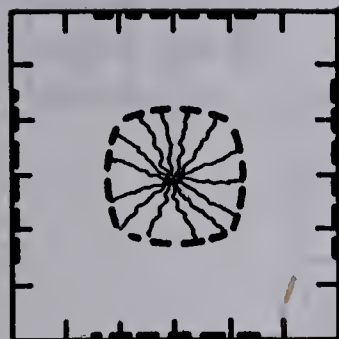


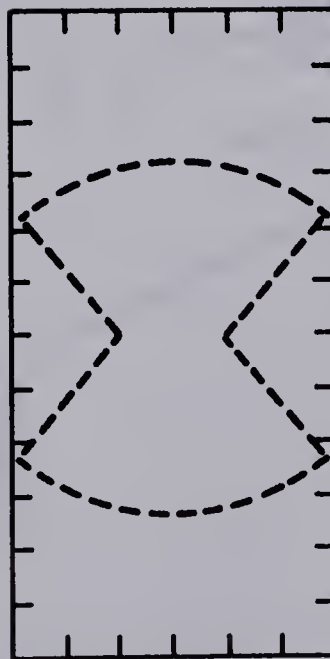
FIGURE 5.46 LOAD-MAXIMUM DEFLECTION CHARACTERISTICS OF FIXED EDGE PLATE, $\frac{b}{a} = 1.0$, $\mu = 0$, CONCENTRATED LOAD AT CENTER



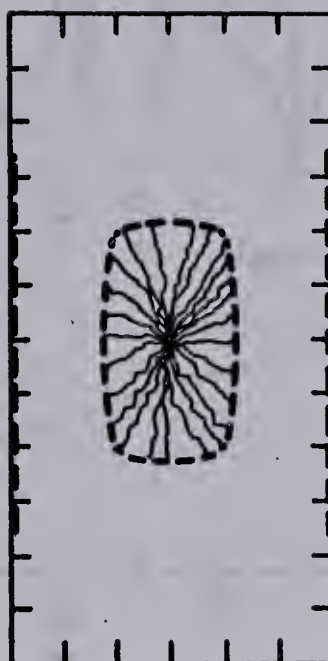
FOR SIMPLY SUPPORTED
PLATE, $\mu = 0$, $b/a = 1.0$
CONCENTRATED LOAD
AT CENTER



FOR FIXED EDGE PLATE
 $b/a = 1.0$, $\mu = 0$
CONCENTRATED LOAD
AT CENTER



FOR SIMPLY SUPPORTED PLATE, $b/a = 0.5$
 $\mu = 0$, CONCENTRATED LOAD AT CENTER



FOR FIXED EDGE PLATE, $\mu = 0$, $b/a = 0.5$
CONCENTRATED LOAD AT CENTER

YIELD PATTERNS

FIGURE 5.47 CONCENTRATED LOAD AT CENTER

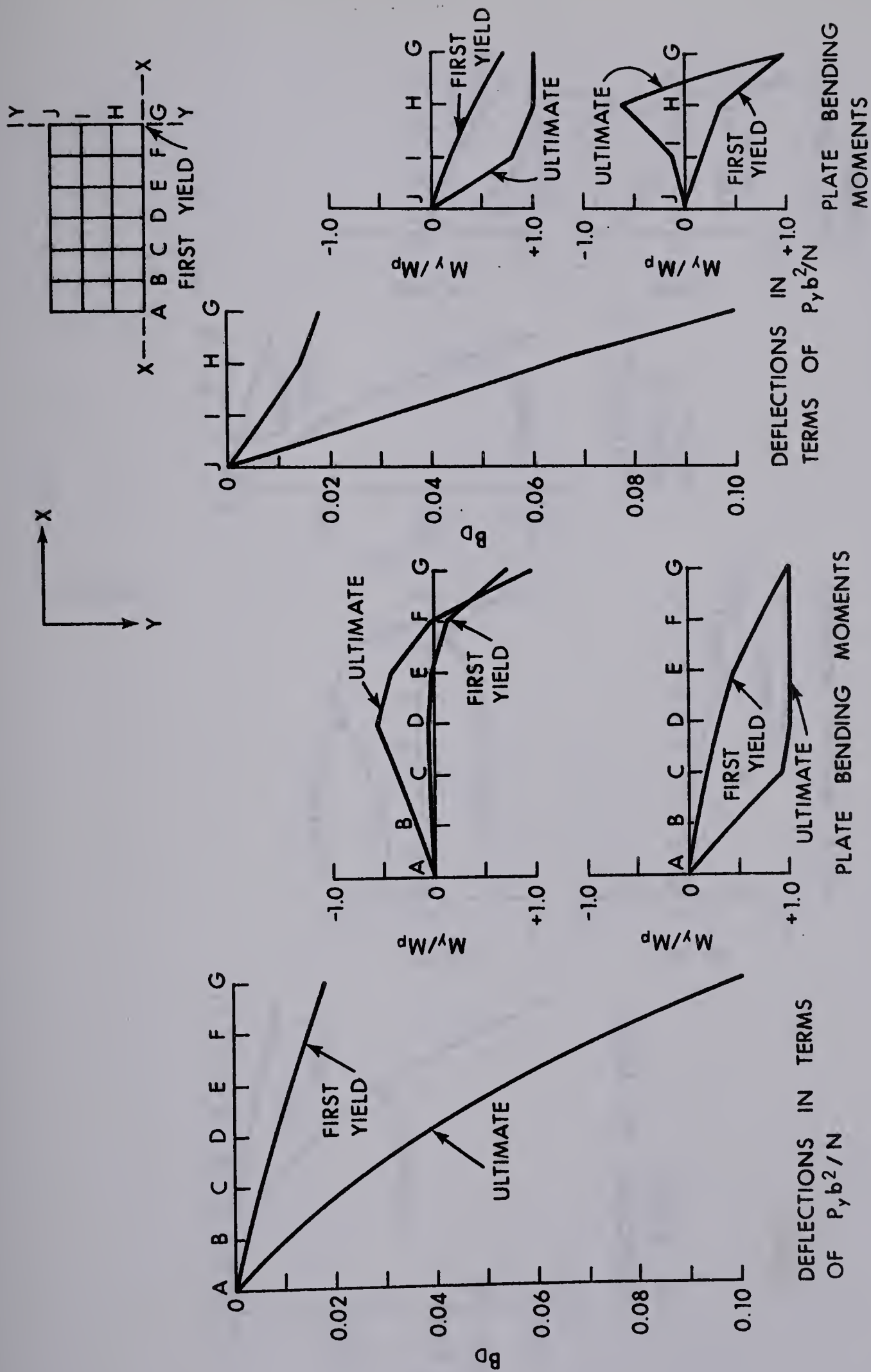


FIGURE 5.48 DEFLECTIONS AND BENDING MOMENTS ALONG LINES X-X AND Y-Y OF SIMPLY SUPPORTED PLATE, $\frac{b}{a} \approx 0.5$, $\mu = 0$, CONCENTRATED LOAD AT CENTER

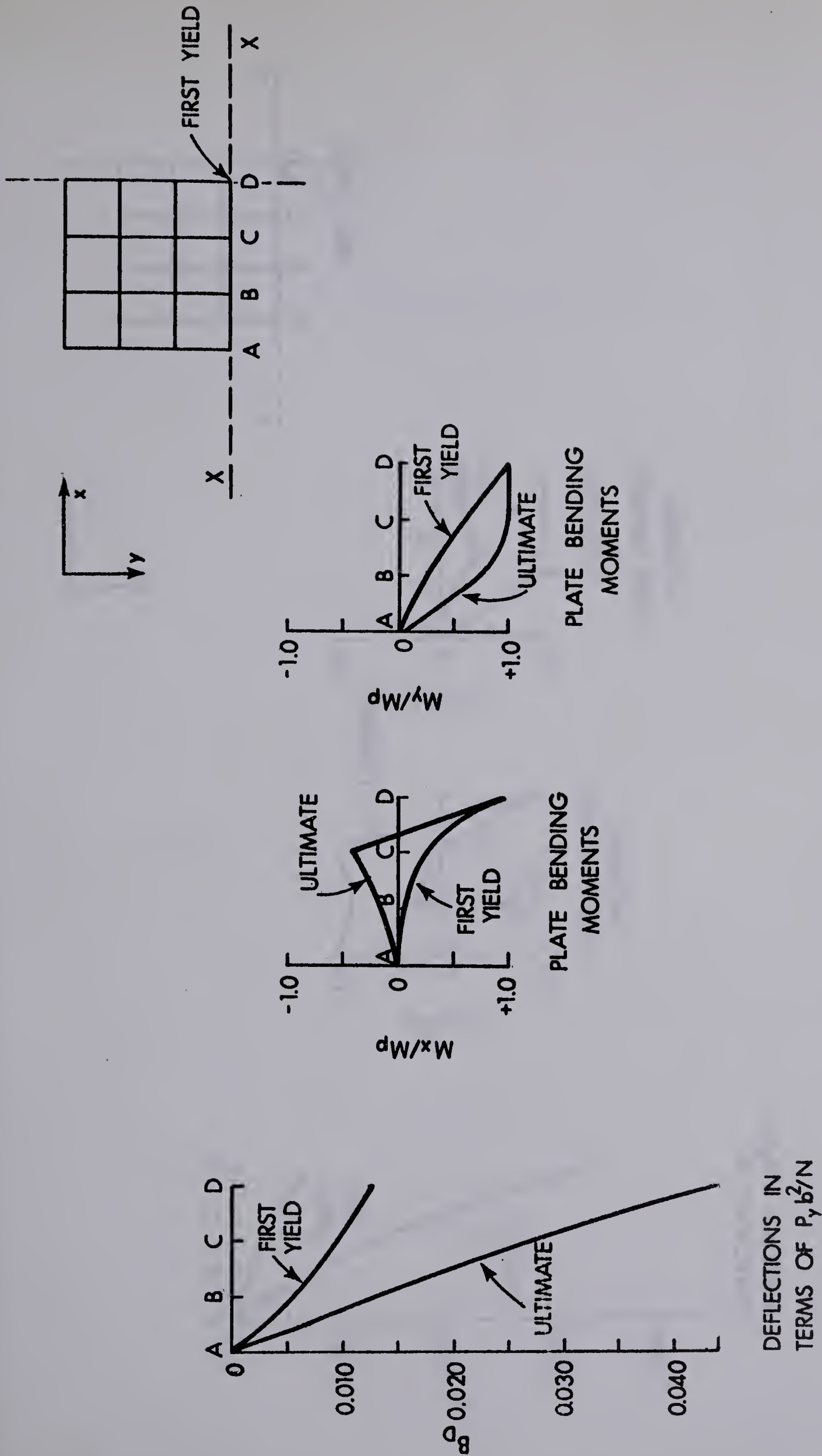
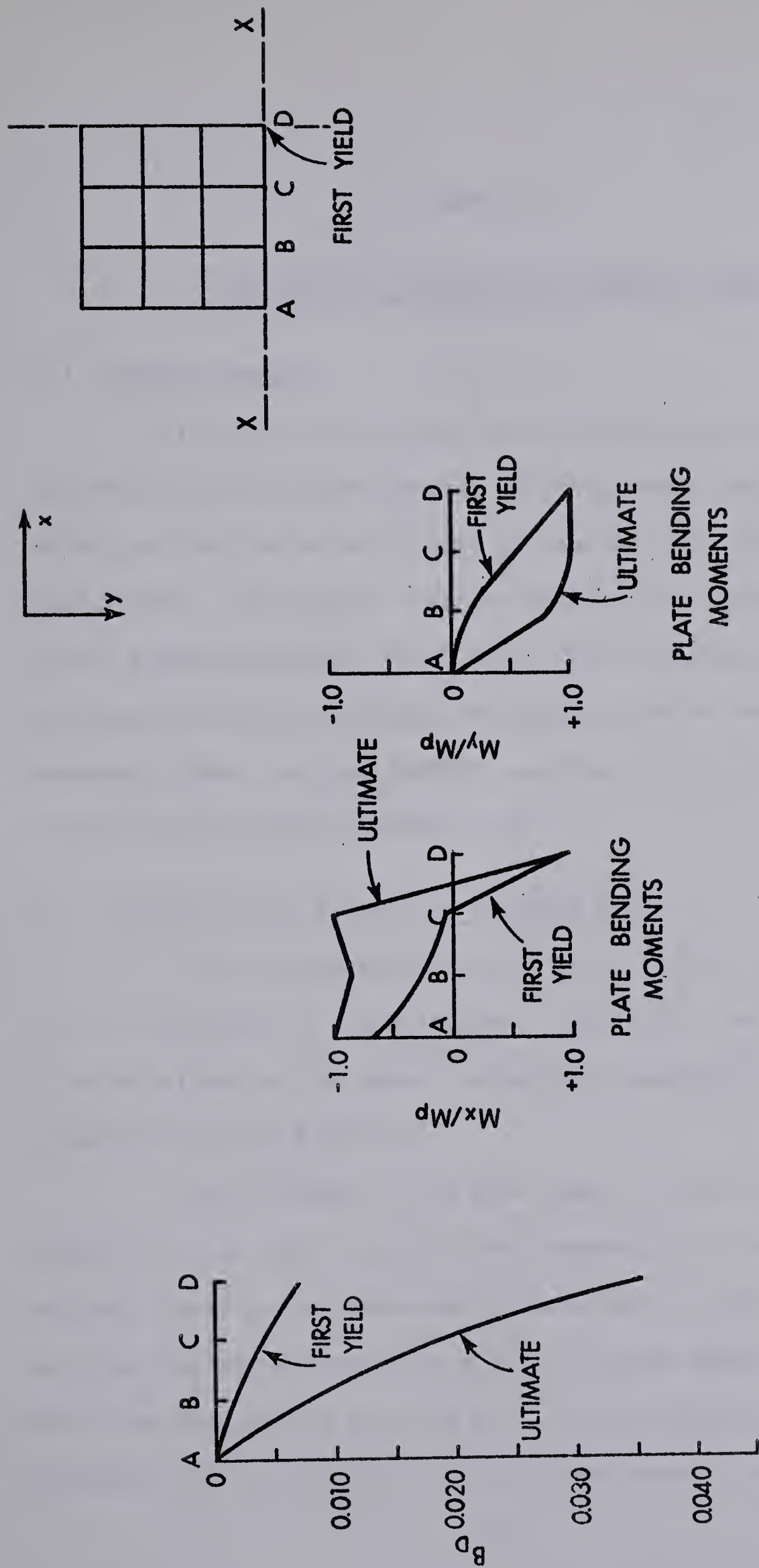


FIGURE 5.50 DEFLECTIONS AND BENDING MOMENTS ALONG LINES X-X AND Y-Y OF SIMPLY SUPPORTED PLATE, $\frac{b}{a} = 1.0$, $\lambda = 0$, CONCENTRATED LOAD AT CENTER



DEFLECTIONS IN
TERMS OF $P_y b^2/N$

FIGURE 5.51 DEFLECTIONS AND BENDING MOMENTS ALONG LINE X-X OF
FIXED EDGE PLATE, $\frac{b}{a} = 1.0$, $\mu = 0$, CONCENTRATED LOAD AT CENTER

CHAPTER VI

APPLICATION TO REINFORCED CONCRETE SLABS

6.1 General Remarks

The aim of this study is, as mentioned in previous CHAPTERS, to obtain a better understanding of the strength and behavior of building slabs, so that the results might in some way help in formulating a design method. Although the results are strictly applicable to perfect elasto-plastic material, which will yield according to "square yield criterion", they are extended for application for design of reinforced concrete slabs. In this CHAPTER, application for design will be restricted to the case of uniform loading only.

6.2 Stiffness of a Reinforced Concrete Slab

The computed deflection of a reinforced concrete slab depends on the assumption of the stiffness. Generally, the stiffness computation is based either on the gross, uncracked transformed section or on the cracked transformed section.

The stiffness (N) in this study is the stiffness of the unyielded parts of the slab, and thus the computation of the stiffness should be strictly based on the uncracked transformed section. However, the unyielded zone near the yielded area will be cracked whereas the zone further away from the yielded area may still be relatively uncracked. The true stiffness (N) as a whole of the unyielded zone is somewhere between those

for the cracked and uncracked sections. For this reason the average of the transformed cracked and uncracked stiffnesses is assumed for application.

6.3 Comparison of Theoretical Deflection with Measured Value

Theoretical load-deflection plot of a fixed edge square plate from the analyses is compared with measured load-deflection plot from tests by Vanderbilt, Sozen and Siess (15) in FIGURE 6.2. Measured load-deflection plot was obtained from FIGURES 5.92 and 5.93 of Reference (15) in which a nine panel reinforced concrete square slab was loaded to failure, with all panels loaded uniformly.

As indicated in FIGURE 6.2, the deflections from the analyses agree very well with measured values, especially at higher loads, and at ultimate load. The deviations at lower loads and closer agreements at higher loads may be explained as follows. Average stiffness (N) as described in SECTION 6.2 was used for computations of theoretical deflections, and the true stiffness (N) of the unyielded parts of the slab may be larger than the assumed stiffness (N) at lower loads, thus resulting in higher theoretical deflections at lower loads. However, at higher loads, the true stiffness (N) of the unyielded parts of the slab may be almost equal to the assumed stiffness (N), thus giving closer agreements between the theoretical and measured deflections. Calculations for theoretical deflection at ultimate load are given below.

The pertinent data of the test slab on deep beams from Reference (15) is:

Overall slab dimensions = 15' x 15'

Panel dimensions = 5' x 5'

Thickness of the slab = 1.5"

Concrete cover (approx.) = 0.25"

% age of steel = 0.314%

f'_c = 3020 psi

f_y = 42,000 psi

E_c = 3×10^6 psi

From FIGURE 5.92 of Reference (15), measured cumulative deflection of the center panel for the load of 395 lb/ft² = 0.27". Beam deflection from FIGURE 5.93 of Reference (15) = 0.07" \therefore Net slab deflection = 0.20"

Using the above data, the theoretical deflection at ultimate load is computed as shown below.

Using ACI 318-63 Section 1601 (a),

Ultimated moment (M_p) for the test slab = 206 ft-lb/ft of slab

From FIGURE 5.19 of this study,

First yield load (q_y) = $22.4 \times \frac{M_p}{b^2}$

$$= 22.4 \times \frac{206}{25} = 184.5 \text{ lb/ft}^2$$

Ultimate load = $47.1 \times \frac{M_p}{b^2}$

$$= 47.1 \times \frac{206}{25} = 388 \text{ lb/ft}^2$$

Deflection at ultimate load = $K_D \frac{q_y b^4}{N}$

$$= \frac{0.0062 \times 184.5 \times (5)^4}{N}$$

Moment of Inertia of transformed uncracked section =

$$3.4938 \text{ in}^4/\text{ft of slab}$$

Moment of Inertia of transformed cracked section =

$$= 0.5327 \text{ in}^4/\text{ft of slab}$$

Average Moment of Inertia = $2.0132 \text{ in}^4/\text{ft of slab}$

Average stiffness (N) = $E_c \times 2.0132$

$$= 3 \times 10^6 \times 2.0132$$

$$= 6.0396 \times 10^6 \text{ lb-in}^2/\text{ft of slab}$$

$$= 0.0419 \times 10^6 \text{ lb-ft}^2/\text{ft of slab}$$

$$= 0.0419 \times 10^6 \text{ lb-ft}$$

$$\text{Deflection at ultimate load} = \frac{0.0062 \times 184.5 \times (5)^4}{0.0419 \times 10^6}$$

$$= 0.017 \text{ ft}$$

$$= \underline{\underline{0.204''}}$$

The close agreement of the theoretical deflection with measured value suggests that the use of the average stiffness (N) for unyielded parts of this particular test slab is satisfactory. Incidentally, it is found that the average stiffness (N) of a reinforced concrete slab ($p = 0.2\%$ to 1%) is close to the value of the stiffness (N) based on the moment of inertia of $\frac{b'd^3}{12}$. The stiffness (N) based on $\frac{b'd^3}{12}$ is about 10% to 30% smaller than the average stiffness (N), depending on the percentage of steel in the slab. The stiffness (N) of the unyielded parts of a reinforced concrete slab may therefore be related to $\frac{b'd^3}{12}$ by a coefficient C_s so that the stiffness (N) = $C_s \frac{b'd^3}{12} \times E_c$. C_s may, however, depend on such variables as the percentage of steel,

concrete cover, thickness of the slab etc. But, for most typical slabs the stiffness (N) based on $\frac{b'd^3}{12}$ will give a slightly larger slab deflection but of the right order of magnitude.

6.4 Suggested Procedure for Design of a Reinforced Concrete Slab

Since the stiffness (N) based on $\frac{b'd^3}{12}$ slightly overestimates the deflection, and since it is much easier to compute, it will be used for design application.

A typical interior panel of a building floor may be represented by a fixed edge slab. Steps involved in the design of such a slab are shown below by an example.

Assume:

Slab dimensions	= 15' x 15'
Live load	= 100 lb/ft ²
f'_c	= 3000 psi
f_y	= 40,000 psi
E_c	= 3×10^6 psi
E_s	= 30×10^6 psi
Concrete cover	= 1"

STEP 1: Compute Design Loads

Assume $t = 4''$

$d = 3''$

Dead load = $\frac{4}{12} \times 150 = 50$ lb/ft²

Live load = 100 lb/ft²

Using ACI 318-63 Section 1506 (a),

Design loads = $1.5 \times 50 + 1.8 \times 100 = 255$ lb/ft²

STEP 2: Compute Required M_p and Required p

From FIGURE 5.19,

$$q = 47.1 \times \frac{M_p}{b^2}$$

$$255 = 47.1 \times \frac{M_p}{225}$$

$$\therefore M_p = \frac{255 \times 225}{47.1} = 1220 \text{ lb}$$

From FIGURE 6.1, required p is approximately equal to 0.4%.

But, from ACI 318-63,

For $d = 3''$ and $p = 0.35\%$, $M_p = \underline{\underline{1225 \text{ lb}}}$

\therefore Use $d = 3''$ and $p = 0.35\%$

STEP 3: Check Maximum Deflection

$$w = K_D \frac{q_y b^4}{N}$$

From FIGURE 5.19, $q_y = 22.4 \frac{M_p}{b^2}$

$$N = \frac{3 \times 10^6 \times (3)^3}{144} = 0.562 \times 10^6 \text{ lb-ft}$$

$$\text{Ultimate load} = 255 \text{ lb/ft}^2 = 47.1 \frac{M_p}{b^2}$$

$$\therefore \text{Working load} = 150 \text{ lb/ft}^2 = \frac{150}{255} \times 47.1 \frac{M_p}{b^2}$$

$$= 27.7 \frac{M_p}{b^2}$$

From FIGURE 5.19, for this working load,

$$K_D = 0.0021$$

$$w \text{ at working load} = K_D \frac{q_y b^4}{N}$$

$$= \frac{0.0021 \times 22.4 \times 1225 \times 225}{0.562 \times 10^6}$$

$$= \underline{\underline{0.0232}} \text{ ft}$$

Allowable deflection from ACI 318-63 Section 909 (f)

$$= \frac{b}{360} = \frac{15}{360} = 0.042 \text{ ft}$$

The deflection is therefore satisfactory under short-time loads, and from FIGURE 5.19, it is seen that there will be a few cracks developed along the fixed edges of the slab. However, if the long-time deflection is taken as three times the short-time deflection, as suggested by ACI 318-63 Section 909 (d), the deflection is unsatisfactory. For this case, the design cycle can be repeated by slightly increasing the thickness of the slab without increasing the reinforcements until the deflection requirement is satisfied.

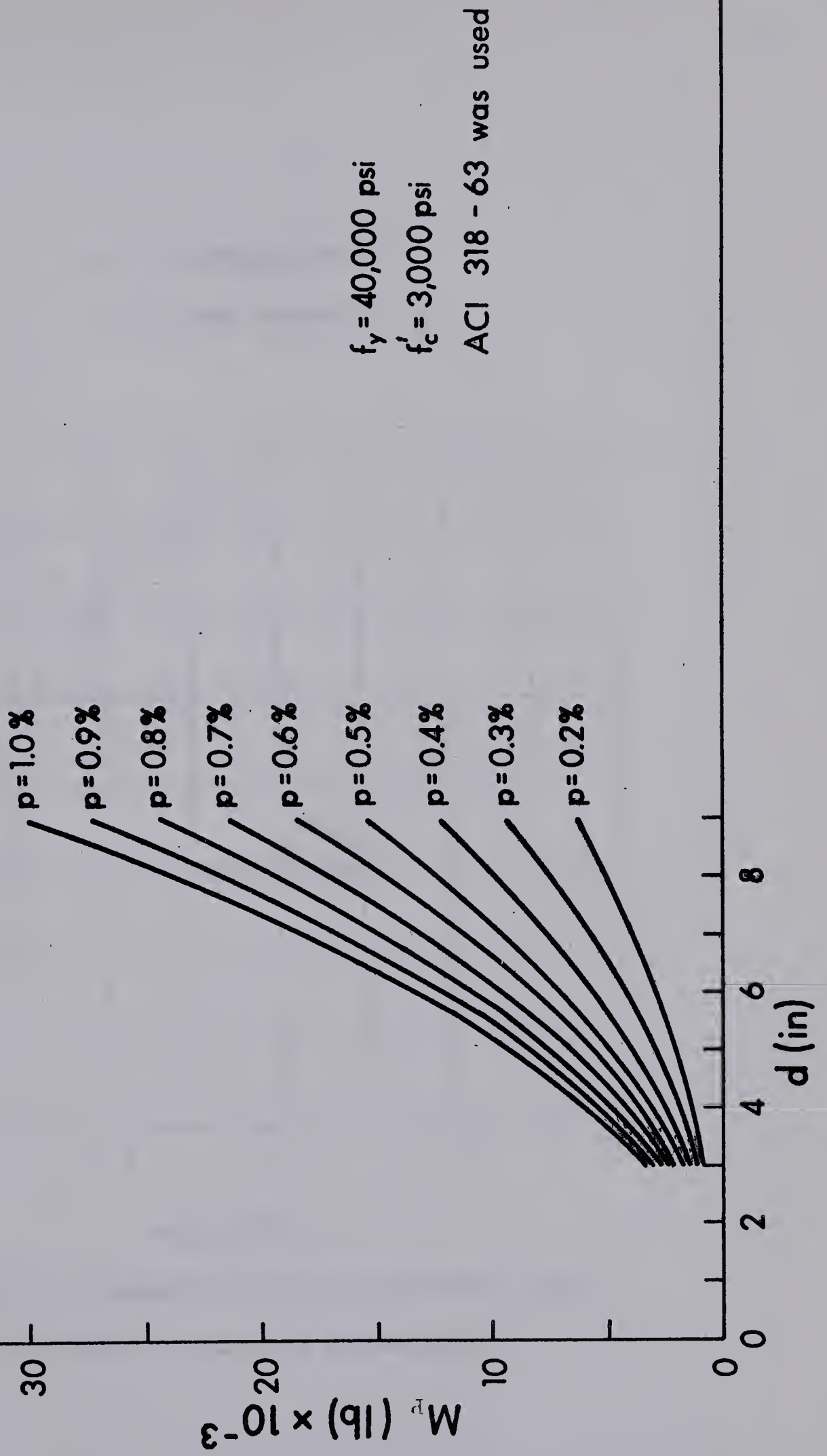


FIGURE 6.1 ULTIMATE MOMENT PER UNIT WIDTH - EFFECTIVE DEPTH
RELATIONSHIP FOR REINFORCED CONCRETE SLAB

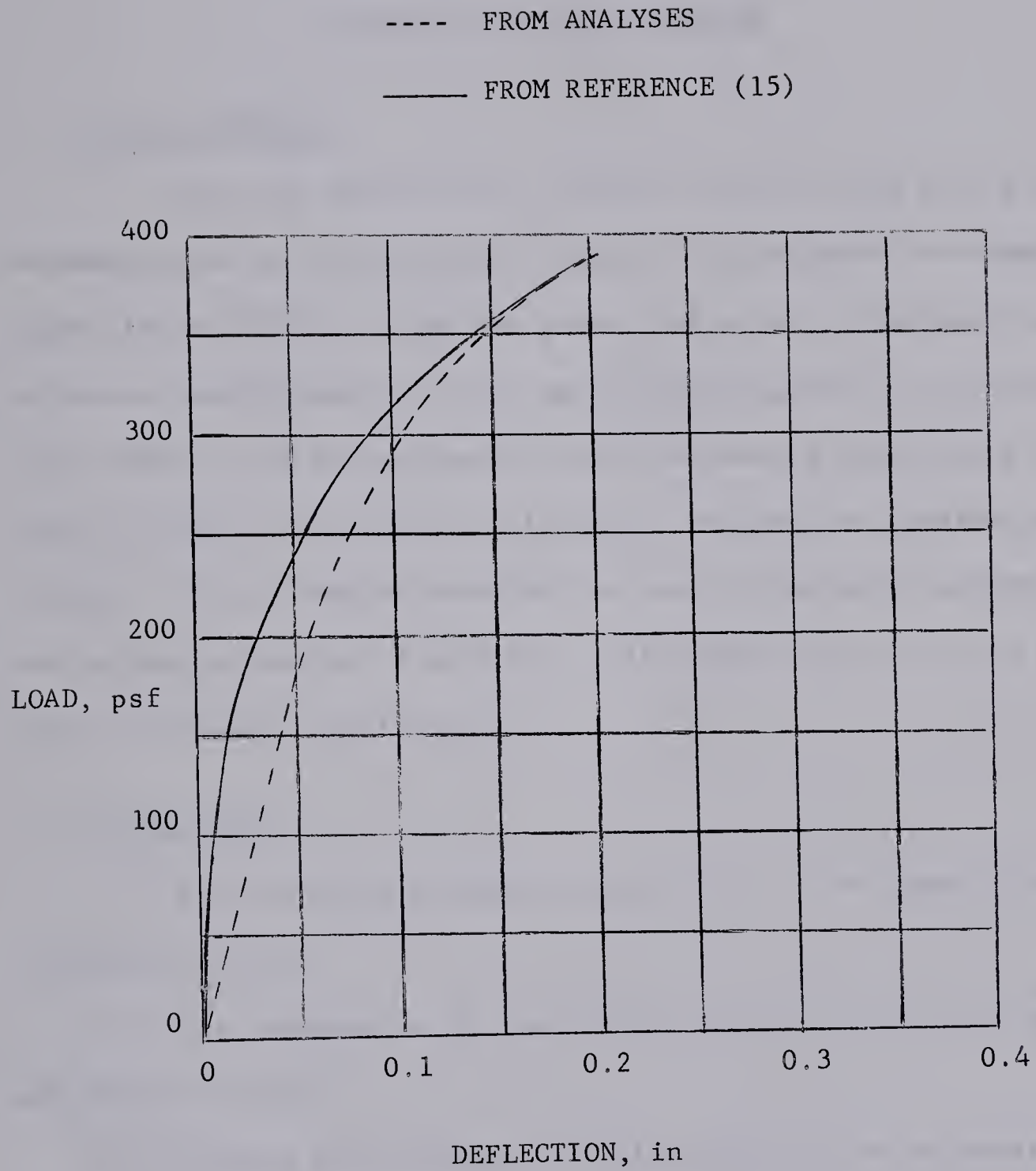


FIGURE 6.2 COMPARISON OF LOAD-DEFLECTION PLOTS
FROM ANALYSES AND FROM REFERENCE (15)

CHAPTER VII

CONCRETE AND STEEL STRAINS

7.1 General Remarks

From the deflection at ultimate load at each grid point, the maximum values of curvature are computed and presented as dimensionless quantities in TABLE 7.1 for the plates subjected to uniform load. These curvature coefficients are used in the investigation of reinforced concrete slabs to determine whether strain-hardening has taken place in the steel or whether the concrete strain has reached its limiting value in flexure. This is rather important as one of the basic assumptions in developing the method of analysis is the applicability of the idealized moment-curvature relationship.

7.2 Assumptions

The following assumptions are used in the computation of concrete and steel strains.

- (1) The computation of the ultimate moment of the slab by using ACI 318-63 is valid.
- (2) Two-way slab thickness requirements will be according to the provisions of ACI 318-63, Section 2002 (e).
- (3) The slab is underreinforced and the percentage of reinforcements ranges from 0.2% to 1%.
- (4) Strain at which the steel begins to strain-harden is 0.015.

- (5) Limiting strain in flexure for concrete is 0.0038.
- (6) Poisson's ratio is zero.
- (7) Average stiffness used in CHAPTER VI is applicable.

7.3 Investigation Based on Average Stiffness

From TABLE 7.1, the maximum curvature is at the mid-point of a longer fixed edge of a reinforced concrete slab with aspect ratio $(\frac{b}{a}) = 0.5$.

Assume: Slab dimensions = 10' x 20'

$$f'_c = 3000 \text{ psi}$$

$$f_y = 40,000 \text{ psi}$$

$$E_c = 3 \times 10^6 \text{ psi}$$

$$E_s = 30 \times 10^6 \text{ psi}$$

$$n = 10$$

Since the slab is underreinforced, the neutral axis moves up as the load is increased, and c_1 shown in FIGURE 7.1 becomes smaller and smaller until the concrete strain reaches its limiting value in flexure. For the computation of steel and concrete strains shown below, the two limits of c_1 , and the two limits of percentage of steel from Assumption (3) will be considered. If the steel and concrete strains are satisfactory, i.e. do not exceed 0.015 and 0.0038 respectively, for the above-mentioned limiting cases, they can be assumed to be satisfactory for cases between these limits.

(i) Reinforced Concrete Slab with $p = 0.2\%$

From ACI 318-63 Section 2002 (e),

$$\text{Minimum allowable thickness} = \frac{60 \times 12}{180} = 4''$$

$$\text{Use } t = 5''$$

$$d = 4''$$

From FIGURE 6.1, for $p = 0.2\%$ and $d = 4''$,

$$M_p = 1260 \text{ ft-lb/ft of slab}$$

$$\text{Average computed stiffness (N)} = 1.44 \times 10^6 \text{ lb-ft}^2/\text{ft of slab}$$

$$\text{Maximum curvature from TABLE 7.1} = 8.852 \text{ } M_p/N$$

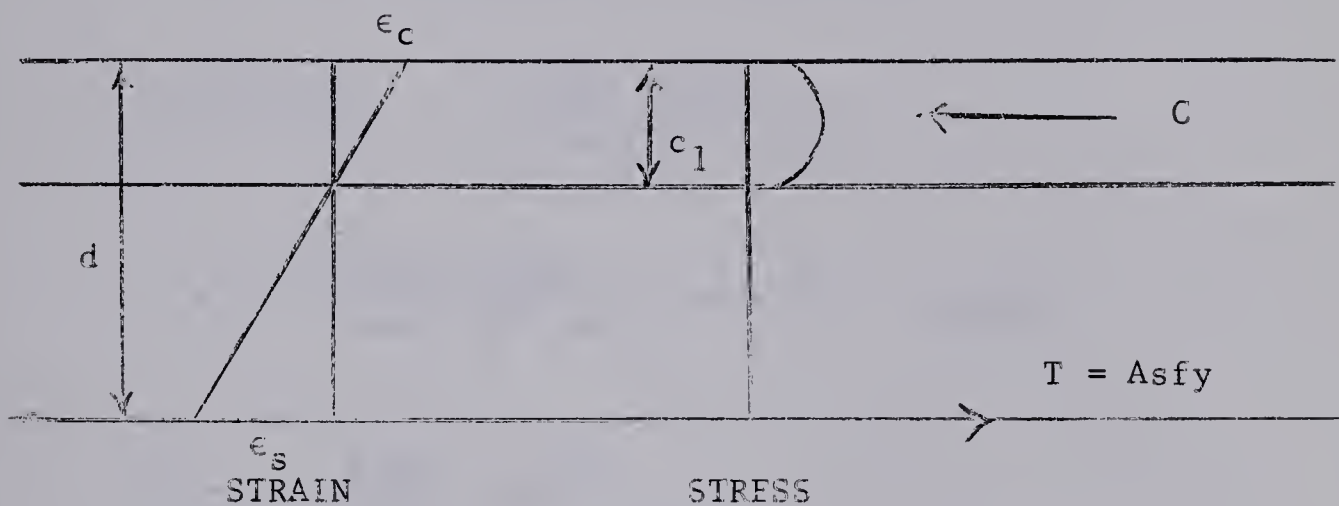


FIGURE 7.1

Assume the smallest c_1 and use ACI 318-63, Section 1503 (g)

$$c_1 = \frac{0.002 \times 4 \times 12 \times 40,000}{0.85 \times 3000 \times 12 \times 0.85} = 0.148''$$

$$\frac{\epsilon_s}{(4 - 0.148)} = \frac{8.852 \times 1260}{1.44 \times 10^6 \times 12}$$

$$\epsilon_s = \frac{8.852 \times 1260 \times 3.852}{1.44 \times 10^6 \times 12} = \underline{\underline{0.00248}}$$

$$\frac{\epsilon_c}{0.148} = \frac{8.852 \times 1260}{1.44 \times 10^6 \times 12}$$

$$\epsilon_c = \frac{8.852 \times 1260 \times 0.148}{1.44 \times 10^6 \times 12} = \underline{\underline{0.0001}}$$

Assume the largest c_1 which is obtained as follows:

$$\begin{aligned}
 k &= \sqrt{(pn)^2 + 2pn} - pn \\
 &= \sqrt{(0.002 \times 10)^2 + 2 \times 0.002 \times 10} - 0.002 \times 10 \\
 &= 0.181
 \end{aligned}$$

$$kd = c_1 = 0.181 \times 4 = 0.724''$$

$$\frac{\epsilon_s}{(4 - 0.724)} = \frac{8.852 \times 1260}{1.44 \times 10^6 \times 12}$$

$$\epsilon_s = \frac{8.852 \times 1260}{1.44 \times 10^6 \times 12} \times 3.276 = \underline{\underline{0.00212}}$$

$$\frac{\epsilon_c}{0.724} = \frac{8.852 \times 1260}{1.44 \times 10^6 \times 12}$$

$$\epsilon_c = \frac{8.852 \times 1260}{1.44 \times 10^6 \times 12} \times 0.724 = \underline{\underline{0.00047}}$$

(ii) Reinforced concrete slab with $p = 1.0\%$

$$t = 5''$$

$$d = 4''$$

$$p = 1\%$$

From ACI 318-63, $M_p = 5900$ ft-lb/ft of slab

Average computed stiffness (N) = 1.86×10^6 lb-ft/ft of slab

Assume the smallest c_1 and use ACI 318-63

$$c_1 = \frac{0.01 \times 4 \times 12 \times 40,000}{0.85 \times 3000 \times 12 \times 0.85} = 0.739''$$

$$\frac{\epsilon_s}{(4 - 0.739)} = \frac{8.852 \times 5900}{1.86 \times 10^6 \times 12}$$

$$\epsilon_s = \frac{8.852 \times 5900 \times 3.261}{1.86 \times 10^6 \times 12} = \underline{\underline{0.00763}}$$

$$\epsilon_c = \frac{8.852 \times 5900 \times 0.739}{1.86 \times 10^6 \times 12} = \underline{\underline{0.00173}}$$

Assume the largest c_1 which is obtained as follows:

$$\begin{aligned} k &= \sqrt{(pn)^2 + 2pn} - pn \\ &= \sqrt{(0.01 \times 10)^2 + 2 \times 0.01 \times 10} - 0.01 \times 10 \\ &= 0.358 \end{aligned}$$

$$kd = c_1 = 0.358 \times 4 = 1.43''$$

$$\frac{\epsilon_s}{(4 - 1.43)} = \frac{8.852 \times 5900}{1.86 \times 10^6 \times 12}$$

$$\epsilon_s = \frac{8.852 \times 5900 \times 2.57}{1.86 \times 10^6 \times 12} = \underline{\underline{0.00601}}$$

$$\epsilon_c = \frac{8.852 \times 5900 \times 1.43}{1.86 \times 10^6 \times 12} = \underline{\underline{0.00335}}$$

In the above computations the concrete and steel strains are derived for two limiting cases of c_1 , and the actual c_1 will be between

these two limits.

Since in no case have the steel strains and concrete strains exceeded 0.015 and 0.0038 respectively, it may be concluded that for the slabs considered, neither strain-hardening in the steel nor crushing of concrete has taken place at the formation of collapse mechanisms.

It should be pointed out that there can be cases where although the moment at a point in the slab under the applied load is equal to the ultimate moment given by ACI 318-63, the steel strain at this point is less than 0.0013. This is because, in these cases, the section of the slab under consideration is relatively uncracked and the concrete is taking tensile stresses. This statement can be verified by studying FIGURE 37 of Reference (16) in which the measured steel strains are given for various loadings applied to a test slab. Using ACI 318-63, the ultimate moment of this test slab is 206 ft-lb/ft. This moment is attained at mid-point of the supporting edge of the interior panel for a load of 160 lb/sq.ft., and the corresponding steel strain is only 0.0002. However, the shape of the curve suggests that a small increase in load will cause cracking of the concrete and rapid increase in the steel strain.

Case (10), given in TABLE 7.1 of this study, may be considered as being uncracked with the steel strain being less than 0.0013 when the moment is equal to the ultimate moment given by ACI 318-63. However, it is obvious that the concrete and steel strains, for such a case, are consistent with the assumption of idealized moment-curvature relationship.

TABLE 7.1

COEFFICIENTS OF CURVATURE AT ULTIMATE LOAD

UNIFORM LOAD, POISSON'S RATIO = 0

Plates Considered	Curvature = $K_{mc} M_p/N$	Remarks
	K_{mc} at Ultimate Load	
1. Simply supported, $\frac{b}{a} = 0.5$	3.016	Curvature at center (short direction)
2. Fixed edge, $\frac{b}{a} = 0.5$	6.336	Curvature at center (short direction)
3. Fixed edge, $\frac{b}{a} = 0.5$	8.852	Curvature at mid-point of long fixed edge
4. Simply supported, $\frac{b}{a} = 0.6$	1.942	Curvature at center (short direction)
5. Fixed edge, $\frac{b}{a} = 0.6$	4.830	Curvature at center (short direction)
6. Fixed edge, $\frac{b}{a} = 0.6$	7.464	Curvature at mid-point of long fixed edge
7. Simply supported, $\frac{b}{a} = 0.75$	1.378	Curvature at center (short direction)
8. Fixed edge, $\frac{b}{a} = 0.75$	3.328	Curvature at center (short direction)
9. Fixed edge, $\frac{b}{a} = 0.75$	5.890	Curvature at mid-point of long fixed edge
10. Simply supported, $\frac{b}{a} = 1.0$	1.010	Curvature at center
11. Fixed edge, $\frac{b}{a} = 1.0$	1.946	Curvature at center
12. Fixed edge, $\frac{b}{a} = 1.0$	4.358	Curvature at mid-point of fixed edge.

CHAPTER VIII

SUMMARY AND GENERAL CONCLUSIONS

8.1 Summary

A method of analysis was developed to make a theoretical investigation of the ultimate strength and behavior of single panel rectangular plates. The method is based on a modification of Newmark's plate analog and the superposition of elastic solutions. The required finite difference operators were derived using this physical model at each stage of yielding in the plate, and the solutions were superposed to establish the progressive yielding of the plate until the formation of a collapse mechanism. The deflections and bending moments at each grid point for every stage of yielding were determined. The twisting moment and elastic bending which are neglected in the yield line theory were taken into consideration. The "square yield criterion" was used as the yield criterion for the plates.

Four parameters, namely, aspect ratio, support conditions, loading pattern and Poisson's ratio were considered in this study. Aspect ratio ($\frac{b}{a}$) was varied from 0.5 to 1.0, support conditions were for simply supported and fixed edge cases, and the types of loading considered were uniform load, symmetrical line load and concentrated load at the center. The variation of Poisson's ratio was from 0 to 0.3.

An electronic digital computer IBM 7040, was used to perform

the required numerical calculations. The load-deflection characteristics were plotted and the progression of yielding traced for all the plates considered.

A suggested procedure for the application of results in the design of reinforced concrete slabs is given in CHAPTER VI, and the investigation of concrete and steel strains for these slabs at ultimate load is presented in CHAPTER VII.

8.2 Conclusions

In general, the results from the analyses give some insight into the ultimate strength and behavior of plates, and they lead to the following conclusions.

Uniform Load

(1) The ultimate loads obtained from the analyses are within $\pm 5\%$ of the corresponding values from the yield line theory for both simply supported and fixed edge plates.

(2) The final yield patterns from the analyses agree with the yield patterns from the yield line theory and with the yield patterns obtained from tests for the plates considered. The yield patterns from the analyses consist of yield bands instead of yield lines.

(3) The greater values of Poisson's ratio give greater widths of yield bands for both simply supported and fixed edge plates.

(4) For a simply supported plate, the higher value of Poisson's ratio lowers the first yield load if the position of first yield is at the center.

(5) The first yield load of a fixed edge plate is independent of

the value of Poisson's ratio.

(6) Poisson's ratio has significant influence on the behavior with respect to first yield and progression of yielding for the simply supported square plates. For the plate with $\mu = 0$, yielding begins at the corners and progresses towards the center. For the plate with $\mu = 0.1$, yielding essentially takes place simultaneously along the diagonals. However, for the plate with $\mu = 0.2$ or $\mu = 0.3$ the position of first yield is at the center, and yielding progresses towards the corners.

(7) For simply supported plates, the ratio of the ultimate load to first yield load increases with increasing value of Poisson's ratio and decreases with increasing value of aspect ratio ($\frac{b}{a}$). In general, the ultimate load is about 1.0 to 1.3 times the first yield load.

(8) For fixed edge plates, the ratio of the ultimate load to first yield load is independent of Poisson's ratio, and varies from about 2.0 for a square plate to about 2.4 for a rectangular plate.

(9) The ultimate load of a simply supported or a fixed edge plate is independent of the value of Poisson's ratio.

(10) In general, for both simply supported and fixed edge plates, the ratio of the maximum deflection at ultimate load to the maximum deflection at first yield load decreases with increasing values of aspect ratio ($\frac{b}{a}$) and increases with increasing values of Poisson's ratio. This ratio varies from 1.0 to 3.0 for simply supported plates, and 4.0 to 10.0 for the fixed edge plates.

(11) The higher value of Poisson's ratio gives smaller deflection in the elastic range, and causes greater deflection at ultimate load for

a given simply supported or fixed edge plate.

Line Load

(12) For a simply supported or a fixed edge plate, subjected to symmetrical line load the yielding takes place along the axis of symmetry until it is right close to the supports.

Concentrated Load

(13) The final yield pattern of a simply supported square plate subjected to concentrated load at the center is similar to the final yield pattern of the plate subjected to the uniform load. The ultimate load from the analyses for this yield pattern is about 13% higher than the corresponding value from the yield line theory.

(14) The mode of failure for a fixed edge square plate under the concentrated load is similar to the conical collapse mode except that in the final yield pattern from the analyses there is some negative yielding along the fixed edges. The ultimate load from analyses is within 2% of the corresponding value of the conical collapse mode.

(15) For the simply supported plate with $\frac{b}{a} = 0.5$, subjected to concentrated load at the center, the final yield pattern is similar to the collapse mode with circular fans shown on page 29 of Reference (5). The ultimate load from the analyses is within 7% of the corresponding value given in Reference (5).

(16) The fixed edge rectangular plate fails in the same manner as the fixed edge square plate except that there is rectangular collapse mechanism in the middle of the plate for the former case.

(17) For both simply supported plates and fixed edge plates, subjected to concentrated load at the center, the ratio of the ultimate load to the first yield load varies from about 2.0 for a square plate to 2.6 for a rectangular plate with $\frac{b}{a} = 0.5$.

(18) For simply supported plates, subjected to concentrated load at the center, the ratio of the deflection at ultimate load to deflection at first yield load varies from 3.5 for a square plate to 5.6 for a rectangular plate with $\frac{b}{a} = 0.5$.

(19) For fixed edge plates, the ratio of the deflection at ultimate load to deflection at first yield load varies from 5.1 for a square plate to 7.0 for a rectangular plate with $\frac{b}{a} = 0.5$.

Reinforced Concrete Slabs

(20) If the thickness of a typical two-way reinforced concrete slab satisfies the requirements of ACI 318-63, and if the percentage of steel varies from 0.2% to 1%, it is unlikely that the strain-hardening will take place in the steel at the formation of a collapse mechanism. The concrete strain will also be less than its limiting value in flexure. The above statements apply to simply supported and fixed edge slabs with aspect ratio ($\frac{b}{a}$) ranging from 0.5 to 1.0, and subjected to uniform loads.

(21) The theoretical maximum deflection at ultimate load of the fixed edge square plate subjected to uniform load shows good agreement with the measured value of the test slab given in Reference (15).

(22) The design of a reinforced concrete slab may be made, using one of the load-deflection characteristics plots.

(23) Stiffness (N) for deflection computations may be based on $\frac{b^3 d^3}{12}$ when one of the load-deflection characteristics plots from the analyses is used for design application.

LIST OF REFERENCES

1. Hopkins, H.G. and Prager, W., "The Load Carrying Capacity of Circular Plates" J. Mech. Phys. Solids 2 1953.
2. Hopkins, H.G. and Wang, A.J., "Load-Carrying Capacities for Circular Plates of Perfectly Plastic Material with Arbitrary Yield Condition" J. Mech. Phys. Solids 3 1954.
3. Hopkins, H.G., "On the Plastic Theory of Plates". Proc. Roy. Soc. (A) Vol. 241 1957.
4. Mansfield, E.H., "Studies in Collapse Analysis of Rigid Plastic Plates with a Square Yield Diagram". Proc. Roy. Soc. (A) Vol. 241 1957.
5. Wood, R.H., "Plastic and Elastic Design of Slabs and Plates". Thames and Hudson, London, 1961.
6. Brotchie, J.F., "Elastic-Plastic Analysis of Transversely Loaded Plates". ASCE Journal (EM) October, 1960.
7. Johansen, K.W., "Beregning of Krydsarmerede Jaernbetonpladers Brundmoment" Bygningsstatistiske Meddelelsen (Copenhagen), Vol. 3, 1931.
(See also: Johansen, K.W., "Yield-Line Theory" English translation, Cement and Concrete Association 1962).
8. Hognestad, E., "Yield-Line Theory for the Ultimate Flexural Strength of Reinforced Concrete Slabs", ACI Journal, Vol. 49, March, 1953.
9. Metz, G.A., "Flexural Failure Tests of Reinforced Concrete Slabs" ACI Journal, January 1965.
10. Crawford, R.E., "Limit Design of Reinforced Concrete Slabs", ASCE Journal (EM) October, 1964.
11. Timoshenko, S.P., and Woinowsky-Krieger, S, "Theory of Plates and Shells" McGraw-Hill, 1959.
12. Ang, A., "The Development of a Distribution Procedure for the Analysis of Continuous Rectangular Plates". Structural Research Series No. 176, University of Illinois, 1959.
13. Prescott, W.S., Ang, A, and Siess, C.P., "Analysis of Clamped Square Plates Containing Openings with Stiffened Edges". Structural Research Series No. 229, University of Illinois, 1961.

LIST OF REFERENCES (Continued)

14. Simmonds, S.H. and Siess, C.P., "Effects of Column Stiffness on the Moments in Two-Way Floor Slabs". Structural Research Series No. 253, University of Illinois, 1962.
15. Vanderbilt, M.D., Sozen, M.A. and Siess, C.P., "Deflections of Reinforced Concrete Floor Slabs". Structural Research Series No. 263, University of Illinois, 1963.
16. Gamble, W.L., Sozen, M.A. and Siess, C.P., "An Experimental Study of a Reinforced Concrete Two-Way Floor Slab". Structural Research Series No. 211, University of Illinois, 1961.
17. Prager, W., "An Introduction to Plasticity" Addison-Wesley, 1959.
18. Westergaard, H.M. and Slater, W.A., "Moments and Stresses in Slabs" Proc. ACI Vol. 17, 1921.
19. Neal, B.G. "The Plastic Methods of Structural Analysis", John Wiley, 1957.
20. Beedle, L.S., "Plastic Design of Steel Frames" John Wiley, 1958.
21. European Committee for Concrete, Bulletin No. 27, September, 1960.
22. European Committee for Concrete, Bulletin No. 29, November, 1960.
23. European Committee for Concrete, Bulletin No. 35, March, 1962.

APPENDIX A

YIELD CRITERIA

APPENDIX A

YIELD CRITERIA

A.1 Square Yield Criterion

The yield criterion which is used for application to isotropic reinforced concrete slabs is "square yield criterion", and it is shown in FIGURE A.1. As stated by WOOD (5), this criterion in common use is only an approximation for a more complicated yield criterion for reinforced concrete slabs. He further stated that the use of it is roughly suitable for steel plates, for design purposes, especially in view of the beneficial effects of membrane action. Therefore the elasto-plastic plate in this study means the plate which yields according to "square yield criterion". The material of this plate is somewhat like a reinforced concrete with reinforcements in two perpendicular directions

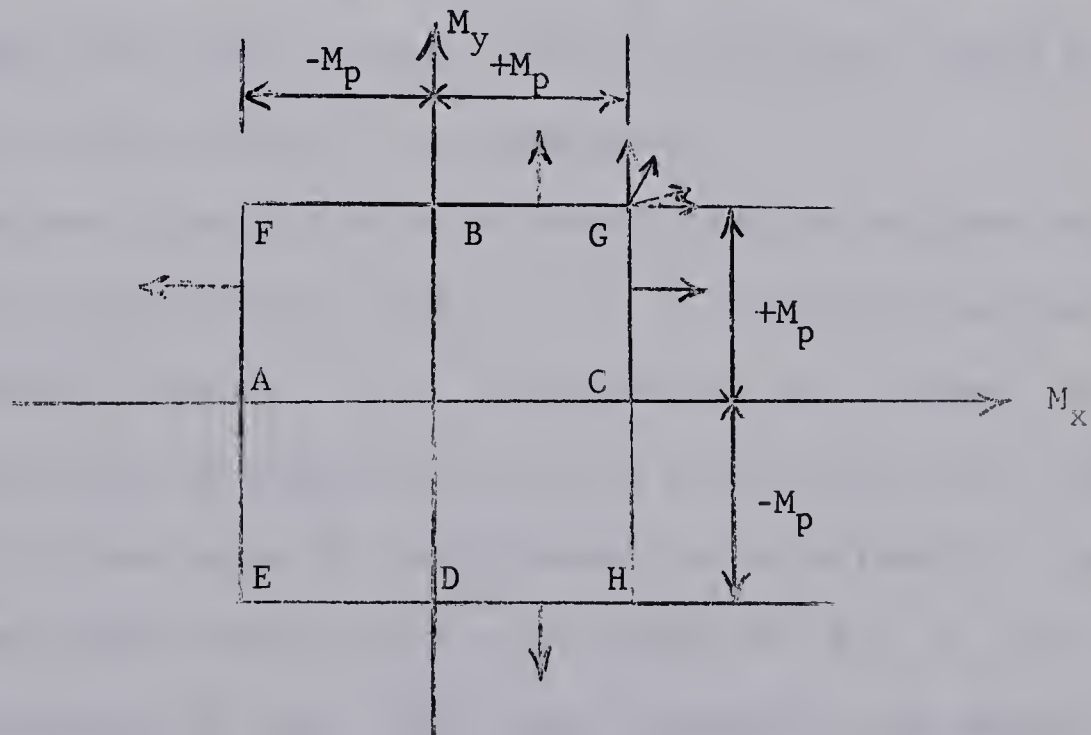


FIGURE A.1

To clarify the use of this criterion better, the explanation will be in terms of isotropic reinforced concrete slab. The slab which is reinforced in the direction of x and y will yield when the bending moment M_x in the x direction reaches $\pm M_p$, or when $M_y = \pm M_p$. The yield moment in one direction in such a case is independent of the yield moment given by the reinforcement at right angles, and whether the latter reinforcement is yielding or not. Yielding as described above is represented in FIGURE A.1 by points on the boundary near A, B, C or D. Points near B and C apply to yielding of a rectangular slab at any point along the axes of symmetry under symmetrical loading, assuming the supports of the slab to be symmetrical, and in x and y directions also. Points A and D represent yielding along the edges of a fixed edge slab. Yielding across any fracture line, which is not in line with the reinforcement axes x and y will compell to yield both sets of reinforcements. This is represented by point E or G in FIGURE A.1. WOOD (5) has expressed that yield moment across such fracture line is likely to exceed M_p , and he has carried our tests to support this view. He has further stated that to this extent the use of "square yield criterion" is conservative.

From the above discussion it is assumed that for a given point in the slab, if the reinforcement in the x or y direction has yielded, and the reinforcement in the y or x direction has not yielded, M_y or M_x can still be increased in magnitude until its value reaches the value of M_p . However, if both sets of reinforcements have yielded for a given point, it is assumed that there will be no increment of M_x , M_y and M_{xy} under further application of load. With these assumptions the method of analysis is developed in CHAPTER II.

A 2 Tresca's Yield Criterion

Tresca's yield criterion is usually stated as: "yielding occurs when the maximum shear stress in the material reaches a certain critical value".

Referring to principal stresses $\sigma_1, \sigma_2, \sigma_3$, the Tresca yield criterion is represented as

$$\sigma_1 - \sigma_3 = \text{constant} = 2 \tau_y \quad (\text{A.1})$$

where $\sigma_1 \geq \sigma_2 \geq \sigma_3$ and τ_y is the maximum permissible shear stress in the material.

For the case of pure tension, we have $\sigma_1 = f_y, \sigma_2 = \sigma_3 = 0$, and therefore from EQUATION (A.1),

$$\sigma_1 = f_y = 2 \tau_y$$

$$\therefore \tau_y = f_y / 2$$

In applying the Tresca yield criterion to plane stress problems like plates, the principal moments instead of principal stresses are usually used, and therefore we have

$$M_I - M_{II} = M_p \quad (\text{A.2})$$

where M_I, M_{II} = principal moments

M_p = plastic moment of the plate

A.3 Von Mises' Yield Criterion

The von Mises' yield criterion was interpreted by Hencky to mean that yielding began when the shear strain energy reached a certain critical value.

The von Mises yield criterion is usually given as

$$(\sigma_1 - \sigma_2)^2 + (\sigma_2 - \sigma_3)^2 + (\sigma_3 - \sigma_1)^2 = 6 \tau_y^2 \quad (\text{A.3})$$

where $\sigma_1, \sigma_2, \sigma_3$ = principal stresses

τ_y = maximum permissible shear stress

For pure tension case, we have $\sigma_1 = f_y$, $\sigma_3 = \sigma_2 = 0$,
and therefore from EQUATION (A.3),

$$2 \sigma_1^2 = 2 f_y^2 = 6 \tau_y^2$$

$$\tau_y = \frac{f_y}{\sqrt{3}}$$

For application of the von Mises yield criterion to plates, the principal moments instead of principal stresses are used, and it may be expressed as shown below.

$$M_I^2 - M_I M_{II} + M_{II}^2 = M_p^2 \quad (\text{A.4})$$

where M_I, M_{II} = principal moments

M_p = plastic moment of the plate

EQUATION (A.4) can be represented diagrammatically as shown in

FIGURE A.3

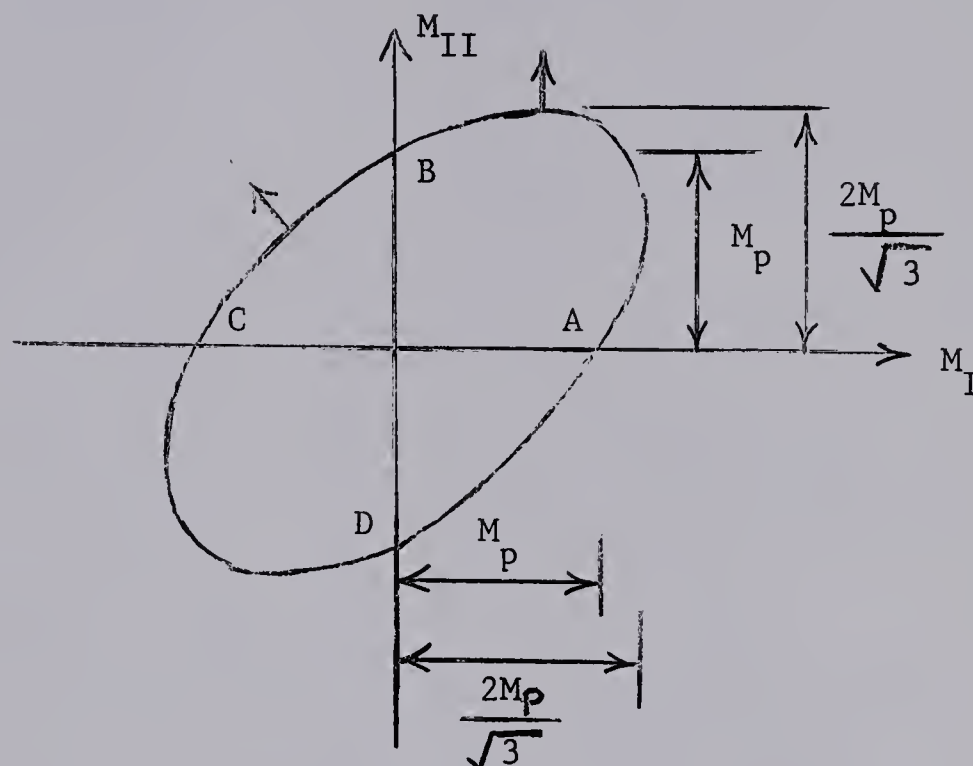


FIGURE A.3

The state of stress of a point in the plate subjected to a load is either within or on the yield locus shown in FIGURE A.3. In the former case the plate remains elastic and rigid at that point, whereas in the latter case it yields plastically, and the flow rule demands that for the point which has yielded, the strain direction be normal to the yield locus.

For the case of symmetrically loaded circular plate, M_r , and M_θ can be taken as the principal moments.

APPENDIX B

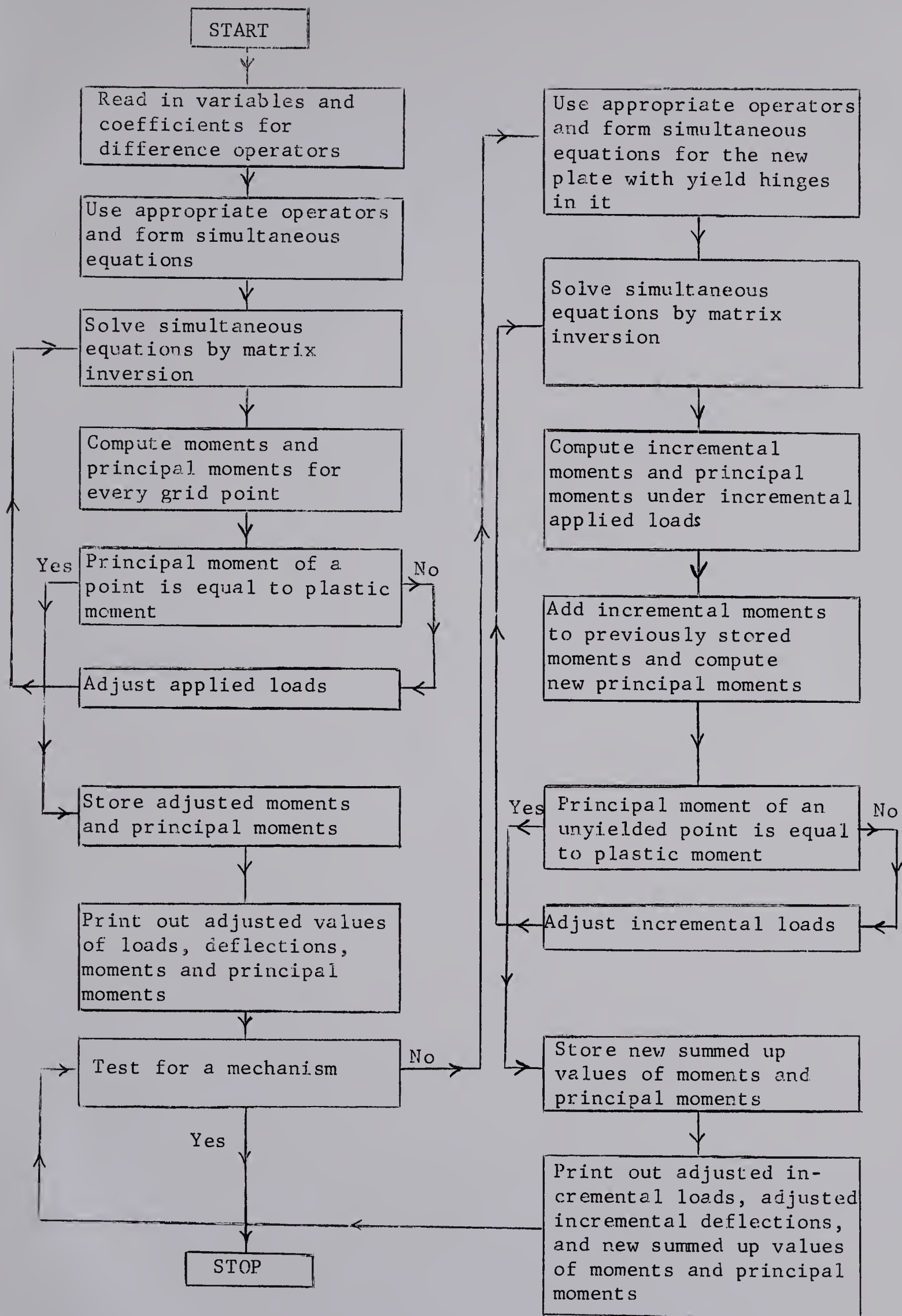


FIGURE B.1 SCHEMATIC FLOW DIAGRAM FOR COMPUTER PROGRAM

B29841